January 1989

Soil Phase Photodegradation of Toxic Organics at Contaminated Disposal Sites for Soil Renovation and Groundwater Quality Protection

W. M. Moore

R. Ryan Dupont

J. E. McLean

Soil Phase Photodegradation of Toxic Organics

at

Contaminated Disposal Sites

for

Soil Renovation and Groundwater Quality Protection

Final Report

for

Award 14-08-0001-G1304

Project Period:
September 22, 1986 through September 21, 1988
Extension through March 21, 1989

Principal Investigator

W.M. Moore

Co-Principal Investigators

R.R. Dupont
J.E. McLean

Utah State University
Utah Water Research Laboratory
UMC 8200
Logan, UT 84322-8200

August 28, 1989

Soil Phase Photodegradation of Toxic Organics

at

Contaminated Disposal Sites

for

Soil Renovation and Groundwater Quality Protection

Final Report

for

Award 14-08-0001-G1304

Project Period:
September 22, 1986 through September 21, 1988
Extension through March 21, 1989

Principal Investigator

W.M. Moore

Co-Principal Investigators

R.R. Dupont
J.E. McLean

Utah State University
Utah Water Research Laboratory
UMC 8200
Logan, UT 84322-8200

August 28, 1989

FOREWORD

The release of refractory, non-biodegradable, hazardous organics to the terrestrial environment via industrial waste discharges and waste disposal practices has severely impacted land and water resources. Photochemical reactions induced by direct light energy adsorption by contaminants (direct photolysis), or by light energy transfer from energy adsorbing/transferring substances (sensitized photolysis) provide potential pathways for the removal of many of these organics, i.e., polynuclear aromatic hydrocarbons (PAHs), phenols, aromatics, substituted and chlorinated aromatics, etc., from contaminated soils. These photochemical reactions have been shown to be effective for a number of pesticides and PAHs, and may prove technically and economically attractive as a treatment approach for renovation of contaminated soil systems for soil detoxification and groundwater contamination prevention.

This document describes findings of a two and one-half year laboratory study on the effectiveness and applicability of soil phase photolysis as a degradation pathway for a number of refractory hazardous organics of environmental concern. In this project, the quantitative nature of direct and sensitized photolysis of various chemicals on a range of soils and soil minerals was investigated in laboratory scale photolysis experiments simulating natural sunlight conditions. The possibility of optimizing the observed photodegradation reactions through the use of soil amendments was also investigated.

The support of the U.S. Geological Survey through Award 14-08-0001-G1304 is gratefully appreciated. The Utah Water Research Laboratory provided experimental and analytical facilities required for the successful completion of this project. In addition, the efforts of students Richard Hoff, Richard Liu, Tom Teng, and Elizabeth Guimarin are greatly appreciated. Nancy Mesner is acknowledged for her monumental efforts in completing the project, while thanks go to Ivonne Cardona Harris for her hard work in typing the manuscript.

The contents of this report were developed under a grant from the Department of the Interior, U.S. Geological Survey. However, those contents do not necessarily represent the policy of that agency, and you should not assume endorsement by the Federal Government.

TABLE OF CONTENTS

TABLE OF CONTENTS (CONT'D)

TABLE OF CONTENTS (CONT'D)

LIST OF TABLES

LIST OF TABLES (CONT'D)

LIST OF TABLES (CONT'D)

LIST OF FIGURES

LIST OF FIGURES (CONT'D)

ABSTRACT

Accurate assessment of the potential for contaminated soil remediation requires detailed knowledge of the fate of waste constituents within the soil environment. For many non-biodegradable organics compounds, photochemical degradation may provide a potential pathway for the removal of such compounds from soil surfaces. A study was conducted to evaluate the rate of photodegradation of ten hazardous organic compounds from three soils, silica gel, and four soil minerals (kaolinite, montmorillonite, illite, and calcite) under conditions of controlled irradiation. In addition, the effect of six amendment treatments (methylene blue, riboflavin, hydrogen peroxide, diethylamine, peat moss, and silica gel) on the rates of compound loss was also investigated. Soil and mineral samples were spiked with various combinations of m-cresol, quinoline, biphenyl, dibenzo[a]furan, fluorene, pentachlorophenol, phenanthrene, anthracene, 9H-carbazole and pyrene at either 500 or 1000 mg/kg initial soil concentration of each chemical. Amendments were applied to the soils and minerals and duplicate samples were irradiated in petri dishes under ultraviolet or visible light while spike controls were incubated in the dark. Linear regression of soil/mineral contaminant concentration data showed that first order kinetic modeling best described the degradation process. Significant loss of anthracene occurred on all surfaces tested although the rate of loss varied with surface type and, for some surfaces, with the spiking solution concentration and chemical mixtures. Anthracene loss from silica gel was the most rapid of all reactions observed. Skumpah soil, a light colored alkaline soil, yielded the greatest reduction in contaminant concentrations found in the soil studies. Calcium kaolinite displayed the most rapid kinetics of the mineral surfaces tested. Loss of the other test compounds was observed from only some of the surfaces investigated. Anthraquinone and fluorenone were identified as the major degradation products of the photoreaction of anthracene and fluorene. Under the conditions of this study, soil and mineral type, as well as surface renewal via mixing, were found to have more effect on degradation rates than any of the amendments that were tested.

INTRODUCTION

The remediation of former hazardous waste disposal sites is a major public concern. The Office of Technology Assessment (1983) indicates that 255 to 275 million metric tons of hazardous waste are generated annually in situations controlled by federal or state regulations. Additionally, some 15,000 uncontrolled disposal sites were contained in the EPA's Emergency 1 Remedial Response Information System at the time. Another 80,263 sites which were identified by the EPA contained contaminated surface impoundments (pits, ponds or lagoons), 90 percent of which were believed to pose potential threats to groundwater resources. Of the 418 uncontrolled hazardous waste sites listed on the National Priority List (NPL), 347 were considered to pose a direct threat to drinking water supplies.

From the data presented above it becomes obvious that the extent of surface and subsurface contamination by hazardous waste treatment, storage, and disposal facilities (TSDFs) has reached alarming proportions. Hazardous waste management practices which were acceptable in the past, particularly landfills, surface impoundments and lagoons, also constitute a substantial threat to public health and the environment due to the migration of hazardous constituents away from these facilities into surrounding areas. All TSDFs, whether operating or abandoned, are required by law to remove or detoxify all hazardous constituents at the site and "... take all steps to prevent threats to human health and the environment ..." (Federal Register 40 CFR 264.113) from their facility upon closure. Post-closure monitoring is required for 30 years following closure to assure that migration of hazardous constituents from the site is not occurring.

It is apparent that an urgent need exists for the development and evaluation of innovative techniques for the remedial, in-place treatment of hazardous constituents at uncontrolled, abandoned, and active waste disposal sites. To provide optimal control techniques and alternative strategies for site remediation, one must understand the nature of biological and physicochemical reactions that detoxify or immobilize hazardous constituents in soil systems. The extremely toxic nature of many hazardous organic constituents significantly reduces the effectiveness of hazard reduction by biological means in many soil/waste systems. Reduced biological activity, the nature of many of these complex organics, and their potential for photoreactivity led to the initiation of this feasibility study in which direct photolysis and possible photosensitizing amendments were used to renovate soil systems that had been contaminated with a subset of hazardous organics. The hazardous organics came from wood preserving wastes which have become both a health and an environmental concern at many abandoned sites across the country.

The objective of this project has been to broaden the knowledge base regarding the role of soil-phase photolysis in the degradation of refractory, hazardous organic constituents in the terrestrial environment.

Specifically the project was designed to meet the following objectives:

1. To evaluate the role that soil-phase photolysis plays in the fate of hazardous constituents in the soil environment through the quantitative description of photochemical reactions as a function of reaction conditions (sensitizer/donor type and concentration, substrate concentration and soil and mineral type) for selected PAHs and aromatics (anthracene, m-cresol, fluorene, pyrene, pentachlorophenol, phenanthrene, dibenzofuran, quinoline, biphenyl, and 9 H-carbazole) occurring in refractory hazardous wastes.

2. To investigate photochemical intermediates occurring from the photodegradation of these parent compounds.

3. To identify feasible management options for the control and optimization of photodegradation reactions for constituent and overall waste hazard reduction.

LITERATURE REVIEW

Environmental Fate of Hazardous Compounds in Soils

Degradation and immobilization of hazardous organic constituents can be accomplished through a variety of physical, chemical, and biological processes. The study of the biological degradation of hazardous organic compounds in soils has been extensive, especially in the fields of pesticide degradation and the development of substrate specific strains of microorganisms (Moos 1983, Guthrie 1984, Moersen and Rehm 1987).

While there is an abundance of biological degradation information on some hazardous compounds, only limited investigations have been directed toward an evaluation of the importance of non-biological degradation mechanisms to the fate of hazardous organics in soils (Bulman et al. 1985). For a non-biological degradation process to be successful for a chemical compound that is stable at normal temperature and pressure, a significant energy input is required to initiate a reaction, based on activation energy considerations. Sunlight is a readily available and abundant energy source and, consequently, photolysis may be one of the principle mechanisms for the transformation of biologically recalcitrant compounds. The importance of photochemical transformation in the atmosphere is well documented (Altschuller and Bufalini 1971, Leighton 1961). Photodegradation of specific hazardous organic compounds on atmospheric particulates is known to occur; however, the mechanisms are not clearly understood (Korfmacher et al. 1980, Behymer and Hites 1985). Comparatively little is known about photodegradation of pollutants in water or on soils where other competing processes such as biodegradation, hydrolysis, and adsorption occur (Zepp and Cline 1977). In soil and water systems, biodegradation is often the major pathway for elimination of organic compounds. When these systems include refractory species, however, biodegradation is too slow to be effective and photodegradation may become the most important degradation pathway for these compounds.

Photolysis Fundamentals

Direct photolysis occurs when the chemical molecule itself absorbs light and undergoes reaction from its excited state. Transformations of organic pollutants by direct photolysis depend upon the absorption of energy in the UV spectrum. Though many polycyclic aromatic hydrocarbons absorb strongly in the far ultraviolet, direct photolysis is generally an inefficient environmental process due to the fact that virtually no light below 295 nm reaches the earth's surface (Zepp and Cline 1977).

Chemical activity is not restricted to the absorbing molecule because excitation energy can be transferred in a number of ways to the species that ultimately undergo chemical change, a process referred to as photosensitization. This indirect photolysis reaction occurs when another chemical species, called a sensitizer molecule, absorbs light energy and then transfers this energy from its excited state to another chemical which undergoes reaction (Mabey et al. 1982). Photosensitization requires a sensitizer which absorbs the available light, (i.e., in the visible region where there is a wealth of energy reaching the earth's surface) and transfers it to a non-absorbing species to form a reactive intermediate.

The electronically excited sensitizing molecule, or triplet sensitizer, is usually unstable at this new level of energy, and by a deactivation process it reverts to a lower, less energetic stable state. Triplet sensitizers return to ground state by transferring energy to molecular oxygen or organic substrates present in the system which are non-absorbing in this same wavelength region. For energy transfer to occur between molecules, the energy gap between ground state and the first excited state of a molecule must be less than the energy gap between the triplet state of the sensitizer and its ground state, which is on the order of 50 kcal/mole for common sensitizing organic dyes. Most organic molecules require more energy to be excited than is available from a triplet sensitizer. Oxygen, however, is unusual because its ground state is a triplet and the energy gap between ground state and the first excited state, which is a singlet, is unusually low (22 kcal/mole). The favorable energy gap differential between many organic compounds and oxygen results in the selective transfer of sensitizer energy to oxygen even if oxygen is present only in trace amounts (Foote 1968, Sargent and Sanks 1976). Singlet oxygen is a strong oxidizing agent with an average half-life of 2 μ seconds (Kearns 1971), capable of quickly oxidizing substrate molecules.

Much scientific research has been conducted on dye-sensitized photooxidation; however, engineering application of the photolysis process to water, wastewater, and soil treatment has received little attention. Spikes and Straight (1967) reported that many organic compounds including alcohols, nitrogen heterocycles, organic acids, olefins, benzenoids, phenols, and aromatic compounds undergo sensitized photooxidation in natural systems. According to Foote (1968) many organic compounds are capable of absorbing light to initiate these photochemical reactions. Some will sensitize only very specific reactions, while others will sensitize the photooxidation of many substrates. Investigations by Sargent and Sanks (1974, 1976) indicate that common dyes such as methylene blue, toluidine blue, rose bengal and neutral red are effective non-specific sensitizers for photooxidation reactions.

It has been shown that organic dyes can be used to generate singlet oxygen in solutions containing hazardous materials. In some cases the hazardous material is oxidized to a compound which is more susceptible to further degradation by other processes. One of the most popular dyes has been methylene blue because of its high absorptivity in the visible light range. Several fungicides, pesticides, and PNAs have been degraded by photosensitization (Acher and Rosenthal 1977, Naeger 1985, Watts 1983). The dyes are slowly degraded themselves but they have a high efficiency of singlet oxygen generation and will cause the oxidation of many organic molecules which are stable to normal oxygen.

Photoreactions in the Soil Systems

The extent and rate of photolysis of a compound is known to be affected by the solvent in which it is associated, especially if the solvent becomes intimately involved in the photochemical reaction taking place (Miller and Zepp 1983, Lemaire et al. 1982). Although the occurrence of photoreaction of chemicals adsorbed on solid surfaces (in particular pesticides), has been implicated (Choudhry and Webster 1985), the importance of this reaction as compared to aqueous or vapor photoreactivity and reaction pathways through which the reaction occurs have not been completely identified.

To a large extent, the relative importance of the photoreaction of a chemical on a soil depends upon its partitioning among the air-water-soil media within the soil system. For nonpolar, nonionic compounds, partitioning of the compound into the lipophilic organic constituents of soil may be thought of as partitioning into a natural soil solvent system. Thus, the type of organic matter present in soil and its interaction with the contaminant molecule would be expected to affect the photoactivity of that molecule.

Ionic compounds will react more strongly with solid soil surfaces than the nonionic compounds which simply partition into soil organic matter. Binding mechanisms of organic molecules to soil clay minerals have been elucidated by studying shifts in a molecule's infrared absorption spectrum. This technique has been used to examine the nature of clay-organic complexation for a wide variety of organics including: pesticides, organic acids, amino acids, proteins, polymers, and surfactants (Mortland 1970, Farmer 1971, Mingelgrin et al. 1978). The type of binding, (i.e., hydrogen binding, ion exchange, ligand exchange, etc.), between the organic contaminant and soil surfaces will affect the molecule's spatial configuration and, consequently, its chemical, photochemical, and biological activity. Organic chemicals retained by clays in inner sphere complexes may not participate in photoreactions. Compounds held in outer sphere complexes may be available to participate in photoreactions; however, reaction pathways and consequently reaction products may be significantly different from those of non-sorbed compounds due to alterations in their chemical, spatial, and/or conformational properties following interaction with the soil surface.

Both direct and sensitized photolysis have been observed for pesticides in aqueous, soil, and vapor phases (Miller and Zepp 1983). Miller and Zepp (1983) found that factors including soil particle size, mineral composition, light absorption characteristics, and moisture content affected the nature of the photoreactions of pesticides. Soil characteristics such as transition metal content (Nilles and Zabik 1975), soil pigment content (Hautala 1978), and soil water content (Burkhard and Guth 1979) have also been identified as affecting the nature and extent of photochemical reactions in soil systems. Some sensitized photolysis mechanisms were shown to be sensitive to the pH of the system, suggesting that soil pH might also have an influence on soil photolysis rates (Fife and Moore 1979).

The literature on the photophysical and photochemical properties of humic materials has been reviewed by Choudhry (1984). Studies suggest that the active components of soil seem to be the fulvic and humic acids. Under suitable conditions these materials photogenerate singlet oxygen in small concentrations (Gohre and Miller 1983) and undergo other photochemical reactions. Miles and Brezonik (1981) have reported a reaction cycle

involving the humic materials of iron in an oxidative cycle where iron is photoreduced from ferric to ferrous forms and then the ferrous state is returned to ferric state by dissolved oxygen. This could account for the low dissolved oxygen levels in waters which are highly colored by organics. Zepp et al. (1977) found that there is a steady-state soil concentration of singlet oxygen of approximately 10^{-14}M. Gohre and Miller (1983) have evidence for the production of singlet oxygen in soil at a level capable of oxidizing an olefin present at parts per billion levels in soil. The singlet oxygen production in all of these cases is extremely small, but there is reason to believe that the production is stable over a long period of time.

Despite the observations of soil photodecomposition, little substantive information exists to allow accurate predictions of the importance of soil surfaces on general chemical photodecomposition. As Helling et al. (1971) indicated in 1971 and Miller and Zepp (1983) repeated 12 years later, soil and chemical properties which alter soil photodecomposition, i.e., soil sensitization, reaction quenching, radical formation, light adsorption characteristics, and soil characteristics (particle size, organic content, and temperature), remain poorly understood.

A group lead by De Mayo has published a series of papers (Johnston et al. 1982; Bauer et al. 1982, 1984; De Mayo et al. 1984) on the photolysis of polycyclic aromatic hydrocarbons on silica gel, metal oxides, and glass surfaces. They found that the nature of the bonding between the surface and the organic compounds being photolyzed was significant in determining the nature and extent of photolysis. Likewise, Dunston et al. (1989) concluded that of the subfractions in coal ash, the strongest adsorbent for pyrene also had the greatest ability to stabilize pyrene to photochemical reactions.

Simulated atmospheric particulates, including fly ash and carbon black, as well as silica gel and alumina were used as solid surfaces in the work of Korfmacher et al. (1980), Yokley et al. (1986), and Behymer and Hites (1985). Comparisons of the rates of photolysis of compounds including anthracene, pyrene, and phenanthrene in solution (organic solvent) with those on the solids led to the conclusion that the color, or relative internal reflectance of the solids, affected reaction rates. If the adsorbate is present as a monolayer or less on the adsorbent, the probability of a photon encountering and exciting a molecule of the adsorbate is very low compared to the probability of passing through the adsorbate and reaching the surface of the adsorbent. The adsorbent then acts as an internal filter for the light, either strongly absorbing it or reflecting it back through the layer of organic molecules. Multiple passes of the light through the organic material increase the chances of absorption and the production of an excited state, thus increasing the probability of a subsequent reaction.

Photoreactions of halogenated aromatic compounds have also recently been of interest because of a 2,3,7,8-tetrachlorodibenz-p-dioxin (TCDD) release near Seveso, Italy in 1976 (Choudhry and Hutzinger 1982). Photolysis of TCDD on soil surfaces was reported by Crosby et al. (1971) in the presence of suitable hydrogen sources in the form of polar solvents. Plimmer and Klingebel (1973) indicated that methanol used as a solvent for TCDD photooxidation experimentation also acted as a hydrogen donor in the photolysis reaction. Investigations of the use of alternative hydrogen donors for <u>in situ</u> treatment of

contaminated surfaces in the Seveso area was reported by Wipf et al. (1978). Solutions of 80 percent olive oil and 20 percent cyclohexane at 350 L/ha and a 40 percent aqueous emulsion with 4 percent biodegradable emulsifying agent at 400 L/ha were used to produce a thin film on vegetation and other smooth surfaces to provide a maximum reaction surface for TCDD photolysis. Under laboratory conditions, the oil and emulsion solutions reduced the half life of TCDD by a factor of 25 when irradiated with light of approximate solar wave-length distribution. Liberti et al. (1978) reported that a 1:1 solution of ethyl oleate and xylene used as hydrogen donors also resulted in complete TCDD degradation on building surfaces within approximately 1 hour at 2 mW/cm^2 and 72 hours at 20 $\mu W/cm^2$ light intensity.

An alternative treatment was reported by Christensen and Weimer (1979) for the soil photodegradation of polybrominated biphenyl waste using tertiary amines (1 percent by weight). The treated soil was exposed to sunlight for four days in closed containers. The polybrominated biphenyls were degraded by 40 percent in the amine treated soil samples and only by 6 percent in the untreated soil samples. Amines are known to be good hydrogen donors in photochemical processes. They also form charge transfer complexes that may aid in stimulating photodecomposition reactions. The limited evidence presented by Christensen and Weimer suggests that it was the charge transfer complexes that were undergoing photodegradation in their experiments.

The photochemistry of methylene blue and other thiazine dyes has been studied extensively as described above. Bonneau et al. (1975) found that methylene blue was more effective as a sensitizer at pH 7 to 9 than at acidic pH levels. Riboflavin photosensitizes oxygen in a manner similar to methylene blue but the effective pH range for its triplet state is 3 to 8 (Fife and Moore 1979). Riboflavin is a more reactive molecule than methylene blue and it can transfer energy to other molecules as well as oxygen. Acher and Rosenthal (1977) utilized riboflavin and methylene blue to generate singlet oxygen for the degradation of herbicides and other toxic materials.

As a continuation of this concept, Naeger (1985) has shown that refractory compounds such as acridine, anthracene, naphthalene and quinoline can be altered in the presence of singlet oxygen photogenerated by methylene blue. The quantum efficiencies ranged from 0.5 percent to 10 percent depending on the pH and the dye and substrate concentrations. It had been shown previously by Watts (1983) that oxygen saturation of reacting solutions was also necessary for optimal reaction conditions.

This technique of oxygen production which uses sensitizer dyes has not been reported in the literature for contaminated soil treatment. A multitude of compounds may quench the photoactivity of sensitizer dyes in soils; however, if the approach were successful, lower molecular weight compounds would be formed and degradation processes would be accelerated through this sensitized photodegradation mechanism.

MATERIALS AND METHODS

Characterization of Materials

Compound Selection. One of the most prevalent hazardous wastes in the United States is generically termed creosote waste. Creosote is commonly used as a wood preservative and is a mixture of phenols, phenolic derivatives, and polycyclic aromatic hydrocarbons obtained either by destructive distillation of wood tar or fractional distillation of coal tar (Verschueren 1983). Typical constituents of creosote are given in Table 1. Because of their resistance to biodegradation and their persistence in contaminated soils (Sims et al. 1986), a subset of creosote constituents was selected for photodegradation studies (Table 2). Compounds selected were also considered based on their listing as EPA hazardous constituents (40 CFR, Appendix VIII), their presence in coal tar (Merck 1983), the presence of specific functional groups, low vapor pressure to minimize volatility (Verschueren 1983), and their expected recalcitrance or reactivity under experimental conditions.

Chemical structures for the test compounds used in the study are shown in Figure 1, and select physicochemical properties commonly used for environmental fate models and parameter estimations are listed in Table 3. A limited number of biodegradation half-lives in soils are also listed in Table 1, however, the high variability in reported rates makes their interpretation difficult without detailed information about the experimental conditions applied.

Although the solar spectrum is strongly attenuated in the ultraviolet region, the interaction of the compounds used in this study with light energy is limited to the region from 300 to 400 nm. Because of the importance of this region to photochemical activity of the selected compounds, the absorption spectra for each compound was quantified in the ultraviolet region from 220 to 400 nm as indicated in Figures 2 and 3 for solution concentrations in the range of 10^{-5} M. These solutions were prepared in methylene chloride. Those compounds which showed a significant absorption maxima above 300 nm are indicated in Table 2. All compounds except fluorene, biphenyl, dibenzofuran and cresol exhibited major absorption peaks above 300 nm. The compounds with absorption peaks above 300 nm may be photoreactive due to direct photolysis in the soil systems, i.e.,they do not require addition of a sensitizer. Those compounds without absorption peaks above 300 nm require sensitizer addition if photodegradation is to be accomplished.

Table 1. Constituent analysis of creosote derivative wastes.

Compound	Weight % (1)	Weight % (2)
Acenaphthene	2-5	9
Anthracene	1.2-1.8	2
Biphenyl		1.2
Carbazole	1.8-2.7	2
Dibenzofuran		5
Fluoranthene	2-5	10
Fluorene	2-4	10
Naphthalene	7-28	3
Phenanthrene	9-14	21
Pyrene	2-3	8.5

(1) High temperature creosote (Winslow 1973).
(2) Creosote oil, data are ± 0.7 percent (Lorenz and Gjovik 1972)

Table 2. Ultraviolet absorption data for selected compounds.

Compound	Molecular Weight	Absorption Maxima > 300 nm (log extinction coefficient)
Quinoline	129.2	315 (3.7)
Pentachlorophenol	266.3	302 (3.3)
Carbazole	167.2	320 (3.7), 330 (3.7)
Fluorene	166.2	None
Phenanthrene	178.2	316 (3.0)
Biphenyl	154.2	None
Pyrene	202.3	320 (4.5), 335 (4.8)
Dibenzofuran	168.2	None
m-Cresol	108.2	None
Anthracene	178.2	356 (4.0), 374 (4.0

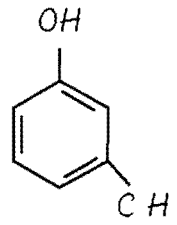

m-Cresol

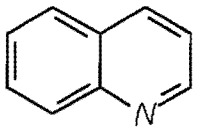

Quinoline

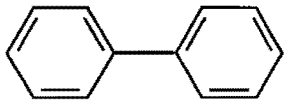

Biphenyl

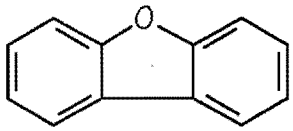

Dibenzofuran

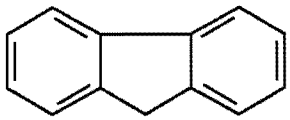

Fluorene

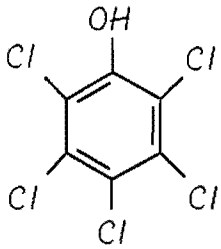

Pentachlorophenol

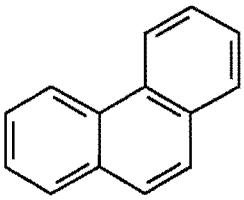

Phenanthrene

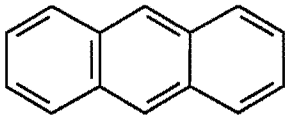

Anthracene

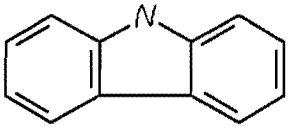

Carbazole

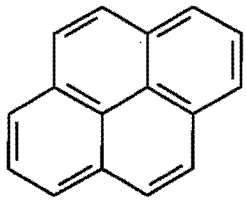

Pyrene

Figure 1. Structures of test chemicals used in the study.

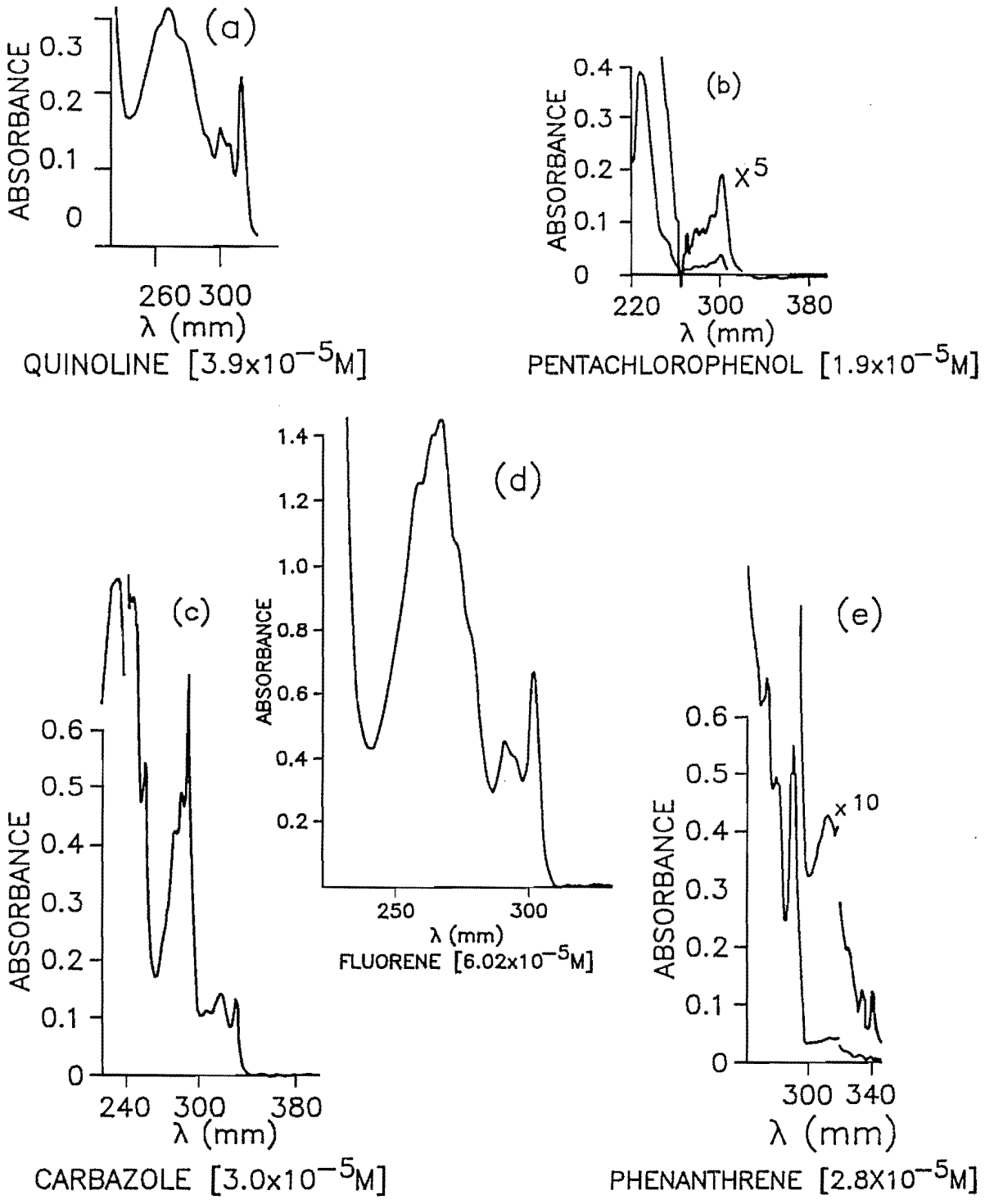

Figure 2. UV adsorption spectra for selected compounds in the study.

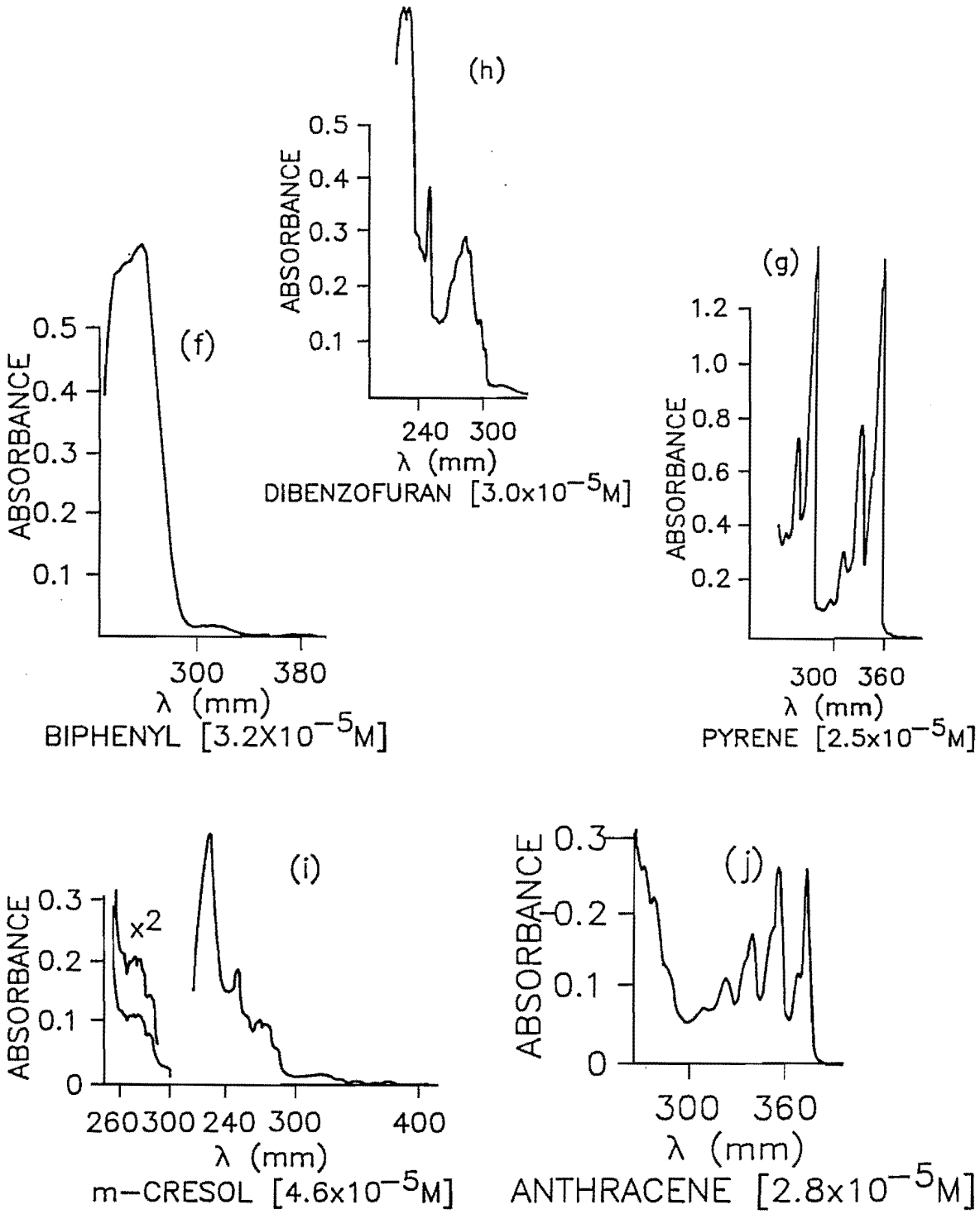

Figure 3. UV adsorption spectra for selected compounds in the study.

Table 3. Environmental fate assessment parameters

	log K_{ow} (1)	Water Solubility (mg/L, 298K)	Vapor Pressure (mm Hg, 298K)	log K_{oc}	Half-Lives (288-298K) (days)
Anthracene	4.45	7.10 E-1 (2)	6.00 E-6 (2)	4.42 (8)	17-260 (10,11)
Biphenyl	4.06	7.50 E+0 (3)	1.64 E-2 (5)	3.80 (9)	
Carbazole	3.51	1.50 E+1 (4)	1.25 E-6 (5)	3.28 (9)	
m-Cresol	1.98	2.59 E+4 (3)	4.85 E-1 (5)	1.35 (7)	
Dibenzofuran	4.12	5.23 E+0 (4)	1.74 E-3 (5)	3.85 (9)	
Fluorene	4.12	1.98 E+0 (3)	6.00 E-4 (2)	3.85 (8)	2-46 (11,12)
PCP	5.12	1.74 E+1 (3)	4.37 E-5 (5)	2.95 (8)	28 (13)
Phenanthrene	4.45	1.29 E+0 (3)	1.21 E-4 (2)	4.36 (8)	10-69 (10,14)
Pyrene	4.88	1.35 E-1 (3)	4.50 E-6 (2)	4.98 (8)	3-1900 (11,12)
Quinoline	2.02	6.00 E+3 (3)	9.12 E-3 (6)	2.76 (9)	

(1) Hansch and Leo (1979), (2) Wasik et al. (1983) (experimental), (3) Verschueren (1983), (4) Lyman et al. (1982), Equation 2-18, (5) Mackay et al. (1982), (6) Smith et al. (1978) (experimental), (7) Roy and Griffin (1985), (8) Kenaga and Goring (1980), (9) Lyman et al. (1982), Equation 4-9, (10) Sims (1986), (11) Coover (1987), (12) Sims and Overcash (1983), (13) Murphy et al. (1979), (14) Bulman et al. (1985)

One important component of creosote waste is anthracene. Anthracene is unique among the compounds selected in that it absorbs strongly in the near UV region, with an absorption maxima at 353 nm. A dilute solution of creosote waste in methylene chloride shows only the distinctive absorption spectrum of anthracene. Anthracene has a proven ability to act as a photosensitizer in aqueous systems (Mansnovi et al., 1984, Naeger 1985). It is suspected to be a potential photo-sensitizer for the degradation of other components in the experimental synthetic waste mixture.

Soil/Mineral Selection and Preparation

Test Soils. Three soils were selected which represent three climatic regions of the U.S. with diverse soil physical and chemical properties. These regions include: the arid west (Skumpah silty clay loam from Wendover, Utah), the humid south (McLaurin sandy loam from Wiggins, Mississippi), and the moderate climate zone of the southern Great Plains (Durant clay loam from Ada, Oklahoma). These soils were classified as: a fine silty, mixed, Typic mesic, Natrirgid; a course loamy, siliceous, thermic, Typic, Palendults; and a fine, montmorillonite, thermic, Vertic Agtigustolls, respectively. Bulk quantities of the soils were air dried and sieved mechanically through a 2 mm mesh sieve. The fraction of

the sieved soil passing a Number 60 USA Standard sieve was obtained by hand and stored under air dried conditions. In order to maintain a fairly uniform matrix, only this fraction was used for the photodegradation experiments.

Test Minerals. Because of the low organic content of the test soils (< 2.5 percent) and the role clay mineral surfaces play in soil surface reactions (hydrolysis, adsorption, ion exchange, etc.) pure mineral studies were conducted to more fully evaluate their effect on observed soil photolysis reactions. Based on the mineralogical composition of the test soils, the following pure minerals were evaluated in the study: kaolinite, two calcite samples, montmorillonite, and illite. Three of these minerals, kaolin (Twiggs Co., Georgia), illite bearing shale (Rochester, New York), and Na-montmorillonite (Spur Clay, Wyoming) were obtained from Ward Natural Science, Inc. Purecal U and Purecal T calcite samples were obtained from the Wyandotte Chemical Co. (Wyandotte, MI). The calcite samples required no further processing.

The clay minerals were purified and the less than 2 μm fraction was collected using the procedure of Jackson (1956). Prior to dispersion of the clay suspension, the minerals were treated with 2N sodium acetate solution, buffered to pH 5.0 for removal of carbonates; then they were treated with sodium citrate-sodium bicarbonate-sodium dithionite solution for the removal of Mn and Fe oxides. After this, the minerals were dispersed with a 2 percent sodium carbonate solution. The less than 2 μm fraction was removed from the bulk sample using continuous centrifugation with a feed rate of 217 mL/min and a rotational speed of 750 rpm.

The minerals were then saturated with either Ca or Al using 0.1M solutions of the respective Cl salts. The minerals were repeatedly rinsed with distilled water to remove excess Cl ion. Preparation of minerals in this fashion allowed for the evaluation of the saturating ion's effect upon the observed photolysis reaction rates within the model mineral systems. A schematic of the mineral preparation procedure is shown in Figure 4.

Silica Gel. Commercial silica gel (Aldrich Chemical, surface area = 507.5 m^2/g, pore volume = 0.75 cm^3/g, mean particle size range = 70 to 230 mesh) was utilized in all silica gel experiments. In all experiments, silica gel samples were pretreated by heating them at 500°C for 20 minutes.

Soil and Mineral Properties

Physical/Chemical Properties. The Soil, Water, and Plant Analysis Laboratory, Utah State University, determined the routine soil and mineral physical/chemical properties which are pertinent to photoreactivity evaluation using standard soil property measurement techniques (Page 1982, Klute 1986). The soil analyzed was the less than 60 mesh fraction. The results of these determinations are shown in Tables 4 and 5. A complete description of the physical/chemical properties of the soil for the less than 2 mm and the less than 60 mesh fractions are given in the Appendix.

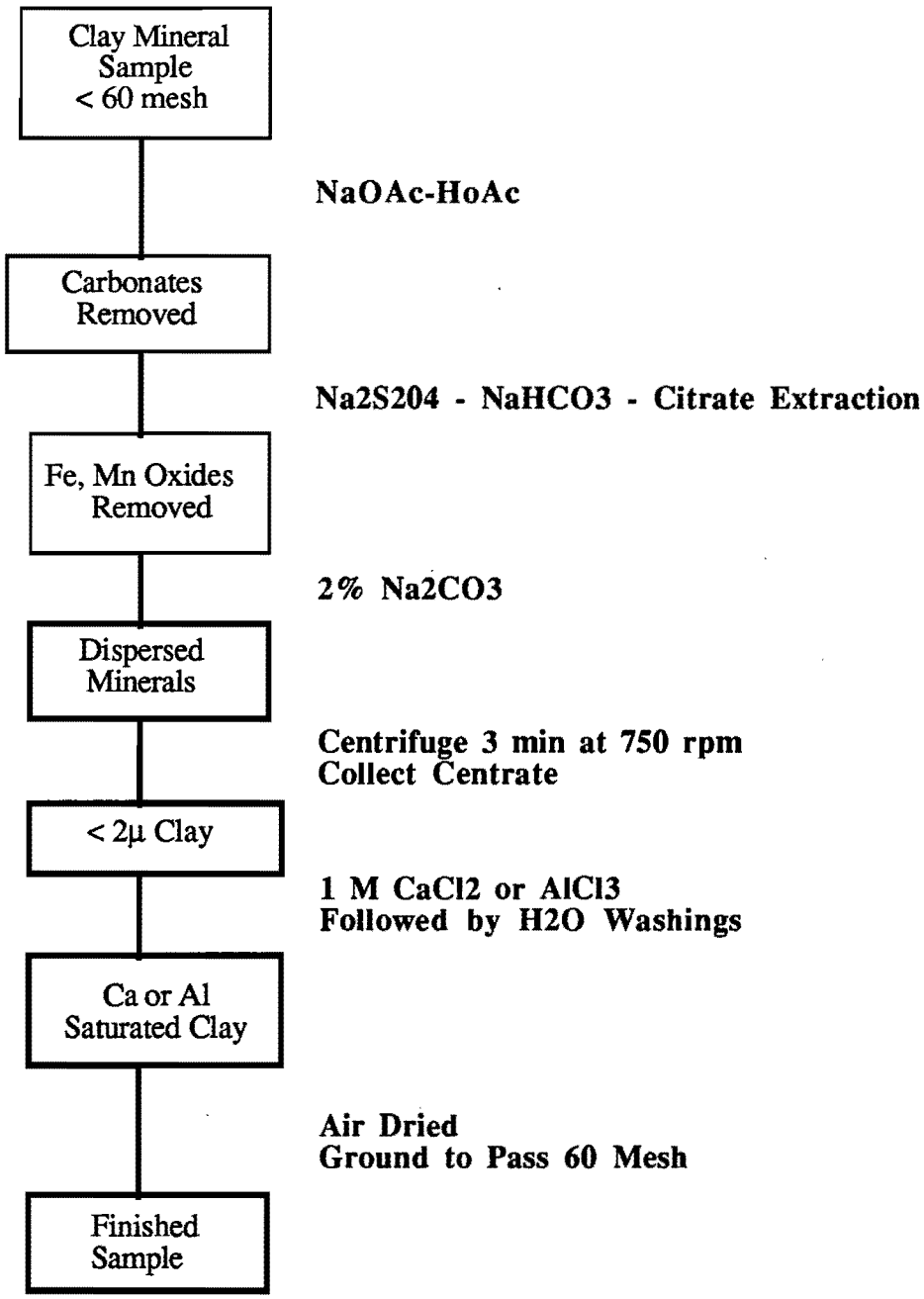

Figure 4. Mineral preparation procedures utilized in this study. After Jackson (1956).

Table 4. Physical properties of soils and minerals used in the study.

	Particle Size Distribution			Surface Area		Surface Charge
	Clay	Silt	Sand	Total	External	Density
	kg/kg	kg/kg	kg/kg	m^2/g	m^2/g	C/m^2
Ca Kaolinite				24.9	36.4	0.236
Al Kaolinite				23.1	29.5	0.263
Ca Montmorillonite				578.6	36.5	0.165
Al Montmorillonite				514.0	44.6	0.155
Ca Illite				120.6		0.162
Al Illite				86.9	52.9	0.184
Calcite (Pure Cal U)				13.6	13.6	
Calcite (Pure Cal T)				2.0	2.0	
Silica Gel				507.5	500.0	
Skumpah	0.32	0.52	0.16	57.2	13.4	0.210
McLaurin	0.08	0.41	0.51	4.8	2.7	0.793
Durant	0.3	0.46	0.24	128.3	33.9	0.194

	Relative Surface Reflectance at a Given Wavelength				Munsell
	300nm	350nm	400nm	500nm	Color Designation
Ca Kaolinite	41	53	66	74	
Al Kaolinite					
Ca Montmorillonite	21	35	48	62	
Al Montmorillonite					
Ca Illite	29	32	41	50	
Al Illite					
Calcite (Pure Cal U)	100+	100+	100+	100+	
Calcite (Pure Cal T)	100+	100+	100+	100+	
Silica Gel					
Skumpah	25	29	35	45	10YR7/2 (light grey)
McLaurin	15	17	21	30	10YR6/3 (pale brown)
Durant	20	21	24	29	10YR4/2 (dark greyish brown)

Table 5. Chemical properties of soils and minerals used in the study.

	Organic Carbon kg/kg	CEC cmol/kg	pH sat'd paste	Surface Acidity, Ho Unheated	Heated to 500°C
Ca Kaolinite	0.008	6.1	8.1	>+1.5	-3.0 to -8.2
Al Kaolinite	0.007	6.3	5.1	-3.0 to -8.2	-3.0 to -8.2
Ca Montmorillonite	0.003	98.9	8.0	>+1.5	+1.5 to -3.0
Al Montmorillonite	0.003	82.6	5.0	-3.0 to -8.2	-3.0 to -8.2
Ca Illite	0.005	20.3		>+1.5	+1.5 to -3.0
Al Illite	0.004	16.6	6.2	-3.0 to -8.2	-3.0 to -8.2
Calcite (Pure Ca U)			11.2	>+1.5	
Calcite (Pure Cal T)			11.2	>+1.5	
Silica Gel			6.4	>+1.5	>+1.5
Skumpah	0.007	12.5	8.3		
McLaurin	0.007	3.8	5.3		
Durant	0.022	24.9	6.8		

Total and external surface area of the soils and minerals were determined using the ethylene glycol monoethylether (EGME) retention method of Carter et al. (1986). External surface area measurements were based upon collapsing the mineral lattice structure following standard acid/hydrogen peroxide pre-treatment (this was accomplished by heating the sample at 500°C for 40 minutes prior to surface area determinations). Soils were pretreated, as per standard methods, with hydrochloric acid and 30% hydrogen peroxide. For most agricultural soils, this type of pretreatment does not significantly affect mineral properties of the soil. However, for the Skumpah soil, which contains approximately 20 percent carbonates (calcite and dolomite), this pretreatment significantly affects the measured surface area (Table A1, Appendix A).

Results from the non-treated sample are thought to be a more realistic measurement of the surface area for a calcite containing soil than that derived using standard pretreatment procedures because of the effect of pretreatment on Skumpah soil constituents. These non-treated values for Skumpah were used for all reaction calculations carried out in the study.

Korfmacher et al. (1980) and Behymer and Hites (1985) have shown internal surface reflectance and its macroscopic indicator, soil color, to have a significant effect on observed soil phase photolysis rates. Consequently, these data were quantified for the soils and minerals used by using diffuse reflectance spectroscopy and Munsell Soil Color designation, the results of which are indicated in Table 4. These color designations using standard Munsell Soil Color Charts (Kollmurgen Corp., Baltimore, MD) are based upon a qualitative comparison of sample color to standard color chips to provide a uniform color designation for soil samples.

Surface acidity for the minerals was measured using the Benesi's procedure (1956) to indicate relative surface pH and potential surface reactivity. In this procedure, surface acidity is measured by observing the color of the adsorbed form of selected indicators which have a range of pKa values. The subset of indicators presented by Benesi (1956) which was used in the study included: benzeneazodiphenylamine (pKa = +1.5), dicinnamalacetone (pKa = -3.0), and anthraquinone (pKa = - 8.2). Results indicate that the surface acidity of calcium saturated minerals, the calcites, and silica gel are greater than +1.5; whereas, the acidity of the aluminum saturated minerals is -3.0 to -8.2. Drying the minerals at 500°C for 40 minutes increased the acidity of the surfaces of the calcium saturated minerals.

Soil Mineralogy. Random powder mounts were used for bulk mineralogical analysis of the three test soils. The general procedure entails the grinding of 1 to 2 g of air-dried sample with a ceramic mortar and pestle to pass a No. 140 sieve. The sample was then mounted on a glass slide using a thin layer of vaseline as an adherent. X-ray diffraction was conducted on this sample over a range of 2 to 60 degrees two-theta.

Oriented clay mounts were used for specific clay mineralogical analyses. In these clay mount procedures, 50 g of air-dried soil were mixed with 50 mL of calgon solution (≈0.5 N with respect to sodium) and dispersed by mixing in a Warring blender on low speed for 5 minutes. The suspension was then transferred to a settling tube and brought to 1 L volume with deionized water. The soil suspensions were allowed to equilibrate at room

temperature (≈ 25°C) for 36 hours. After temperature equilibration, soil suspensions were agitated in the settling tubes with a stainless steel plunger to resuspend the sediment. Seven and one half hours after agitation, the upper 10 cm of the suspension (particles less than 2 μm diameter) were siphoned out of the settling tube into a 500 mL flask. Two mL of this clay suspension were then mounted on a glass slide and allowed to dry overnight.

To determine mineralogy of the clay fraction, each soil suspension sample was scanned as follows:

1. One run on air-dried samples from 2 to 30 degrees two-theta.

2. One run after glycerol solvation (2 hours at 60°C) of the air-dried sample from 2 to 13 degrees two-theta.

3. One run after heating the glycerol solvated air-dried sample to 500°C for 1 hour from 2 to 13 degrees two-theta.

A Siemans X-ray generator was used to generate X-rays using a Cu target with a Ni filter. X-rays were generated at 35 kV, 16 milliampres and 2,000 counts per second. System operating conditions included a baseline = 2.8, a signal width = 4.52, and a scan rate = 2 degrees two-theta per minute. Analysis of X-ray diffraction peaks and interpretation of diffraction patterns to determine mineralogy were aided by and based on procedures detailed in Jackson (1956), Carrol (1970), and Stakey et al. (1984).

Results of the X-ray diffraction data collected from the oriented clay mounts used for identifying specific clay mineralogy are presented in Table 6. The diffraction pattern obtained from the Skumpah soil suggested a mineralogy of allophane or imogolite, both of which are amorphous to X-rays. Being amorphous to X-rays suggests that the discrete clay particles exist at sizes smaller than an X-ray can detect, or that the particles do not exhibit a long range ordered atomic arrangement. Optical inspection of the Skumpah soil (bulk sample) with a petrographic microscope revealed the presence of cryptocrystalline quartz and rhombs of calcite.

The infrared spectra of the three soils were collected using both pressed KBr pellet and photoacoustic spectroscopy (Figures 5 to 7). There were no measurable differences in the qualitative nature of the spectra obtained between these methods. The McLaurin soil shows a great deal of definition in the region from 3,600 to 3,700 cm^{-1} which indicates the presence of kaolinite. The other two soils show only a strong maximum in this region likely due to a high level of metallic cations, particularly calcium. The spectrum for the Durant soil indicates the presence of montmorillonite (bands at 3620, 1640, 1040, and 1010 cm^{-1}).

Table 6. X-ray diffraction mineralogical analysis of the test soils.

Soil	Bulk Mineralogy	Clay Mineralogy
McLaurin	quartz	Vermiculite and possibly some kaolinite
Durant	quartz	Smectite-illite randomly interstratified, and kaolinite
Skumpah	quartz, calcite dolomite	Traces of illite, kaolinite, calcite and dolomite; pattern suggests clay material to be amorphous to X-rays

Throughout the spectrum from 3000 to 500 cm^{-1}, the McLaurin and Durant soils are similar and indicate a typical soil structure. The characteristic absorption bands for quartz at 800 and 780 cm^{-1} are apparent in these soils. The bands at 910 cm^{-1} may indicate dioctrahedral composition for the 2:1 layer silicate or may be due, in part, to kaolinite. The peaks at 870 and 712 cm^{-1} in the Skumpah soil indicate the presence of calcite and dolomite. Several very sharp peaks at 2520 and 1790 cm^{-1} also were observed in the Skumpah soil sample. These peaks are not typical for soils and were not definitely identified in the study.

Experimental Methods

Spiking Procedure. Two spiking procedures were used. The first for initial soil studies using large photoreactors (20mm x 150mm), and the second for all mineral studies and soil studies using small photoreactors (15mm x 50mm).

Large Photoreactor Spiking Procedures. A spike solution was prepared by adding the test compounds to methylene chloride to yield a 2500 mg/L solution of each compound. The test compounds were anthracene, fluorene, cresol, carbazole, quinoline, biphenyl, dibenzofuran, phenanthrene, PCP, and pyrene. Batches of soil were prepared for incubation in 1 L beakers. Sufficient spike solution was added to the soil samples to achieve a concentration of 500 mg/kg soil of each test compound, and additional methylene chloride was added to produce a stirrable slurry. The solvent was allowed to evaporate (≈3 to 4 hours at room temperature) under a hood in the dark. The soil was stirred occasionally with a stainless steel stirring rod. After solvent evaporation, soils were weighed in 40 g aliquot into 20 mm x 150 mm Pyrex® petri dishes, and were spread to form a 2 to 3 mm

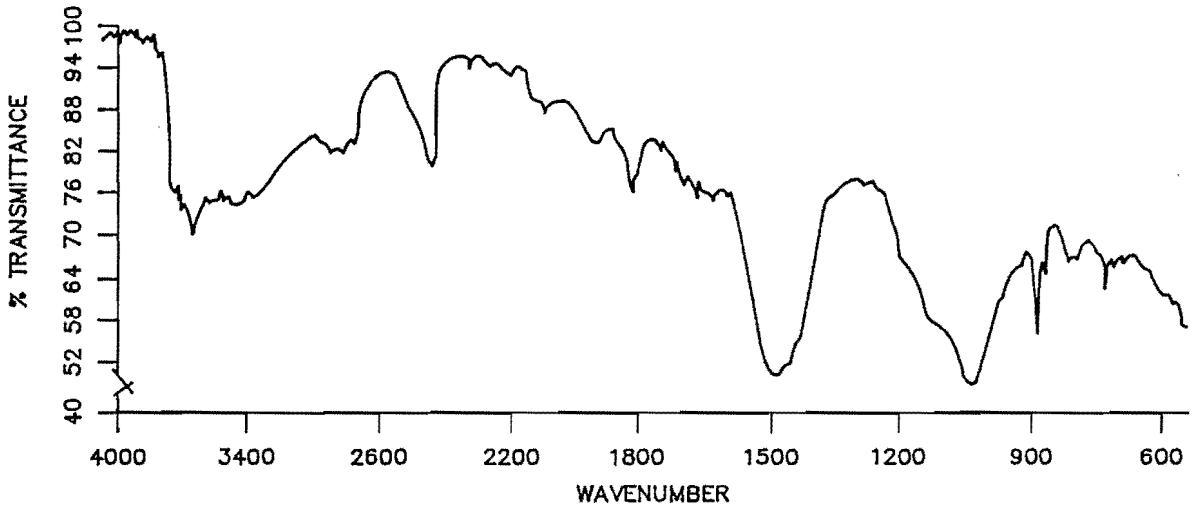

Figure 5. IR absorbance spectra of Skumpah soil, no treatment.

Figure 6. IR absorbance spectra of McLaurin soil, no treatment.

Figure 7. IR absorbance spectra of Durant soil, no treatment.

continuous layer in each dish. Triplicate dishes (40 g soil) of each test sample were extracted immediately, without irradiation, to determine initial compound soil concentrations and soil specific compound recovery efficiencies. Sample dishes were covered with 2 mm thick Pyrex® lids and were placed under lights or in the dark for specified time periods.

Small Photoreactor Spiking Procedures. Spiking solutions were prepared by adding the test compound to methylene chloride so that the solution contained 1000 mg/L of each compound. Three different mixtures of chemical were used: the ten compound mixture used in the large photoreactor study; a seven compound mixture containing the same compounds with the exception of dibenzofuran, PCP, and carbazole; and anthracene alone. Batches of minerals and soils were prepared for incubation in 20mm x 150mm petri dishes (Pyrex®, Corning Glass Works). Sufficient spike solution was added to the mineral samples to achieve a concentration of either 500 or 1000 mg/g of each compound. Additional methylene chloride was added to produce a stirrable slurry. The solvent was allowed to evaporate (≈3 to 4 hours) in the dark at room temperature. After solvent evaporation, 1 g of each mineral or soil was weighed into 15 mm x 50 mm Kimax® petri dishes and the samples were spread to form a 0.5 to 1 mm layer. Triplicate dishes were

extracted immediately, without irradiation, to determine the initial compound concentrations and mineral/soil specific compound recovery results. The petri dishes were covered with 2mm thick Kimax® lids and placed under light or in the dark for specified time periods. These procedures were used for all mineral and silica gel studies and for the seven compound soil studies.

Soil/Mineral Amendments

Soil amendments were selected based upon their known photochemical properties in other systems and upon their potential for large scale application to in situ soil decontamination or to waste treatment site remediation. Relative costs were not considered in this "proof-of-concept" investigation. Table 7 shows the soil/amendment combinations evaluated for their effect on photoreactivity.

Table 7. Soil/mineral/amendment combinations evaluated during the study.

	Amendment					
Soil/ Mineral	None	Organic Dye	Hydrogen Peroxide	Peat Moss	Diethyl-amine	Silica Gel
McLaurin	X	X	X	X		
Durant	X	X	X		X	
Skumpah	X	X		X	X	X
Ca Kaolinite						X

Organic Dyes. Riboflavin and methylene blue are organic dyes with bright visible colors and absorption maxima in the visible region (maxima at 440 nm and 370 nm, log extinction coefficient = 4.0, for riboflavin, and a broad maximum at 660 nm, log extinction coefficient = 4.8, for methylene blue, Figure 8). Both of these dyes have been shown to be effective sensitizers for the generation of singlet oxygen. Riboflavin was found to be most effective in a pH range from 3 to 8 (Fife and Moore 1979). The dyes were purchased from Sigma Chemical Company (Gibbstown, NJ) in commercial grade and used as received. Both dyes were added to the soils in a mass ratio of 0.1 mg dye/g soil. Methylene blue was found to be soluble in methylene chloride; thus, it was added to the

soil/spike solution slurry and dispersed by mixing the slurry during solvent evaporation. Riboflavin was insoluble in methylene chloride; consequently, an aqueous solution was prepared by the addition of 0.20 g riboflavin to 1.00 L water (4.18×10^{-4}M). This solution was added to the soil (0.5 mL/g soil), mixed, and allowed to air dry at room temperature for 24 hours. The riboflavin amended air dried soil was then ball milled to pass a 60 mesh sieve and was stored for later use.

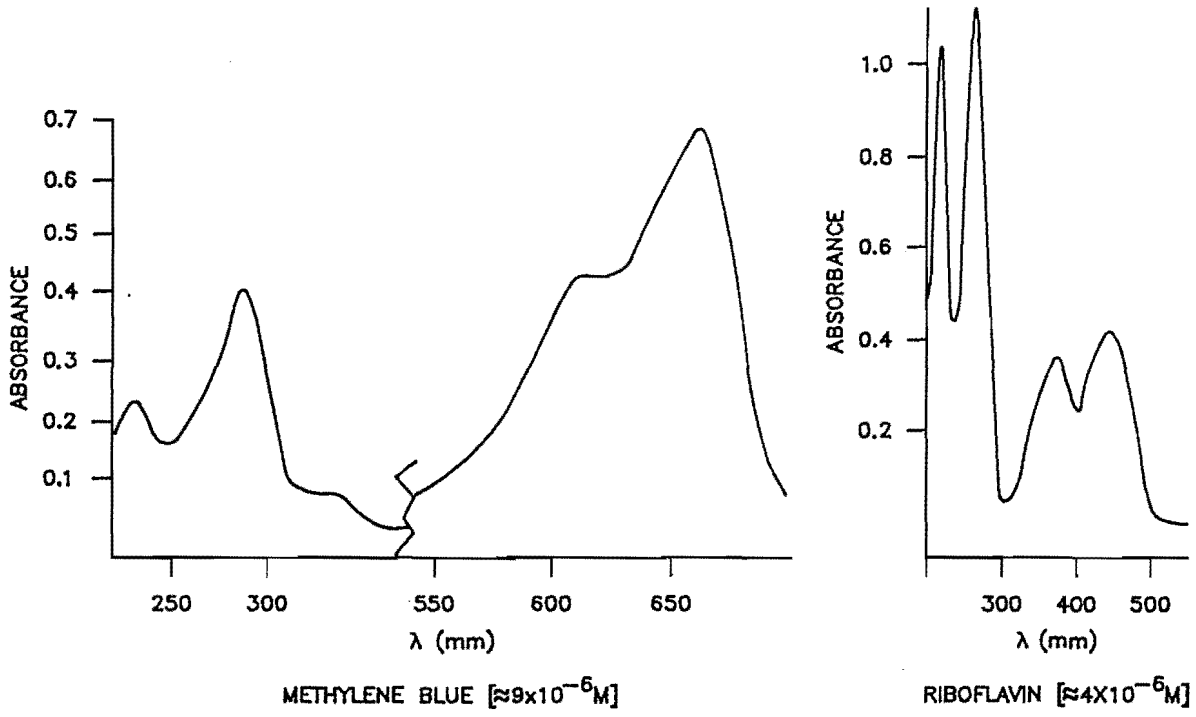

Figure 8. UV absorbance spectra for sensitizers used in the study.

Peat Moss. Gohre and Miller (1983) suggested that the organic content of soils under irradiation was responsible for the generation of small amounts of singlet oxygen and oxidizing radicals. The humic substances in natural waters have been identified as the source of photochemically generated hydrogen peroxide, which in turn produces reactive hydroxyl radicals (Cooper and Zika 1983). However, nonionic organic compounds in the soil systems are known to selectively partition into the organic content of soil (Lambert et al. 1965; Karickhoff 1979, 1981). In order to determine whether increased organic content would enhance photodegradation or if the selective partitioning would render the test compounds unavailable for photolysis, peat moss was added to test soils to artificially increase the soil organic carbon content. The peat moss was a commercial soil amendment from Fisons Western Corporation (Vancouver, B.C.). It was oven dried at 103°C for 24 hours; then it was ball milled and sieved to pass a Number 60 USA Standard sieve. It was stored at room temperature and was added to the soil in a mass ratio of 10 mg peat moss/g soil. The dry peat moss was added to the soil in small batches (less than 200 g of soil) and mixed by stirring. Further mixing occurred during the the compound spiking procedures.

Hydrogen Peroxide. Hydrogen peroxide has been identified as a photolytically generated intermediate in reactions in natural waters (Cooper and Zika 1983). Hydroxyl radicals can be formed through homolysis of the peroxygen bond of either hydrogen peroxide or organic peroxides which are formed by reactions of organic compounds with hydrogen peroxide. The hydroxyl radicals react with organic compounds to form oxidized products, with the overall reaction:

$$H_2O_2 + 2(R)H \rightarrow 2(R)OH + 2H \qquad (2)$$

where (R)H and (R)OH are the starting compound and oxidized product, respectively (Choudhry and Webster 1985). Though all of the results above were obtained in solution, hydrogen peroxide was selected for testing as a soil amendment to evaluate the potential increased generation of hydroxyl radicals in soil systems. A 30 percent hydrogen peroxide solution, obtained from EM Scientific (St. Louis, MO), was sprayed with a calibrated mister directly onto the prepared soil immediately prior to incubation. Each 40 g soil sample received 1.2 to 1.5 mL of the hydrogen peroxide solution. Samples were shaken lightly to disperse the wetter particles before placing them in irradiation or dark control chambers.

Diethylamine. The chemical properties exhibited by amines are highly dependent on the chemical environment. In solution, they can act as hydrogen donors or proton acceptors, depending on the pH of the solution. In photochemistry, they are known to act as hydrogen donors, and they can form charge transfer complexes which can stimulate photodecomposition reactions. Christensen and Weimer (1979) treated soil contaminated with polybrominated biphenyl waste with tertiary amines (1 percent by weight) and exposed the soil to sunlight for a period of four days. They found significant enhancement of photodegradation in the amine treated samples. Diethylamine was chosen for testing, and was applied to soils in methylene chloride solution prepared by dissolving 40.0 g of diethylamine (98% EM Scientific, St. Louis, MO) in 1.00 L methylene chloride. Diethylamine was added to the soil at a concentration of 10 mg/g soil (1 percent by weight).

Silica Gel. Silica gel is composed of silicon atoms tetrahedrally bonded to four oxygen atoms. When activated by high temperature, the surface moieties of silica gel consist of the slightly acidic silanol (Si-OH) group. These silanol groups extend outward from the surface of the silica gel and react with polar or unsaturated moieties by hydrogen bonding or dipole interactions. These hydroxyl surfaces represent highly reactive sites which have been shown by Yokley et al. (1986) and Dunston et al. (1989) to facilitate extensive photodegradation of pyrene (79 percent) and benzo(a)pyrene (93 percent) after only 24 hours of UV irradiation. Commercial grade silica gel was evaluated as a photodegradation media through the direct application and irradiation of the test compounds on activated silica gel as described above. To provide an approximate doubling of the external surface area available for sorption and reaction, silica gel was also evaluated as an amendment for photodegradation reaction enhancement on Skumpah soil and Ca Kaolinite.

Irradiation Chambers

Two banks of fluorescent tubes were used to simulate separate segments of the spectrum of natural sunlight over a large surface area with even intensity. Visible light was provided using Vitalite Full Spectrum 1500 tubes (Duro-test Corp, North Bergen, NJ), while light over a wide spectrum of the UV range was supplied by UVA-351 and UVB-313 tubes (The Q-Panel Company, Cleveland, OH). Light arrays contained 16 tubes on 6 cm centers. The tray supporting the sample dishes was positioned so that the tops of the dishes were 5 cm from the lights. Light intensity measurements were made with a wavelength specific, non-integrating spectroradiometer (Optronic Instruments, Model 742) which was computer calibrated against a hydrogen lamp standard emitting source. The lamp had been calibrated against a National Bureau of Standards light source. The detector for this device has a 1.25 cm aperture. This provided an intensity measurement every 2 nm across a selected range of wavelengths. The approximate integrated intensity of the radiation provided was 20 W/m^2. The emission spectra of the two light sources, as measured after attenuation through the Pyrex® and Kimax® petri dish covers, are compared to that of natural sunlight in Figure 9.

Figure 10 indicates the results of radiometer measurements taken for the UV reactor at the 5 cm irradiation distance. Results for the visible light reactor were similar. Analysis of the outer dimensions of the effective light area indicated a useable irradiation surface of 91.5 cm by 107 cm in the irradiation chambers, providing a total of 42 sample locations per irradiation chamber using the 150 mm petri dishes. Mean light energy was found to be approximately 20 W/m^2, with successive measurements at the same location yielding a reading of $\pm$ 2.5 W/m^2 and a variation of $\approx$ 12 percent. Total light intensity variation of $\approx$ 25 percent, as measured by the radiometer, was observed across the irradiated surface suggesting the need for the rotation of the reaction vessels at regular intervals to ensure uniform irradiation of all samples during each irradiation experiment.

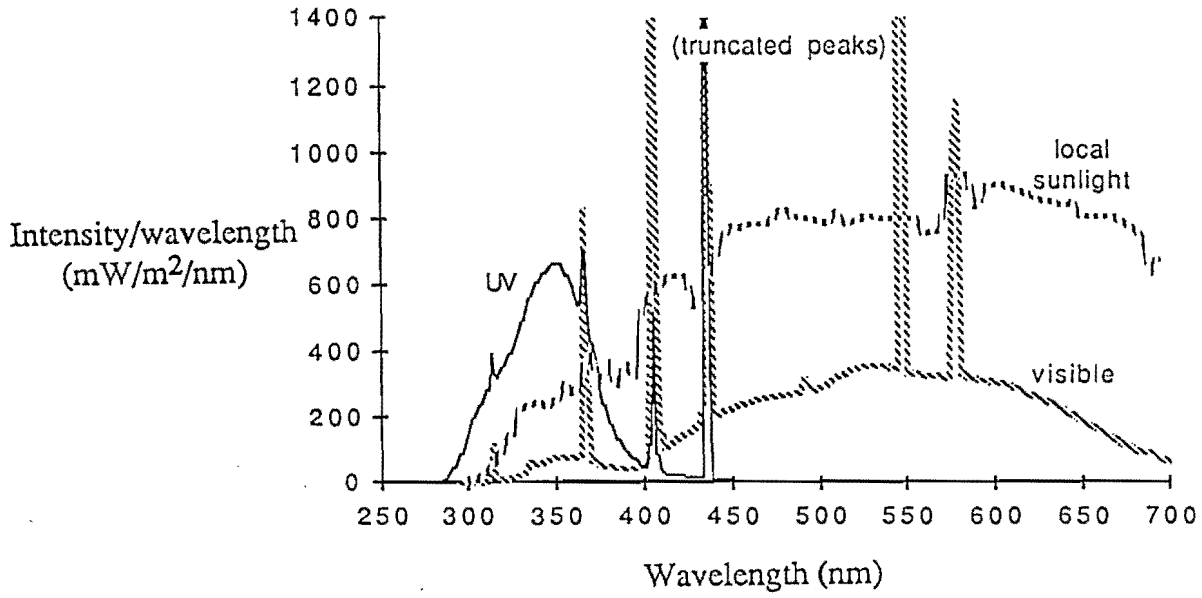

Figure 9. Attenuated irradiance spectra for lights used in UV and visible irradiation chambers compared with local sunlight. Attenuation provided by Pyrex® and Kimax® petri dish covers.

The uncooled irradiation chambers were operated for a continuous eight hour period, resulting in temperatures on the reactor vessel trays of 85°C for the visible and 45°C for the UV light arrays, respectively. Room temperature rose a net of over 10°C. With an ambient air temperature rise of such a magnitude it was determined that cooling of the irradiation chambers by air alone was not adequate.

To estimate the cooling requirements of the simulated solar reactor systems, the visible light array was selected as the limiting case for examining heat flux into the sample tray based on black body radiation calculations (Equation 3), assuming that the temperatures encountered after eight hours represented steady-state conditions. The surface of the lamp assembly had a temperature of 133°C, while the tray temperature was 85°C. Using Equation 3, the heat flux was calculated as:

$$E = \sigma\Delta T^4 = 5.669 \times 10^{-8} \times (406^4 - 358^4) = 612\ W/m^2 \qquad (3)$$

With an irradiation chamber surface area of approximately one square meter, the heat flux into the visible light tray was estimated to be approximately 612 W.

AXIS ACROSS LIGHT TABLE	AXIS ALONG LENGTH OF UV BULBS														
	1	2	3	4	5	6	7	8	9	10	11	12	13	14	15
1	21.5		25.0		22.5		25.5		24.5		24.0				20.0
2															
3	21.0	27.0													
4															
5	19.5		26.0												23.0
6															
7	18.0			23.5											
8															
9	18.5				21.5										
10															18.5
11	18.0					21.0									
12															
13	17.5						20.0								
14															
15	19.0							18.5							19.0
16															
17	18.5								17.5						
18															
19	17.0									17.0					
20															18.5

Figure 10. Radiometer measurements of the UV reactor light output 5 cm from the UV bulbs as a function of light bench location. Values are in W/m^2.

Water cooling was selected as the primary means of removing this heat from both chambers. A metal tray was constructed to fit into the bottom of the sample tray, and 9 m of 0.6 cm OD copper tubing were soldered to this metal tray. Tap water (≈11°C) was passed through the copper tubing at a flow rate of 17 L/mm, and the tray temperature was allowed to reach steady-state before any irradiation experiments were conducted. (With a water temperature increase of 5.5°C, the calculated heat flux was 654 W from the visible irradiation chamber.) The sample tray remained cool to the touch, between 15 and 20°C, and a sample reactor vessel containing water was found to be 35°C at the end of a 36 hour sampling period. Further chamber temperature reduction was provided by a fan and air ducting during the entire study.

Sample Maintenance & Handling

Large Photoreactor Studies. All irradiated and dark control soil samples were maintained during the irradiation period to simulate tilling and moisture management practices which might typically be employed at a soil remediation or land treatment site. On a daily basis, samples were agitated laterally to disturb the soil and to expose a new soil surface to light. Every third day the dishes were randomly rotated with respect to their positions under the light array to minimize inconsistencies in light exposure among samples. The samples were misted weekly, wetting each sample with 1.2 to 1.5 mL deionized water. On the second day following wetting, the soil was stirred with a stainless steel spatula to simulate tilling (all of the clumps formed by the wetting and drying of the soil were broken up). The insides of the dish tops were routinely wiped with moist cheesecloth to remove dust accumulation which might attenuate transmitted light. All of these activities were performed with minimal loss of soil dust from the dishes.

Dark controls were incorporated into the experimental design to allow for the determination of test compound loss from the treated soils due to soil irradiation. These controls were corrected for biological and/or other physical/chemical losses observed in the non-irradiated soils. These dark controls were incubated in light sealed boxes at the same ambient temperatures as the irradiated samples; they were wetted and mixed on a schedule identical to that of the irradiated samples to eliminate sample handling as a variable affecting compound photoreactivity.

Small Photoreactor Studies. Sample handling procedures were modified in the small photoreactor studies due to the rapid reaction rates observed for the compounds in these reactors. In all silica gel/anthracene alone experiments, sample dishes were shaken at 10 minute intervals during irradiation experiments. Sample dishes in the silica gel experiments using the test compound mixtures were shaken hourly. Every two hours the pure minerals were shaken for both the anthracene and the test compound mixtures. The McLaurin, Durant and Skumpah soils were shaken daily. Due to the short term nature of the small photoreactor experiments, no moisture management was employed in these studies. Dark controls were also included in all mineral studies.

Sample Extraction

Large Photoreactor Studies. Following irradiation, soil samples were extracted using a modification of USEPA Method 3510, "Separatory Funnel Liquid-Liquid Extraction" (USEPA 1986). Samples were transferred from the Petri dishes into 250 mL glass centrifuge bottles, and the soil was suspended in 75 mL distilled water. The suspension was then extracted for 30 s using a Tissumizer® mechanical/ sonic homogenizer (Tekmar, Cincinnati, OH) with a model SDT-1810 motor, SDT-1182EEN shaft and generator assembly, and TR-20 speed control. The solution pH was then adjusted to 12 by dropwise addition of 6 M NaOH. Fifty mL of pesticide grade methylene chloride was then added to the sample, and the sample was tissumized for an additional 30 s. The entire mixture was centrifuged at 1500 rpm for 15 minutes, and the centrate was decanted into a 250 mL separatory funnel. Extraction of the soil remaining in the centrifuge bottle was repeated twice with 75 mL volumes of methylene chloride. The organic and aqueous phases in the separatory funnel were allowed to separate. The entire organic phase was passed through a glass drying column containing 60 g of anhydrous sodium sulphate and collected in a 200 mL volumetric flask. The volume was brought up to 200 mL with methylene chloride added as necessary. The extract was mixed; an aliquot was transferred into a Teflon® lined, screw topped, glass vial and the sample was labeled as the base/neutral (B/N) extract and retained for analysis. The water phase remaining in the separatory funnel was then washed back into the centrifuge bottle and its pH was adjusted to 2 by dropwise addition of 6 M HCl. The extraction of this acidified sample was conducted as described above, and these samples were labeled as the acid (A) extracts.

Small Photoreactor Studies. Due to extensive mineral processing requirements and the time involved in this effort, only a small quantity of processed pure mineral (600 to 800 g) was available for experimentation. This required the development of procedures that employed small mineral samples, i.e., 1 g, for reaction, extraction, and quantification. The results of extraction and recovery efficiency studies using modified, mineral specific methods were evaluated in the study to validate the accuracy and reproducibility of these modified sample handling procedures. These data is described in the Results and Discussion section which follows.

The extraction of irradiated mineral samples was carried out using a short-term, shaking procedure followed by centrifugation and centrate filtration prior to GC and/or HPLC analyses. In this modified extraction procedure, 1 g mineral samples were transferred to 8 mL glass vials fitted with Teflon™ lined screw-tops; 8 mL pesticide grade methylene chloride were added to ensure that there was no headspace in the vial. The vials were then vigorously shaken by hand for 30 seconds before being centrifuged for 5 minutes at 2,800 rpm. The centrate was then stored at $\leq 4°C$ prior to analysis. When analyzed by HPLC, all samples were filtered through 0.2 µ HPLC syringe filters prior to injection to prevent contamination and clogging of the HPLC system with dispersed mineral. All procedures were carried out in subdued light, and samples were protected from room light to minimize photoreactions which take place in the extracting solvent prior to quantitative analysis.

Analytical Procedures

GC Analysis. GC analyses were performed on a Shimadzu (Kyoto, Japan) GC-9A Gas Chromatograph with a Shimadzu C-R3A Chromatopac electronic integrator and an AOC-9 Auto Injector. The column used for compound separation was a 30 m x 0.75 mm ID SPB-5 wide bore capillary column purchased from Supelco, Inc. (Bellefonte, PA). The column was operated at a nitrogen carrier flow rate of 8 mL/min with a detector make-up flow of 25 mL/min. The injection port was maintained at 250°C, while the oven temperature program was 5 min at 100°C, 5°C/min to 160°C, 15 min at 160°C, 5°C/min to 225°C and 5 min at 225°C. A hydrogen flame ionization detector (FID) was used for all quantitative determinations. Compounds were quantified by comparison of integrated peak areas to external standards.

Further chromatographic analysis to search for and identify degradation products was carried out using a Varian (Palo Alto, CA) 3400 gas chromatograph coupled with a Finnigan (San Jose, CA) MAT 700 ion trap mass spectrophotometer. The column used was a J & W Scientific (Rancho Cordova, CA) 30 m x 0.25 mm ID capillary column with DB-5 as the stationary phase. Helium was used as the carrier gas at a velocity of 34.0 cm/s. The injection port was maintained at 280°C, and GC operating conditions and temperature programming were identical to those used for GC/FID analyses described above. The ion trap operated with a scan range of 50 to 300 amu and a scan rate of one scan per second. A computer assisted library search using a 25,500 compound data base aided in the identification of compounds which were confirmed by matching their retention time with known standards.

Ultraviolet spectra of reagents used in the experiments were measured on a Carey (Palo Alto, CA) 219 scanning spectrophotometer using solutions of individual compounds at concentrations of approximately 10^{-5} M in methylene chloride. Soil and dish temperature measurements were made with a 0.75 mm diameter Fluke 51 K/J thermocouple thermometer (John Fluke Mfg. Co., Palatine, IL).

HPLC Analysis. All high performance liquid chromatographic (HPLC) analyses were performed on a Shimadzu (Kyoto, Japan) LC-6A equipped with a Shimadzu SPD-6A UV detector set at a wavelength of 254 nm. The column used was a 4.6 mm x 25 cm C-18 column (Supelcosil, LC-PAH, Supelco, Inc., Bellefonte, PA). Chromatography conditions were as follows: isocratic for four min with acetonitrile/water (40/60), linear gradient elution to 25 percent acetonitrile over 18 min, followed by a 5 min hold at 25 percent acetonitrile. The flow rate was 2 mL/min. Compounds and intermediate products were quantified by comparison of integrated peaks to peak responses from external standards.

NMR Analysis. A Varian XL-300 nuclear magnetic resonance (NMR) instrument was used for data collected in this study. All samples analyzed via NMR procedures were solvent exchanged by first evaporating the methylene chloride extract under a hood in subdued light. Deuterated chloroform was then used to re-dissolve the dried sample prior to proton NMR analyses. Proton NMR analyses were conducted on extracts from anthracene only studies to elucidate more clearly anthracene reaction mechanisms and

intermediate products formed. This method is particularly useful for the identification and quantification of reaction intermediates as it is sensitive to proton spin shifts in a molecule, resulting in all reaction products and intermediates having essentially the same detection sensitivity. The reactions observed for anthracene are unique in that the NMR peaks for each of the photoproducts are chemically shifted so that each can be identified and quantified independently even in a complex mixture of anthracene and all other intermediates.

RESULTS AND DISCUSSION

Methylene Chloride Effects

Because the test compounds were applied to soils in a methylene chloride solvent to ensure their adequate and uniform distribution within the soil reactors, questions were raised as to the effect of the solvent on soil properties. All physical/chemical properties of the three test soils were evaluated before and after solvent treatment. Solvent treated soil samples were generated by tumbling 500 g of soil with 200 mL methylene chloride for two hours in a rotary tumbler. Tumbled samples were removed after two hours and the methylene chloride was allowed to evaporate (≈ 15 minutes) before subsamples were collected for the various physical/chemical properties being determined. Standard property (pH, EC, % organic carbon, CEC and exchangeable cations) analyses were conducted to quantify the effects that the solvent treatment had upon soil properties important to compound distribution and photoreactivity in the soil systems. These data are summarized in Tables 1A through 3A in Appendix A. Solvent pretreatment had no significant effect on any chemical characteristic of the soils as shown in these tables; however, soil texture was modified slightly by some aggregation of soil particles, especially in the McLaurin soil. IR spectra were also measured for the three soils treated with methylene chloride, and no changes in these spectra were observed between the soils with and without methylene chloride amendment.

Extraction Efficiency Results

Tissumizer® Extraction Results. Extraction efficiency studies using the Tissumizer® apparatus were conducted to evaluate and optimize extraction procedures. Extractions of unamended spiked soils were conducted at varying spike concentrations between 1 and 1000 mg/kg soil. Based on ANOVA (Feldman et al. 1986) results at $\alpha = 0.05$, these experiments showed no consistent pattern of significant variation in recovery efficiency as a function of concentration, within the range of 10 to 1000 mg/kg soil. Efficiencies ranged from nearly 100 percent to 60 percent for the individual compounds, but the percentages were consistent for each compound over the concentration range studied. These measured extraction efficiencies allowed the accurate determination of 98 percent reduction in compound mass levels in the soils following the concentration of soil extracts. At a concentration of 1 mg/kg soil, however, the variability of results became unacceptably large. An analysis of method error indicated that this was due to a Kuderna-Danish concentration step added to the procedure at low soil concentrations levels. Concentration of extracts was not used for experimental quantification, and minor changes were made in the procedures for handling the samples during extraction. With extract concentration steps included, detection limits for this extraction and analysis procedure ranged from 0.5 mg/kg

soil for several compounds to 1.5 mg/kg soil for pentachlorophenol. Without concentration, the detection limits rose to a high of 50 mg/kg soil for pentachlorophenol and a low of 10 mg/kg soil for most other compounds. Under worst case conditions, these detection limits allowed the accurate determination of 90 percent reduction in soil concentration levels throughout the study.

Each time a soil was spiked during the course of the experiments, an aliquot of soil was extracted to quantify the efficiency and reproducibility of the extraction procedure. Extraction efficiencies were calculated for each treatment by comparison of the concentration of compounds in the extracts to the mass of the compounds spiked onto the soils. An analysis of variance was applied to these data using the Scheffé F test and the Fisher's Protected Least Significant Difference test at $\alpha = 0.05$. A two way ANOVA for soil type and treatment showed that treatment had no significant effect on extraction efficiency, while soil type showed a significant effect for all test compounds.

All data from the extraction of the 500 mg/kg samples were combined to compare extraction efficiencies among soils. Mean extraction efficiencies for each soil/compound combination are summarized in Table 8. ANOVA results showed that for all of the compounds, except quinoline and pentachlorophenol, recoveries from Durant soil were significantly different from both McLaurin and Skumpah soils. For quinoline, Durant soil yielded significantly lower recovery than Skumpah, while for pentachlorophenol, both Durant and Skumpah soils showed significantly lower recoveries than McLaurin soil. The trend in recovery efficiency for most compounds was: McLaurin $\approx$ Skumpah > Durant. It is believed that the low extraction efficiency from Durant soil was due to its "high" organic matter content. This is supported by the relationship shown between the sorption of organic solutes and the organic content of soils (Lambert 1967, Karickhoff et al. 1979, Karickhoff 1981).

Durant also showed much more variability in recovery data than the other two soils. This result supports an experimental observation made in the process of performing the extractions: when the Durant soil was combined with water and methylene chloride and homogenized, an emulsion formed which entrapped virtually all of the solid and liquid content of the extraction vessels. This emulsion was seen to a lesser degree with the other soils. Centrifugation, which was normally effective in breaking the emulsion with Skumpah and McLaurin samples, did not have a measurable effect on the Durant emulsion. Freedman and Cheung (1981) described a phenomenon of solvent absorption by soil organic matter, causing the organic matter to swell and form a gel of the type observed in the Durant soil.

Table 8. Extraction efficiencies and standard deviations for the test compounds on the test soils using Tissumizer® procedures, expressed as percentages. All data are for extractions at 500 mg/kg spike concentration.

	Skumpah		McLaurin		Durant	
Compound	Extraction Efficiency	Standard Deviation	Extraction Efficiency	Standard Deviation	Extraction Efficiency	Standard Deviation
Anthracene	89	7	92	8	77	18
Biphenyl	90	7	89	9	76	19
Carbazole	93	9	95	9	82	17
Cresol	57	10	71	9	65	11
Dibenzofuran	94	6	92	8	77	19
Fluorene	93	7	93	8	78	19
Pentachlorophenol	70	12	83	12	62	20
Phenanthrene	93	7	93	8	76	19
Pyrene	93	10	94	10	75	21
Quinoline	90	6	86	9	82	13
	Number of Measurements					
	n=22		n=25		n=25	

Manual Shaking Extraction Results. Table 9 shows the results of extraction efficiency data for anthracene (1000 mg/L) and anthraquinine (1000 mg/L) for the minerals using the hand shaking method. Both extraction study and t = 0 extraction test results are summarized in Table 9. Extraction efficiencies vary among minerals with the Ca- and Al-illite having relatively low percent recoveries. Anthraquinone recovery was greater than 80 percent from the kaolinite clays but was less than 60 percent for the two 2:1 clays. The recovery of anthraquinone after 8 hr incubation in the dark was similar to mineral extraction data at time zero, with the exception of Al-illite.

A long term extraction efficiency study of anthraquinone from Ca-montmorillonite was also conducted. After 96 hr, 51.4 ± 2.1 percent of the added anthraquinone was extracted compared with 59.2 ± 2.6 percent extracted at time zero. Extraction efficiency of anthraquinine and other photoproducts appears to decrease over time due to binding of these compounds with the mineral surfaces.

Table 9. Recovery efficiency results for anthracene and anthraquinone from test minerals using manual shaking procedure. Values presented are mean ± standard deviation.

Mineral/ Soil	Extraction Study Hand Shaking Compound	Co	% Recovery**	t = 0 hr Samples Hand Shaking Compound	Co	% Recovery**
Kaolinine						
Ca-	Anthracene	1000	70.6±9.5	Anthracene	1000	86.4±12.1
	Anthraquinone	1000	79.3±7.6	Anthracene	500	91.5±18.3
	Anthraquinone - 8 hr	1000	85*			
Al-	Anthracene	1000	71.7±11	Anthracene	1000	67.0±11.6
	Anthraquinone	1000	87.9±8.1			
	Anthraquinone - 8 hr	1000	86*			
Montmorillonite						
Ca-	Anthracene	1000	59*	Anthracene	1000	85.5±21.4
	Anthraquinone	1000	63*	Anthracene	500	99.2±7.2
	Anthraquinone - 8 hr	1000	62*			
Al-	Anthracene	1000	61*	Anthracene	1000	78.0±6.1
	Anthraquinone	1000	57*			
	Anthraquinone - 8 hr	1000	44*			
Illite						
Ca-	Anthracene	1000	47*	Anthracene	1000	54.4*
	Anthraquinone	1000	63*			
	Anthraquinone - 8 hr	1000	61*			
Al-	Anthracene	1000	47*	Anthracene	1000	78.4*
	Anthraquinone	1000	74*			
	Anthraquinone - 8 hr	1000	49*			
Calcite (SA=13)				Anthracene	1000	93.5±22.8
Calcite (SA=2)				Anthracene	1000	85.5*
Silica Gel						
	Anthracene	1000	72.1±6.4	Anthracene	1000	112±27.8
	Anthraquinone	1000	78.8±7.2			
	Anthraquinone - 8 hr	1000	68*	Anthracene	500	99.1±9.9

* = Mean of Duplicate Samples.
** = Mean of Triplicate Samples.

Table 10 lists results of extraction efficiency data for the minerals and soils for all test compounds added in the seven and ten compound mixtures at 500 or 1000 mg/kg. With the exception of cresol, recoveries were generally greater than 80 percent.

Table 10. Recovery efficiency results for 10 and 7 compound mixtures from minerals and soils using the manual shaking method. Values presented are mean ± standard deviation.

Mineral	Ca Kaolinite					Ca montmorillonite			
Mixture	10	10 w/ silica gel	10	7	7	10	10	7	7
Concentration mg/L	1000	1000	500	1000	500	1000	500	1000	500
Chemical									
Anthracene	91.5±13.7	80.3	105±14.6	99.3±9.2	90.1±8.5	103±16.9	116	102±9.2	105±12.9
Fluorene	87.6±15.0	72.8	95.7±11.5	90.9±10.0	80.0±7.6	101±14.4	111	101±10.5	98.52±15.6
Cresol	56.7±2.18	60.7	50.8±9.0	56.2±3.05	54.2±5.5	57.4±4.9	63.28±1.4	82.44±6.4	86.68±14.7
Biphenyl	80.3±20.1	61.1	91.8±12.4	77.4±15.1	65.6±16.5	99.7±12.9	112	102±10.4	101±13.5
Phenanthrene	7.5±10.8	77.1	93.9±11.2	92.2±7.5	84.2±4.8	97.4±14	107	101±10.3	101±13.9
Pyrene	91.0±12.6	77.6	98.87±12.1	96.2±10.1	87.0±5.2	102±15.1	110	90.86±9.8	89.45±19.8
Dibenzofuran	5.6±17.7	70.3	97.69±10.6			102±13.6	114		

Mineral	Silica Gel				Skumpah		Durant	McLaurin
Mixture	10	10	7	7	7	7 w/silica gel	7	7
Concentration mg/L	1000	500	1000	500	500	500	500	500
Chemical								
Anthracene	98.7±3.3	110±7.4	97.0±13.2	96.5±7.1	96.6±3.7	98.3±9.3	88.2±18.0	100±13.4
Fluorene	96.1±3.8	103±8.6	100±15.1	96.7.2	90.8±3.4	93.4±9.2	79.6±16.7	90.8±13.5
Cresol	36.6±12.0	32.5±10.4	49.2±15.5	42.8±11.7	80.3±3.9	83.8±3.6	72.4±9.2	64.9±7.2
Biphenyl	95.9±3.5	104±8.4	99.6±15.8	96.0±7.2	84.4±3.5	88.4±6.8	71.7±15.2	73.2±9.3
Phenanthrene	93.4±4.1	101±8.6	98.6±14.7	95.5±7.7	91.5±4.0	93.8±9.3	81.1±17.5	93.0±14.3
Pyrene	97.5±4.2	106±9.6	99.3±15.3	95.82±7.9	82.2±7.5	85.4±16.8	80.1±16.5	92.2±14.8
Dibenzofuran	98.0±4.9	106±10.6						

The manual shaking method used only methylene chloride in the extraction and thus may not be as effective of a method for removal of the more hydrophilic photoproducts from soil as is the acid/base-neutral Tissumizer® method. The extraction efficiency of the manual shaking method was evaluated for the three soils using two photoproducts, anthraquinone and fluorenone. Results, listed in Table 11, indicate that the shaking method was effective in extracting anthraquinone and fluorenone from both the McLaurin and Durant soils even after 216 hours incubation in light or in the dark. The extraction efficiency of these compounds, however, decreased after 216 hours for the Skumpah soil. Loss was observed in both light and dark incubated samples indicating that irreversible sorption of these compounds occurred over time. The greater loss in the light exposed samples in the Skumpah soil suggests that the two photoproducts may undergo further oxidation to unknown intermediates.

Table 11. Recovery efficiency results for anthraquinone and fluorenone from soils using the manual shaking procedure. Values presented are mean ± standard deviation.

Soil	Sampling Time (hr)	Experimental Condition	Anthraquinone % Recovery	Fluorenone % Recovery
Skumpah	0	-	101±3.5	113±4.4
	216	light	64.6±3.8	80.1±5.2
	216	dark	83.3±1.8	93.8±2.0
McLaurin	0	-	93.2±8.5	92.1±9.2
	216	light	90.2±17.2	72.8±15.8
	216	dark	88.1±5.8	87.8±1.4
Durant	0	-	98.7±3.9	97.7±3.5
	216	light	93.5±1.7	96.0±3.0
	216	dark	95.3±4.0	93.6±2.6

Kinetic Rate Evaluation-Dark Controls

Large Photoreactor Studies. The dark controls consistently showed a rapid initial loss in soil concentrations over time that appeared exponential up to 15 days, with virtually no change after that time for all compounds except cresol and biphenyl. First order loss of compounds such as pentachlorophenol (Murphy et al. 1979), anthracene (Sims 1982), and phenanthrene (Groenwegen and Stolp 1981) have been reported in soil experiments that

were not specifically investigating photoreactivity. Based upon this experimental precedent (and for mathematical convenience in adjustment of the irradiated loss data to account for loss in the dark controls), first order modeling was applied to all compounds in the control samples.

Incubation results for each of the compounds in the dark control samples were normalized by their initial concentrations, and the natural log of (C_t/C_o) was plotted versus time. The slopes of the lines determined from linear regression of the data yielded apparent first order loss rate constants for each compound/treatment combination. The data used to generate the apparent dark control rate constants were subjected to an ANOVA to examine the effects of soil type and amendment on loss of test compounds from the dark controls. This analysis showed that soil type was a universally significant factor in the determination of loss rates, while amendment had little effect on the loss of test compounds in the dark. Analysis of the data showed that for most compounds, first order modeling was adequate (statistically significant r at 95 percent confidence level for a linear model), with the observed loss significant at $\alpha = 0.05$. Table 12 gives the average apparent dark control first order rate constants which were statistically different from zero.

Table 12. Statistically significant apparent first order loss rate constants for the large photoreactor dark controls (1/day).

	Soil		
	Skumpah	McLaurin	Durant
	Amendment		
Compound	None, Peat Moss, Methylene Blue	None, Peat Moss, Peroxide Riboflavin	None Riboflavin, Peroxide
Anthracene	0.002	0.003	0.005
Biphenyl	0.008	0.017	0.006
Carbazole	-	0.004	-
m-Cresol	0.02	0.03	0.02
Dibenzofuran	0.002	0.006	-
Fluorene	0.002	0.004	-
Pentachlorophenol	-	-	0.006
Phenanthrene	0.001	0.002	0.001
Pyrene	-	0.004	-
Quinoline	0.002	0.008	0.002

Small Photoreactor Studies. Based upon results from the large photoreactor studies, dark controls were only sampled at the completion of the irradiation period for the small photoreactor studies. First order kinetics were also applied to these control sample results. Table 13 provides the average dark control apparent first order rate constants for these studies.

Table 13. Apparent loss rate constants for the dark controls for the small photoreactor studies (1/hr).

Mineral	Ca Kaolinite					Ca montmorillonite			
Mixture	10	10 w/ silica gel	10	7	7	10	10	7	7
Concentration mg/L	1000	1000	500	1000	500	1000	500	1000	500
Chemical									
Anthracene	0.0004	0.0007	*	0.0004	0.0006	0.0009	0.003	0.0007	0.001
Fluorene	0.0006	0.0002	*	0.0001	*	0.0004	0.002	*	0.0004
Cresol	0.001	0.0018	0.0002	0.0014	0.0009	0.0008	0.002	0.0007	0.002
Biphenyl	0.001	0.0003	*	0.001	0.0001	0.0004	0.002	*	0.0004
Phenanthrene	0.0004	0.0001	*	0.0008	*	0.0005	0.002	*	0.0004
Pyrene	0.0005	*	*	0.0009	*	0.0005	0.002	*	*
Dibenzofuran	0.0005	0.0007	*			0.0003	0.002		

Mineral	Silica Gel				Skumpah		Durant	McLaurin
Mixture	10	10	7	7	7	7 w/silica gel	7	7
Concentration mg/L	1000	500	1000	500	500	500	500	500
Chemical								
Anthracene	0.0039	0.0035	0.0005	0.0014	0.0001	*	0.002	0.002
Fluorene	0.0047	0.0024	0.0004	0.0011	0.001	*	0.001	0.002
Cresol	0.0113	*	0.001	0.0044	0.001	0.001	0.003	0.002
Biphenyl	0.0037	0.0035	0.0006	0.0015	0.001	*	0.002	0.005
Phenanthrene	0.0045	0.0025	0.0005	0.0011	0.001	*	0.001	0.002
Pyrene	0.0044	0.0027	0.0005	0.0014	0.001	*	0.002	0.002
Dibenzofuran	0.004	0.0006						

* No loss observed in the dark controls

Significance of Dark Control Losses

The loss of test compounds in the dark controls must be explained in order to assert that experimental methods were effective in isolating photodegradation as the cause of compound loss in the irradiated samples. Loss of test compounds in the dark can be accounted for through destructive and/or non-destructive mechanisms. Destructive mechanisms are those which chemically alter the compound, while non-destructive mechanisms by processes such as transport or immobilization render the unaltered compound unavailable for analysis. Biodegradation is a destructive mechanism, and its effects on creosote waste constituents have been studied by several investigators (McKenna and Heath 1976, Groenewegen and Stolp 1981, and Bulman et al. 1985). No chemical or physical soil sterilization techniques were used to control biodegradation in this study because of their potential for altering soil and mineral structure and photoreactivity.

Immobilization in the soils and minerals was a possible mechanism for non-destructive loss. In work done with the extraction of anthracene, pyrene, and phenanthrene from sediments, it was found that the extractability of these compounds decreased in proportion to the length of time between spike and extraction (Haddock et al. 1983). Use of radioactive C^{14} labeled anthracene confirmed the mass balance between the extract and sediment and ruled out volatilization as a source of apparent loss. This intractable adsorption onto soil has been related to soil composition, specifically to the percentage of clays and organic matter in a soil (Karickhoff et al. 1979, Karickhoff, 1981). Karickhoff et al. (1979) suggested that the increase of inextractability with time is related to diffusive transport of the organic compound into sediment particles, or movement into interclay lattices.

Volatilization of organic chemicals is another non-destructive loss mechanism possible in these experiments. While volatilization was not quantitatively determined, parameters were estimated to allow a comparison of volatilization potential among the test compounds. Estimates of the relative potential for each compound's volatilization were made based upon the method described by Swann et al. (1983) using the relationship described by Equation 4.

$$\text{Volatilization Potential} \equiv \frac{V_p}{(WS) \cdot K_{oc}} \tag{4}$$

In Equation 4, Vp is the vapor pressure of the compound in mm Hg, WS in the water solubility in mg/L, and K_{oc} is the soil organic carbon partition coefficient.

This estimation is based on the assumption that the test compounds in the soil matrix partition into the organic fraction of the soil. While this assumption is believed to be valid for highly hydrophobic aromatic molecules, it may not hold for ionizable molecules with significant water solubilities or for sorption of chemicals by clay minerals. These molecules can bind strongly to mineral surfaces of the soil by mechanisms suggested by Karickhoff, 1981). This interaction with soil clay minerals should render the bound

molecules much less susceptible to volatilization. For those experiments where ionizable compounds, including cresol, pentachlorophenol and carbazole, were used, Equation 4 provides a worst case estimate of volatilization potential.

Input parameters for Equation 4 are listed in Table 3, while the results of the relative volatilization parameter calculations for the test compounds are shown in Table 14. These values predict that the volatilization potential for cresol is greater than that of any of the other test compounds. Biphenyl is second in volatility, with a calculated volatilization parameter that is one to four orders of magnitude larger than that of the remaining compounds. This is consistent with the results of the dark controls which displayed high loss rates for cresol and biphenyl. The fact that the highest losses of these two compounds were observed with the McLaurin soil, the soil with the lowest surface area, is consistent with the relationship between the limited binding of compounds to these surfaces and volatilization potential.

Table 14. Estimation of volatilization potential at 298K (Swan et al. 1983). Values are normalized to yield a carbazole volatilization potential = 1.

Compound	Volatilization Potential ($\times 2.5 \times 10^{-10}$)
Anthracene	8
Biphenyl	8,644
Carbazole	1
m-Cresol	20,895
Dibenzofuran	1,176
Fluorene	1,070
Pentachlorophenol	70
Phenanthrene	102
Pyrene	9
Quinoline	66

Dark loss of the test compounds was greater from the silica gel surface than from the minerals (Table 13). Silica gel had the highest surface area of all test materials. The dark loss rates from silica gel may be due to the nonextractability of chemicals binding with this surface, or other chemical reaction mechanisms which occurred in the dark on this highly reactive surface. Loss of test compounds from all minerals was similar.

The potential for volatilization is directly related to temperature of the matrix from which volatilization is taking place. Though measures were taken to maintain both control and irradiated samples under identical environmental conditions, the radiant heat energy from the different light sources produced temperature differences among the samples. The

high power output visible lights resulted in a much higher temperature being produced in the visible chamber compared to the UV chamber. The cooling system lowered the average temperature of the soil samples in the visible light chamber to room (control) temperature; however, a temperature gradient was observed within the soil samples. This gradient, measured in the Durant soil under visible light, is illustrated in Figure 11. Control samples were maintained at a uniform temperature of 299 to 300°K, while the samples under UV light also a showed slight temperature gradient with mean temperatures ranging from 296 to 297°K. This temperature gradient and the presence of an elevated temperature in a thin layer at the top of the soil had the potential to cause volatilization in the irradiated samples; however, this was not accounted for in the controls.

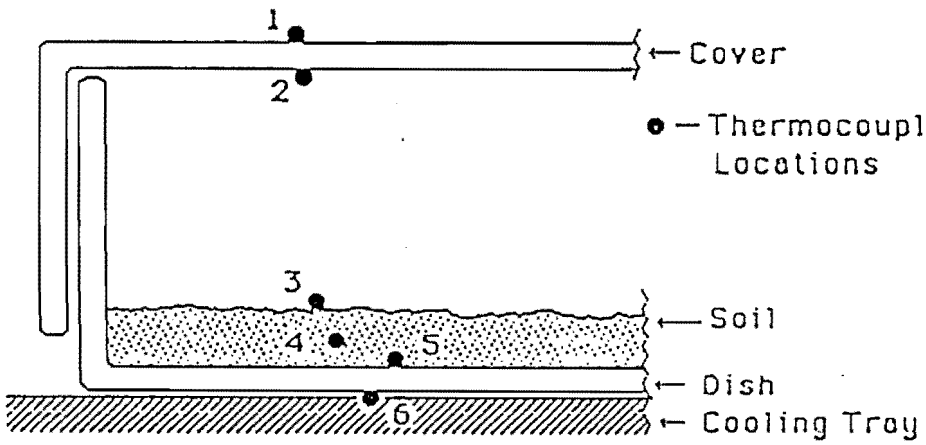

Temp (°K)	Location Number
316.3	1
314.1	2
304.0	3
302.9	4
298.6	5
293.8	6

Figure 11. Temperature profile observed in Durant soil sample under visible light (±0.3K).

A final source of non-destructive loss in these experiments is the physical loss of material. In the course of handling the soil in the irradiation reactors, a very fine dust inevitably resulted, which could be lost due to the high velocity air convection encountered in the laboratory hoods. This loss was quantified by subjecting soil/mineral blanks to the same handling procedures as the actual sample dishes, but on an accelerated schedule. With the equivalent of 50 days of sample maintenance, the mean loss of mass in these blanks was not significant compared to other analytical variation observed in the study. Since this loss was also present in the dark controls, the dark controls were assumed to adequately account for this type of non-photodegradation loss observed in the irradiated samples.

Kinetic Rate Evaluation--Irradiated Samples

Plots of compound concentrations from irradiated soil/mineral samples versus time were clearly exponential, especially for those compounds which showed the highest photoreactivity. Experimental evidence for first order photolysis on soils has been provided by Gohre and Miller (1983) who found that degradation of 2,5-dimethylfuran by photolysis on soil was adequately described by first order kinetics. In support of the use of first order modeling for soil photolysis, the following derivation is provided.

If the organic compounds of interest can be modeled as an optically thin layer on solid soil particles, their absorption of incident light can be approximated by an application of Beer's Law:

$$A = \varepsilon l [B] \tag{6}$$

where absorption A is equal to the extinction coefficient, ε (which is normally expressed as a base 10 logarithm) times the path length, l, and the concentration of the adsorbent, [B]. The proportion of incident light, I_o, adsorbed by the organic compound, I_a, is given by:

$$I_a = I_o (1 - e^{-2.3 \varepsilon l [B]}) \tag{7}$$

For small x, $(1-e^{-x}) \approx x$, which allows Equation 7 to be rewritten as:

$$I_a = I_o (2.3 \varepsilon l [B]) \tag{8}$$

If a direct photooxidation mechanism is assumed for the adsorbed organic molecule as shown in Equations 9, 10, and 11, the kinetic expression for the concentration of excited organic molecule [B*] can be written as shown in Equation 12:

$$B + h\upsilon \rightarrow B^* \tag{9}$$

$$B^* + O_2 \xrightarrow{k_1} BO_2 \tag{10}$$

$$B^* \xrightarrow{k_2} B + \text{energy (deactivation)} \tag{11}$$

$$\frac{d[B^*]}{dt} = I_a - [B^*] (k_1 [O_2] + k_2) \tag{12}$$

If the steady-state assumption is applied to the intermediate, B*, the concentration of B* is given by:

$$[B^*]_{ss} = \frac{I_a}{(k_1 [O_2] + k_2)} \tag{13}$$

This can be used to solve the kinetic expression for the change in concentration of the absorbent molecule with time, d[B]/dt:

$$\frac{-d[B]}{dt} = k_1 [B^*]_{ss} [O_2] \tag{14}$$

$$\frac{-d[B]}{dt} = \frac{I_a k_1 [O_2]}{(k_1 [O_2] + k_2)} \tag{15}$$

If $k_1 [O_2] << k_2$, then substitution for I_a from Equation 8 yields:

$$\frac{-d[B]}{dt} = \frac{I_o (2.3 \varepsilon l [B]) k_1 [O_2]}{k_2} \tag{16}$$

Equations 14 and 15 show that the change in B with time should be first order with respect to the concentration of B, and mixed order with respect to the concentration of O_2. If deactivation is an important process in the chemical reaction, the kinetics should be first order with respect both to absorber B and oxygen concentration, as shown in Equation 16.

It would not be appropriate to assert that all of the loss seen in the irradiated samples can be attributed to photodegradation; therefore, a correction must be applied to the photodegradation data whenever there is significant loss in the corresponding dark control samples. For those samples which demonstrated significant first order loss in the dark, the following expression describes the first order change in concentration of the test compounds:

$$C_{dark} = C_o e^{-(k_{dark})t} \quad (17)$$

In this expression, k_{dark} is the rate constant for dark control loss as reported in Tables 12 and 13. Assuming that first order modeling is appropriate for the results of the irradiation experiments, and that the loss in the irradiation experiments is due to the sum of the effects of mechanisms operating in the dark and to photochemical mechanisms, the following expression can be written for the concentration of test compounds in the irradiated samples:

$$C_{light} = C_o e^{-(k_{dark} + k_{photo})t} \quad (18)$$

where k_{photo} represents the pseudo first order photolysis rate constant for a particular compound under particular experimental conditions. Taking the natural logarithm of Equation 18 and substituting from Equation 17 yields an expression which can be used to solve for k_{photo} by comparison of dark control and irradiated data:

$$\ln\frac{C_{light}}{C_{dark}} = -(k_{photo})t \quad (19)$$

This rate constant is corrected for the loss observed in the dark and represents the direct contribution of photodegradation to the observed loss of the test compound in the soil/mineral systems. Equations 18 and 19 are equivalent expressions for correcting the photodegradation rate constant for the dark reaction. Equation 19 was used for all calculations. For those soil/amendment/compound combinations which did not show significant loss in the dark controls, Equation 18 applies, with $k_{dark} = 0$.

Figure 12 is a plot of typical dark control and irradiated sample data for anthracene, a compound which showed significant loss in the dark controls. The data used in the plot of the results in Figure 12 were corrected as described in Equation 19. For the more reactive surfaces, the linear relationship breaks down over time. The validity of applying first order kinetics over the entire time period of irradiation depends on there being no competition for light absorption by the photoproducts generated. The linear relationship could be expected to hold for no more than two half lives of the compound due to photoproduct interference, consequently, only the linear portion of the first order plots was used to calculate these k_{photo} values. Figure 13 displays this breakdown in linearity of first order kinetics with time for anthracene on silica gel.

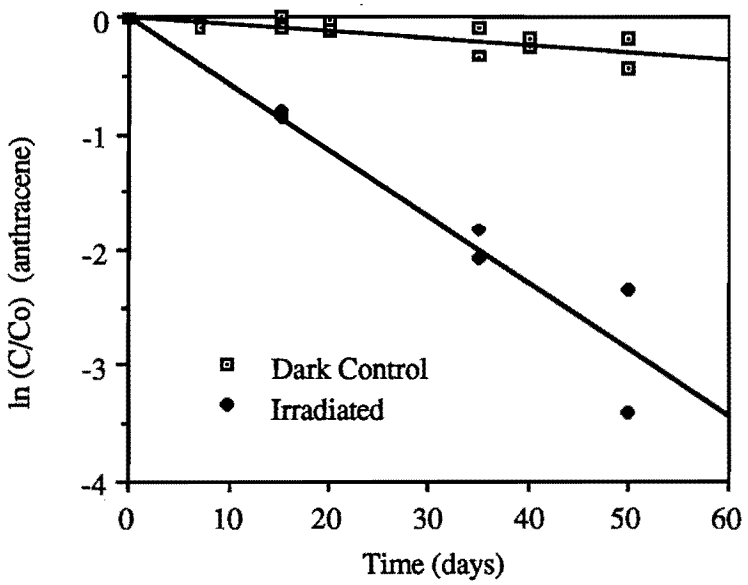

Figure 12. First order plot of the dark control and visible irradiation data for anthracene on McLaurin soil.

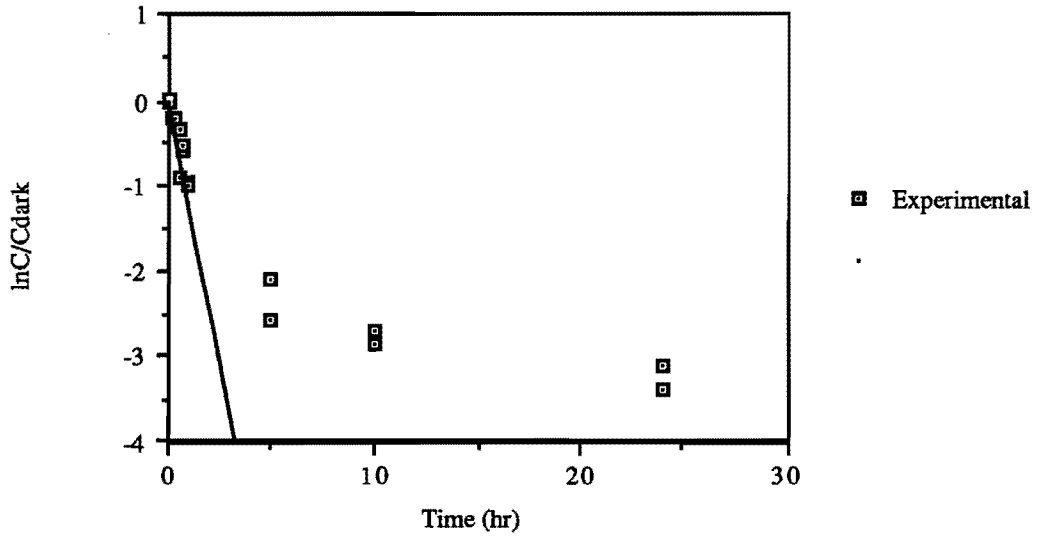

Figure 13. First order plot of anthracene on silica gel.

Theoretically, the regression lines should go through the origin at (0,0) since ln C_t/C_o must equal zero at time zero. The equation for a regression line with the intercept equally zero is given in Nester and Wasserman (1974). This equation was used for calculating the rate constants in all photoreactor studies.

The corrected first order rate constants for the large photoreactor studies are summarized in Table 15 . Combinations of experimental conditions in the large photoreactor studies that produced data which were determined to belong to the same population (α =0.05) were combined to determine one rate constant for a group of experimental conditions. Tables 16 to 23 present a summary of first order photodegradation rate constants and $t_{1/2}$ values for the small photoreactor studies.

Analysis of Calculated Degradation Rate Constants

Large Photoreactors

Statistically significant first order photodegradation rate constants for the soil and soil/amendment studies conducted using the large photoreactors are summarized in Table 15. To assess the relative photoreactivity of the test compounds, a mean degradation constant was calculated for each compound over all soils and all treatments. This allowed the grouping of the compounds by reactivity into three general categories as shown in Table 24.

The only compounds that did not show significant degradation in all 24 soil/light/amendment combinations were those listed as recalcitrant. However, the most recalcitrant test compound, phenanthrene, showed measurable compound loss in 21 out of 24, or 88 percent, of the soil/light/ amendment combinations. Photodegradation data were examined by comparing the rates of test compound loss for different experimental conditions using ANOVA procedures to determine the effect on observed photodecomposition rates of the three factors: soil type, soil amendment, and type of light used for irradiation.

Soil Type. In general, the reactivity of the soils ranged from Skumpah, the most reactive, to Durant, the least reactive. This is illustrated for anthracene in Figure 14, showing mean and 95% confidence intervals for first order rate constants for each soil/amendment/light combination. As has been mentioned, photochemical activity of soil and other surfaces, including atmospheric particulates, has been positively correlated with color and surface reflectance (Korfmacher et al. 1980, Behymer and Hites 1985). This correlation supports experimental observations made in the soil irradiation experiments which indicate relative soil reactivity matches their qualitative color range: Skumpah (light grey) > McLaurin (pale brown) > Durant (dark greyish brown). This is significant in that other degradation processes, such as biodegradation, have been shown to be fairly independent of soil type (Coover 1987).

Table 15. Statistically significant first order photodegradation rate constants (1/day), with 95% confidence intervals.*

	Skumpah				McLaurin				Durant		
	Light										
	UV		Visible		UV		Visible		UV & Visible	UV	Visible
	Amendment										
Compound	None, Peat moss, Meth. blue	Diethyl-amine	None, Peat Moss, Meth. blue	Diethyl-amine	None, Peat moss, Riboflavin	Hydrogen peroxide	None, Peat Moss, Riboflavin	Hydrogen peroxide	None, Peat moss, Riboflavin	Diethyl-amine	Diethyl-amine
Anthracene			.076±.008				.060±.005			.035±.003	
Biphenyl		.024±.04		.014±.003	.028±.009	.057±.014		.045±.011		.008±.002	
Carbazole	.033±.004	.024±.004	.025±.002	.011±.003	.025±.002	.045±.007		.020±.003	.021±.004		.007±.002
m-Cresol		.097±.01		.077±.007		.059±.007		.041±.003	.070±.008	.036±.007	.057±.009
Dibenzofuran		.009±.02		.005±.001			.013±.003		.007±.003	.005±.003	
Fluorene	.090±.01	.058±.01	.066±.01	.027±.004		.068±.005		.046±.008	.026±.005		.012±.003
PCP			.067±.009				.006±.001		.019±.008	.033±.015	.007±.004
Phenanthrene			.004±.001			.004±.001				.004±.001	
Pyrene	.019±.004	.011±.003	.014±.002	.007±.001			.006±.001		.010±.003		.005±.002
Quinoline		.012±.003		.006±.001	.006±.003		.003±.002		.007±.003	.002±.001	.004±.003

Table 16. First order degradation rates of anthracene on the test minerals.

First order photodegradation of anthracene on calcium kaolinite.					
Application/rate Anthracene only	Co mg/kg	d.f. *	k 1/hr	±95% CI	t1/2 hr
1000 mg/L†	945	7	0.102	0.036	6.80**
500 mg/L†	457	9	0.196	0.107	3.54
1000mg/L††	716	5	0.192	0.032	3.61
Anthracene in a 10 Compound Mixture					
1000 mg/L†	915	7	0.0137	0.0021	50.6
500 mg/L†	526	7	0.063	0.019	10.9
Anthracene in a 7 Compound Mixture					
1000 mg/l†	993	7	0.027	0.008	25.7
500 mg/L†	450	6	0.042	0.0063	16.5

** Calculated half life in excess of irradiation time of 5 hr.

First order photodegradation of anthracene on calcium montmorillonite.

Application Anthracene only	Co mg/kg	d.f.*	k 1/hr	±95% CI	t1/2 hr
1000mg/L†	986	7	0.035	0.003	19.8
500 mg/L†	496	7	0.035	0.008	19.8
1000 mg/L††	692	21	0.067	0.011	10.3
Anthracene in a 10 Compound Mixture					
1000 mg/L†	1027	13	0.096	0.028	7.21
500 mg/L†	580	9	0.160	0.037	4.33
Anthracene in a 7 Compound Mixture					
1000 mg/L†	1016	5	0.041	0.016	16.9
500 mg/L†	527	5	0.064	0.013	10.8

First order photodegradation of anthracene on calcium illite.

Application Anthracene only	Co mg/kg	d.f.*	k 1/hr	±95% CI	t1/2 hr
1000 mg/L†	512	15	0.067	0.007	10.3

Table 16. (Cont'd)

First order photodegradation of anthracene on silica gel.

Application Anthracene only	Co mg/kg	d.f.*	k 1/hr	±95%CI	t1/2 hr
1000 mg/L†	1234	3	3.368	0.625	0.21
500 mg/L†	496	7	6.65	1.12	0.10
1000 mg/L†	960	5	4.207	1.59	0.16
Anthracene in a 10 compound mixture					
1000 mg/L†	987	5	1.216	0.604	0.57
500 mg/L†	551	4	1.850	0.641	0.37
Anthracene in a 7 compound mixture					
1000 mg/L†	970	3	2.650	1.19	0.26
500 mg/L†	482	3	4.080	2.46	0.17

First order photodegradation of anthracene on aluminum kaolinite.

Application/rate Anthracene only	Co mg/kg	d.f.*	k 1/hr	±95% CI	t1/2 hr
1000 mg/L†	668	19	0.090	0.007	7.73

First order photodegradation of anthracene on aluminum montmorillonite.

Application Anthracene only	Co mg/kg	d.f.*	k 1/hr	±95% CI	t1/2 hr
1000 mg/L†	1020	7	0.005	0.002	139**
1000 mg/L††	781	25	0.019	0.007	37***

** Calculated half life in excess of irradiation time of 24 hr.
***Calculated half life in excess of irradiation time of 12 hr.

First order photodegradation of anthracene on aluminum illite.

Application Anthracene only	Co mg/kg	d.f.*	k 1/hr	±95% CI	t1/2 hr
1000 mg/L††	720	15	0.031	0.009	22.6**

** Calculated half life in excess of irradiation time of 12 hr.

First order photodegradation of anthracene on sodium kaolinite.

Application Anthracene only	Co mg/kg	d.f.*	k 1/hr	±95% CI	t1/2 hr
1000 mg/L††	876	11	0.066	0.010	10.5**

** Calculated half life in excess of irradiation time of 8 hr.

Table 16. (Cont'd)

First order photodegradation of anthracene on sodium montmorillonite.					
Application Anthracene only	Co mg/kg	d.f.*	k 1/hr	±95% CI	t1/2 hr
1000 mg/L††	784	11	0.004	0.003	160**

** Calculated half life in excess of irradiation time of 32 hr.

First order photodegradation of anthracene on calcite (SA=13).

Application Anthracene only	Co mg/kg	d.f.*	k 1/hr	±95% CI	t1/2 hr
1000 mg/L††	935	7	0.040	0.025	17.3

First order photodegradation of anthracene on calcite (SA=2).

Application Anthracene only	Co mg/kg	d.f.*	k 1/hr	±95% CI	t1/2 hr
1000 mg/L††	854	5	0.053	0.017	13.0**

* Degrees of freedom associated with the linear portion of the first order plot of data.
** Calculated half life in excess of irradiation time of 10 hr.
† Analyses were done by HPLC with methylene chloride extraction.
†† Analyses were done by GC with methylene chloride extraction

Table 17. First order degradation rates of anthracene on soils.

First order photodegradation of anthracene on Skumpah soil with and without the addition of silica gel.†					
Application/rate Anthracene in a 7 compound mixture	Co mg/kg	d.f.*	k 1/hr	±95% CI	t1/2 hr
500 mg/L Anthracene in a 7 compound mixture with silica gel	482	10	0.014	0.002	49.5
500 mg/L	491	11	0.017	0.002	40.8

First order photodegradation of anthracene on McLaurin soil.†

Application/rate Anthracene in a 7 compound mixture	Co mg/kg	d.f.*	k 1/hr	±95% CI	t1/2 hr
500 mg/L	502	5	0.020	0.004	34.3

First order photodegradation of anthracene on Durant soil.†

Application/rate Anthracene in a 7 compound mixture	Co mg/kg	d.f.*	k 1/hr	±95% CI	t1/2 hr
500 mg/L	441	7	0.007	0.002	103

* Degrees of freedom associated with the linear portion of the first order plot of data.
† All analyses by HPLC with methylene chloride extraction.

Table 18. First order degradation rates of test compounds on silica gel.

First order photodegradation of fluorene on silica gel.†					
Application Fluorene in a 10 compound mixture	Co mg/kg	d.f.*	k 1/hr	±95% CI	t1/2 hr
1000 mg/L	960	15	0.008	0.007	86.6**
500 mg/L	515	14	0.014	0.005	49.5**
Fluorene in a 7 compound mixture					
1000 mg/L	1005	14	0.013	0.004	51.0**
500 mg/L	482	15	0.013	0.004	51.0**

** Calculated half life in excess of irradiation time of 24 hr.

First order photodegradation of pyrene on silica gel.†

Application Pyrene in a 10 compound mixture	Co mg/kg	d.f.*	k 1/hr	±95% CI	t1/2 hr
1000 mg/L	975	15	0.027	0.008	25.7**
500 mg/L	528	12	0.068	0.017	10.2
Pyrene in a 7 compound mixture					
1000 mg/L	993	14	0.028	0.017	24.8**
500 mg/L	479	13	0.056	0.011	12.4

First order photodegradation of cresol on silica gel†

Application/rate Cresol in a 10 compound mixture	Co mg/kg	d.f.*	k 1/hr	±95% CI	t1/2 hr
1000 mg/L	366	11	0.121	0.035	5.73
500 mg/L	162	10	0.191	0.050	3.63
Cresol in a 7 compound mixture					
1000 mg/l	491	12	0.110	0.051	6.28
500 mg/L	214	7	0.300	1.03**	2.31

** Cresol concentration was below the detection limit of the LC within the first 5 hr.

First order photodegradation of biphenyl on silica gel.†

Application	Co	d.f.*	k	±95% CI	t1/2
Biphenyl in a 10 compound mixture	mg/kg		1/hr		hr
1000 mg/L	959	15	0.005	0.006	***
500 mg/L	518	14	0.004	0.004	***
Biphenyl in a 7 compound mixture					
1000 mg/L	996	14	0.006	0.017	***
500 mg/L	480	15	0.0001	0.004	***

Table 18. (Cont'd)

First order photodegradation of phenanthrene on silica gel.†					
Application	Co	d.f.*	k	±95% CI	t1/2
Phenanthrene in a 10 compound mixture	mg/kg		1/hr		hr
1000 mg/L	934	15	0.010	0.007	69.3**
500 mg/L	506	14	0.013	0.005	52.1**
Phenanthrene in a 7 compound mixture					
1000 mg/L	986	14	0.011	0.017	***
500 mg/L	478	15	0.008	0.004	86.7**

** Calculated half life in excess of irradiation time of 24 hr.

First order photodegradation of dibenzofuran on silica gel.†					
Application	Co	d.f.*	k	±95% CI	t1/2
Dibenzofuran in a 10 compound mixture	mg/kg		1/hr		hr
1000 mg/L	980	15	0.003	0.007	***
500 mg/L	531	14	0.011	0.006	52.1**

* Degrees of freedom associated with the linear portion of the first order plot of data
** Calculated half life in excess of irradiation time of 24 hr.
*** Not statistically different than zero-no reaction
† All analyses by HPLC with methylene chloride extraction

Table 19. First order degradation rates of test compounds on calcium kaolinite.

First order photodegradation of fluorene on calcium kaolinite.†					
Application/rate Fluorene in a 10 compound mixture	Co mg/kg	d.f. *	k 1/hr	±95% CI	t1/2 hr
1000 mg/L	876	13	0.002	0.001	289**
500 mg/L	478	11	0.013	0.003	52.5
Fluorene in a 7 compound mixture					
1000 mg/l	909	13	0.009	0.001	73.7
500 mg/L	400	12	0.013	0.003	54.6

First order photodegradation of cresol on calcium kaolinite.†

Application Cresol in a 10 compound mixture	Co mg/kg	d.f.*	k 1/hr	±95% CI	t1/2 hr
1000 mg/L	567	11	0.022	0.004	30.9
500 mg/L	254	7	0.110	0.029	6.3
Cresol in a 7 compound mixture					
1000 mg/l	562	3	0.321	0.069	2.2
500 mg/L	271	5	0.176	0.031	3.9

First order photodegradation of pyrene on calcium kaolinite.†

Application Pyrene in a 10 compound mixture	Co mg/kg	d.f.*	k 1/hr	±95% CI	t1/2 hr
1000 mg/L	910	13	0.003	0.001	365**
500 mg/L	494	13	0.004	0.003	192**
Pyrene in a 7 compound mixture					
1000 mg/L	962	15	0.004	0.001	173***
500 mg/L	434	12	0.006	0.001	115**

First order photodegradation of biphenyl on calcium kaolinite.†

Application/rate Biphenyl in a 10 compound mixture	Co mg/kg	d.f. *	k 1/hr	±95% CI	t1/2 hr
1000 mg/L	803	13	0.001	0.006	346**
500 mg/L	459	13	0.006	0.002	116**
Biphenyl in a 7 compound mixture					
1000 mg/l	774	15	0.004	0.001	173***
500 mg/L	328	12	0.006	0.002	125**

Table 19. (Cont'd)

First order photodegradation of phenanthrene on calcium kaolinite.†					
Application Phenanthrene in a 10 compound mixture	Co mg/kg	d.f.*	k 1/hr	±95% CI	t1/2 hr
1000 mg/L	875	13	**		
500 mg/L	469	13	**		
Phenanthrene in a 7 compound mixture					
1000 mg/l	922	17	0.0030	0.001	204***
500 mg/L	421	12	0.004	0.001	185**

First order photodegradation of dibenzofuran on calcium kaolinite.†

Application Dibenzofuran in a 10 compound mixture	Co mg/kg	d.f.*	k 1/hr	±95% CI	t1/2 hr
1000 mg/L	856	13	****		
500 mg/L	488	13	0.003	0.002	266**

* Degrees of freedom associated with the linear portion of the first order plot of data.
** Calculated half life in excess of irradiation time of 96 hr.
*** Total time of irradiation was 336 hr.
**** Not significantly different than zero-no reaction.
† All analyses by HPLC with methylene chloride extraction.

Table 20. First order degradation rates of the test compounds on calcium montmorillonite.

First order photodegradation of fluorene on calcium montmorillonite†					
Application/rate Fluorene in a 10 compound mixture	Co mg/kg	d.f.*	k 1/hr	±95% CI	t1/2 hr
1000 mg/L	1013	21	0.002	0.002	****
500 mg/L	553	20	0.004	0.003	173**
Fluorene in a 7 compound mixture					
1000 mg/L	1013	12	0.003	0.001	231**
500 mg/L	493	13	0.003	0.001	231**

First order photodegradation of cresol on calcium montmorillonite.†

Application/rate Cresol in a 10 compound mixture	Co mg/kg	d.f.*	k 1/hr	±95% CI	t1/2 hr
1000 mg/L	574	21	0.003	0.002	231**
500 mg/L	316	20	0.004	0.002	173**
Cresol in a 7 compound mixture					
1000 mg/L	824	12	0.009	0.002	77.9
500 mg/L	433	9	0.012	0.004	57.8

First order photodegradation of pyrene on calcium montmorillonite.†

Application/rate Pyrene in a 10 compound mixture	Co mg/kg	d.f.*	k 1/hr	±95% CI	t1/2 hr
1000 mg/L	1019	21	0.004	0.003	173**
500 mg/L	552	20	0.005	0.003	139
Pyrene in a 7 compound mixture					
1000 mg/L	908	12	0.005	0.001	139***
500 mg/L	447	13	0.006	0.001	116***

First order photodegradation of biphenyl on calcium montmorillonite.†

Application/rate Biphenyl in a 10 compound mixture	Co mg/kg	i.f. *	k 1/hr	±95% CI	t1/2 hr
1000 mg/L	997	21	0.001	0.002	****
500 mg/L	560	20	0.002	0.003	****
Biphenyl in a 7 compound mixture					
1000 mg/L	1018	12	0.002	0.001	346***
500 mg/L	506	13	0.002	0.001	346***

Table 20. (Cont'd)

First order photodegradation of phenanthrene on calcium montmorillonite.†

Application/rate Phenanthrene in a 10 compound mixture	Co mg/kg	d.f. *	k 1/hr	±95% CI	t1/2 hr
1000 mg/L	974	21	0.003	0.002	231**
500 mg/L	535	20	0.004	0.003	173**
Phenanthrene in a 7 compound mixture					
1000 mg/L	1012	12	0.003	0.001	231***
500 mg/L	504	13	0.004	0.001	173***

First order photodegradation of dibenzofuran on calcium montmorillonite.†

Application/rate Dibenzofuran in a 10 compound mixture	Co mg/kg	d.f. *	k 1/hr	±95% CI	t1/2 hr
1000 mg/L	1024	13	0.001	0.002	****
500 mg/L	572	12	0.001	0.003	****

* Degrees of freedom associated with the linear portion of the first order plot of data.
** Calculated half life in excess of irradiation time of 143 hr.
*** Calculated half life in excess of irradiation time of 96 hr.
**** Not significantly different from zero-no reaction.
† All analyses by HPLC with methylene chloride extraction.

Table 21. First order degradation rates of the test compounds on Skumpah soil with and without silica gel.

First order photodegradation of fluorene on Skumpah soil with and without the addition of silica gel.†					
Application/rate Fluorene in a 7 compound mixture	Co mg/kg	d.f.*	k 1/hr	±95% CI	t1/2 hr
500 mg/L Fluorene in a 7 compound mixture with silica gel	454	10	0.010	0.001	69.3
500 mg/L	467	11	0.01	0.001	69.3

First order photodegradation of pyrene on Skumpah soil with and without the addition of silica gel.†

Application/rate Pyrene in a 7 compound mixture	Co mg/kg	d.f.*	k 1/hr	±95% CI	t1/2 hr
500 mg/L Pyrene in a 7 compound mixture with silica gel	411	10	0.005	0.001	151
500 mg/L	427	11	0.005	0.001	139

First order photodegradation of cresol on Skumpah soil with and without the addition of silica gel.†

Application/rate Cresol in a 7 compound mixture	Co mg/kg	d.f.*	k 1/hr	±95% CI	t1/2 hr
500 mg/L Cresol in a 7 compound mixture with silica gel	401	8	0.039	0.004	17.8
500 mg/L	419	9	0.034	0.005	20.1

First order photodegradation of biphenyl on Skumpah soil with and without the addition of silica gel.†

Application/rate biphenyl in a 7 compound mixture	Co mg/kg	d.f.*	k 1/hr	±95% CI	t1/2 hr
500 mg/L biphenyl in a 7 compound mixture with silica gel	422	12	0.003	0.001	231
500 mg/L	442	13	0.004	0.001	198

Table 21. (Cont'd)

First order photodegradation of phenanthrene on Skumpah soil with and without the addition of silica gel.†					
Application/rate Phenanthrene in a 7 compound mixture	Co mg/kg	d.f.*	k 1/hr	±95% CI	t1/2 hr
500 mg/L Phenanthrene in a 7 compound mixture with silica gel	457	12	0.003	0.001	248
500 mg/L	469	13	0.003	0.001	209

* Degrees of freedom associated with the linear portion of the first order plot of data.
† All analyses by HPLC with methylene chloride extraction.

Table 22. First order degradation rates of the test compounds on Durant soil.

First order photodegradation of fluorene on Durant soil.†

Application/rate Fluorene in a 7 compound mixture	Co mg/kg	d.f.*	k 1/hr	±95% CI	t1/2 hr
500 mg/L	398	9	0.005	0.001	152**

First order photodegradation of pyrene on Durant soil.†

Application/rate Pyrene in a 7 compound mixture	Co mg/kg	d.f.*	k 1/hr	±95% CI	t1/2 hr
500 mg/L	402	9	0.0005	0.0012	***

First order photodegradation of cresol on Durant soil.†

Application/rate Cresol in a 7 compound mixture	Co mg/kg	d.f.*	k 1/hr	±95% CI	t1/2 hr
500 mg/L	361	5	0.011	0.002	53.3

First order photodegradation of biphenyl on Durant soil.†

Application/rate biphenyl in a 7 compound mixture	Co mg/kg	d.f.*	k 1/hr	±95% CI	t1/2 hr
500 mg/L	359	9	0.002	0.002	***

First order photodegradation of phenanthrene on Durant soil.†

Application/rate Phenanthrene in a 7 compound mixture	Co mg/kg	d.f.*	k 1/hr	±95% CI	t1/2 hr
500 mg/L	406	9	0.001	0.001	***

* Degrees of freedom associated with the linear portion of the first order plot of data.
**Calculated half life in excess of irridiation time of 120 hours.
***Not significantly different than zero--no reaction.
† All analyses by HPLC with methylene chloride extraction.

Table 23. First order degradation rates of the test compounds on McLaurin soil.

First order photodegradation of fluorene on McLaurin soil.†					
Application/rate Fluorene in a 7 compound mixture	Co mg/kg	d.f.*	k 1/hr	±95% CI	t1/2 hr
500 mg/L	454	5	0.0170	0.004	40.8

First order photodegradation of pyrene on McLaurin soil.†

Application/rate Pyrene in a 7 compound mixture	Co mg/kg	d.f.*	k 1/hr	±95% CI	t1/2 hr
500 mg/L	461	7	0.011	0.003	66

First order photodegradation of cresol on McLaurin soil.†

Application/rate Cresol in a 7 compound mixture	Co mg/kg	d.f.*	k 1/hr	±95% CI	t1/2 hr
500 mg/L	325	3	0.021	0.004	30.5

First order photodegradation of biphenyl on McLaurin soil.†

Application/rate biphenyl in a 7 compound mixture	Co mg/kg	d.f.*	k 1/hr	±95% CI	t1/2 hr
500 mg/L	366	5	0.024	0.004	28.4

First order photodegradation of phenanthrene on McLaurin soil.†

Application/rate Phenanthrene in a 7 compound mixture	Co mg/kg	d.f.*	k 1/hr	±95% CI	t1/2 hr
500 mg/L	465	7	0.009	0.003	74.9

* Degrees of freedom associated with the linear portion of the first order plot of data.
† All analyses by HPLC with methylene chloride extraction.

Table 24. Classification of compounds by photoreactivity (mean half-lives in hours*).

Classification		
Reactive (< 360 hours)	Moderately Reactive (< 720 hours)	Recalcitrant (> 720 hours)
m-cresol 230	pentachlorophenol 504	pyrene 1512
anthracene 288	carbazole 696	dibenzofuran 1848
fluorene 312	biphenyl 720	quinoline 2784
		phenanthrene 3336

*Based on I_o = 20 Watts/m^2 and Light intensity = I_o * 4.5 m^2/g.

When treatments common to two soils were compared using ANOVA procedures, a positive test for significance was indicated for the role of soil type. The level of certainty of a significant difference between soil types was much higher for the more reactive compounds than for the recalcitrant ones, such as quinoline, phenanthrene, and pyrene. This implies that soil type directly influences the mechanism by which the reactive compounds were degraded in these experiments. This, along with the relationship between soil color and photochemical activity, provides support for the assertion that the loss of compounds observed in these experiments was due to photochemical activity. Carbazole provided an exception to the observation that reactive compounds were dependent on soil type, however, the results for carbazole added support to the role of photolysis in the degradation observed. Carbazole was one of the moderately reactive compounds in the mixture, yet showed little photoreactivity dependence on soil type, while being significantly affected by the type of light used during irradiation. This strongly suggested that the mechanism by which carbazole undergoes degradation is different from the mechanism of the other reactive test compounds, and that its reaction mechanism depends directly on the wavelength of the irradiation.

Light Type. Knowledge of the relative energy spectrum of visible and UV light, and the nature of the possible photochemical reactions involving the compounds used in these experiments lead to the expectation that degradation rates would be significantly greater under UV light. The light produced by the UV irradiation chamber (Figure 9) was higher in intensity than natural sunlight in the lower wavelengths of its range (≈300 nm). Several compounds in the test mixture strongly absorbed light in this range. Though a higher degradation rate under UV versus visible light was apparent for a number of compound/soil/amendment combinations, the extent of photochemical enhancement was not as great as was expected, nor was it statistically significant in many cases. The nature of the light source may be the cause of this observation.

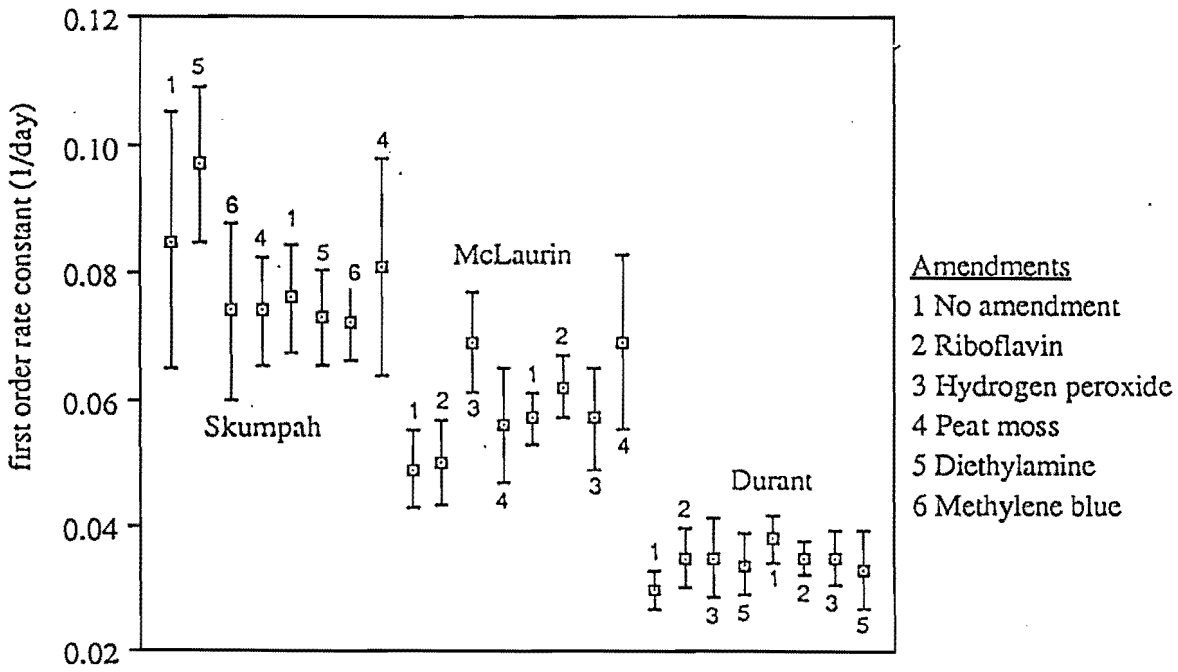

Figure 14. Summarized anthracene first order rate constants and 95% confidence intervals for all soil/amendment combinations.

Both the visible and UV light sources consisted of banks of fluorescent tubes. All fluorescent tubes are dependent on the excitation of mercury and its fluorescent emissions to produce light. The glass used in the tubes and their interior coating transform the mercury emissions into broader spectra. However, as seen in Figure 9, mercury emission lines were still present in the tube output. The broad spectra of the tube output in the irradiation chambers varied as planned between the two chambers, but the light produced in both chambers had strong, common peaks at the mercury emission lines: 313 nm, 365 nm, 407 nm, 435 nm (Calvert and Pitts 1966). A comparison of intensities at selected mercury emission lines is given in Table 25.

Table 25 shows that light intensity is actually higher in the visible irradiation chamber than in the UV chamber at a wavelength of 365 nm, one of the absorption maxima for anthracene. Little difference in anthracene photodegradation rates was observed between identical samples exposed in the different irradiation chambers. This indicates that there is a connection between the rate of anthracene photodegradation and the intensity of light at 365 nm, and implies that absorption of light by anthracene is directly responsible for anthracene photodegradation.

Table 25. Light intensities in irradiation chambers at selected visible and UV mercury emission wavelengths.

Wavelength (nm)	Light intensity at given wavelength ($mW/m^2/nm$)			
	Visible Irradiation Chamber		UV Irradiation Chamber	
	Peak	Background†	Peak	Background†
313	180	5	607	450
365	895	75	761	540
407	2190	75	58	40
435	3270	175	2050	12

†Intensities are compared to the intensity of the broad wavelength bands adjacent to the mercury emissions (background intensity).

The light in the two irradiation chambers does show significant difference in the output at the 313 nm mercury line (Table 25). Several of the test compounds, including quinoline, carbazole, phenanthrene and pyrene, have absorption maxima at or near this wavelength (Table 2). These compounds give positive indication (at $\alpha = 0.05$) of the significance of light when sets of data from identical samples in the UV and visible irradiation chambers are compared. This suggests that at least one of the mechanisms by which these compounds were degraded involved direct absorption of light in the 313 nm region, with subsequent reaction of the excited organic molecule.

Surface Area. While it is difficult to know precisely how optimum concentrations in solution relate to concentrations on a solid matrix, it is possible to obtain a subjective evaluation of the encounter probability of reactants in a soil matrix by estimating the extent to which the surfaces of the soil particles are covered by them. Bauer et al. (1982) and De Mayo et al. (1984) demonstrated a direct relationship between surface coverage and molecular mobility on solid and the dependence of photoreactivity on molecular mobility. Molecular mobility and photoreactivity are greatly enhanced when the reacting species concentration on the surface becomes greater than a monolayer.

Evidence is provided to support the relationship between molecular mobility and the percentage of surface area covered by the results in both the dark controls and irradiated samples. Recall that the two compounds with the highest volatilization parameters were m-cresol and biphenyl (Table 14). Dark control results indicated highest loss rates for these compounds on McLaurin soil, the soil with the smallest surface area. For the irradiated samples, the rates of biphenyl loss were much higher on McLaurin soil. Biphenyl is a hydrophobic compound to which the volatilization parameter estimation method should be applicable. This may indicate that volatilization played a significant role in this apparent loss of biphenyl. The results for m-cresol do not indicate any substantial increase on McLaurin soil. This provides evidence that the estimation method is not accurate for

ionizable compounds and that volatilization is not a dominant factor in observed losses of m-cresol.

To consider the percentage of surface area coverage for the test compounds in these experiments, phenanthrene was used as a model. Using the geometric structure of phenanthrene, the fact that most PAH's are relatively planar, and the approximate bond length of 0.13 nm for carbon-double bonds, the molecule can be approximated as a rectangle with an area of 0.5 nm^2. An expression can then be written using the gram molecular weight of the molecule (Table 2), Avogadro's number (6.02×10^{23}), and the mass concentration at which the molecule was spiked onto the soil to determine the molecular surface area coverage per gram of soil.

$$\frac{0.5\ nm^2}{molecule} \times \frac{6.02 \times 10^{23}\ molecules}{mole} \times \frac{1\ mole}{178.2\ g} \times \frac{10^{-18}\ m^2}{nm^2} \times \frac{5 \times 10^{-4}\ g}{g\ soil} = \frac{0.85\ m^2}{g\ soil} \qquad (19)$$

This molecular surface area coverage can then be compared to the total surface area of the soil, which is included in Table 4. With phenanthrene applied to McLaurin soil, it would cover ≈ 18 percent of the total surface. This can be assumed to be the average coverage of each of the test compounds, to estimate the total coverage achieved with the spike solution.

With ten compounds spiked on the soil, McLaurin soil had more than a monolayer of test compounds on its surface, while the other two soils maintained far less than monolayer coverage during irradiation. McLaurin soil experiments did not display significantly greater photoreactivity than the other two soils, indicating that the extent of surface coverage does not appear to play a determinant role in these experiments.

Small Photoreactors--Minerals

Tables 4A through 12A in Appendix A summarize the calculated half-life values for each test compound and experimental scheme used in the small photoreactor studies. Half-life values within and between mineral and soil types that are not significantly different are indicated in these tables. Statistical tests for detecting significant difference between slopes at $\alpha = 0.05$ were performed using the equations presented by Kleinbaum and Kupper (1978).

To assess the relative photoreactivity of anthracene on the mineral/silica gel surfaces using the small photoreactors, a mean half life for each mineral and silica gel was calculated by averaging the rate constants from the anthracene only studies at the two loading rates used (500 and 1,000 mg/kg) since the slopes of these regression relationships were not statistically different ($\alpha = 0.05$) (Kleinbaum and Kupper, 1978). This allowed the grouping of minerals into three general categories based on relative reactivity as shown in Table 26. Silica gel was the most reactive surface, with a reaction rate an order of magnitude greater than the most reactive clay mineral surface (kaolinite). The two kaolinite clays were more reactive than the two calcites, the illite, or montmorillonite clays. The

calcium saturated clays were more reactive than their aluminum counterparts. The surface area of the two calcite samples had no effect on anthracene loss. The relative reactivity of the mineral surfaces for anthracene, when anthracene was added alone, was: silica gel >> Ca-kaolinite > Al-kaolinite > Ca-illite = Ca-montmorillonite = calcites > Al-illite > Al-montmorillonite.

Table 26. Classification of mineral surface reactivity based on anthracene half-lives from the small photoreactor anthracene-only studies (hr).

Reactive (< 1 hr)	Moderately Reactive (< 24 hr)	Recalcitrant (>24 hr)
Silica Gel (0.14)	Ca-Kaolinite (4.0) Al-Kaolinite (7.7) Cal-Illite (10.3) Ca-Montmorillonite (11.2) Calcite (SA-2) (13.0) Calcite (SA=13) (17.3) Al-Illite (22.6)	Al-Montmorillonite (61*)

*Calculated half-life in excess of irradiation time.

Table 27 summarizes the relative photoreactivities of the test compounds in the seven and ten compound mixtures on the mineral and soil surfaces. A mean half-life was calculated for each compound/mineral combination by averaging rate constants when the regression line slopes were not statistically different at $\alpha = 0.05$.

Anthracene was the only chemical tested that was reactive on all surfaces studied (Table 27). As in the anthracene alone study, silica gel was the most reactive surface tested for both the ten and seven compound mixtures. Rapid loss of both anthracene and cresol was observed from silica gel, their half-lives being less than 5 hr. Pyrene was also reactive on the silica gel. The photoreactivity of pyrene on silica gel has been demonstrated by Yokley et al. (1986) and Dunston et al. (1989), and is confirmed by the results of this study.

Reactivity of anthracene on calcium kaolinite was the only compound/mineral combination that was affected by both solution composition and concentration. The photoreaction rate for anthracene was slowest in the ten compound mixture at the highest loading rate (Table 27) and fastest when anthracene was added alone (Table 26). Anthracene and cresol were reactive on Ca-kaolinite while anthracene was the only chemical that was reactive on Ca-montmorillonite. The rate of anthracene loss was similar for the two clays, but was two orders of magnitude slower than on the silica gel. All other chemicals were relatively non-reactive regardless of mineral surface, compound mixture, or loading rates.

Table 27. Classification of test compounds in the seven and ten compound mixtures by photoreactivity (half-life, hr) on the minerals using the small photoreactors.

Reactive (< 30 hr)	Moderately Reactive (< 70 hr)	Recalcitrant (> 70 hr)
Silica Gel anthracene (0.34) cresol (4.5) pyrene (18.2)	Silica Gel fluorene (60*)	Silica Gel biphenyl (no reaction) Phenanthracene (70*) dibenzofuran (no reaction)
Ca Kaolinite anthracene (13.7) 10 & 7 cpd-500 mg/L anthracene (25.7) 7cpd-1000 mg/L cresol (4.1) 10 & 7 cpd-500 mg/L 7 cpd-1000 mg/L	Ca Kaolinite anthracene (50.6) 10 cpd-1000 mg/L cresol (31) 10 cpd-1000 mg/L fluorene (60) 10 & 7cpd-500mg/L 7 cpd-1000 mg/L	Ca Kaolinite fluorene (289*) 10cpd-1000 mg/L pyrene (212*) biphenyl (194*) phenanthrene 10 cpd-(no reaction) phenanthrene 7 cpd-(194*) dibenzofuran (no reaction)
Ca Montmorillonite anthracene (9.8)	Ca Montmorillonite cresol (64) 7 cpd-both conc	Ca Montmorillonite fluorene (212*) pyrene (142*) cresol (202*) 10 cpd biphenyl (no reaction) phenanthrene (202*) dibenzofuran (no reaction)

*Calculated half-life in excess of irradiation time.

As stated previously, photoreactivity of soils and other surfaces may be related to the color of the surface (Korfmacher et al. 1980, Behymer and Hites 1985). Although silica gel was not included in the surface reflectance analyses (Table 4), it has a high surface reflectance down to 200 nm (Kortum & Braun, 1960). Since all clay minerals and soils absorb radiation below 300 nm, the high reflectance of silica gel accounts in part for its high photoreactivity. The pattern of photochemical reaction potential observed across all test minerals cannot be related exclusively to surface reflectance, however, as based on this reactivity predictor, calcite should be as reactive a surface as silica gel. Chemical reaction

data shown in Tables 26 and 27 clearly indicate this was not the case. Among the other clay minerals, however, reaction order does follow surface reflectance relationships. For the anthracene only study, the most reactive kaolinite has the highest surface reflectance, while montmorillonite and illite, with similar surface reflectance values (Table 4), yield similar anthracene reactivities.

Surface area was another property investigated in relation to the relative reactivity of the mineral surfaces to anthracene. Ranking minerals by total surface yields the following order: Ca-montmorillonite ≈ silica gel ≈ Al-montmorillonite » Ca-illite > Al-illite » Ca-kaolinite ≈ Al-kaolinite > calcite. Assuming that only the external surfaces are important in photoreactions, this order changes to: silica gel » Al-illite ≈ Al-montmorillonite ≈ Ca-montmorillonite ≈ Ca-kaolinite > calcite. Again, surface alone does not account for the photoreactivity observed in the pure mineral studies.

The effect of surface area may, however, explain the relative reactivity of anthracene between mass loading rates on a particular mineral. Equation 19 was used to estimate the percentage of surface area coverage for the test compounds in these experiments. Table 28 lists the percent of each mineral's total surface that was covered by the compounds added under the various loading mixture and loading rate conditions used in this study. For the low surface area Ca-kaolinite, observed photodegradation rates decreased as more compound was added to the clay, whereas photoreaction rates on montmorillonite were not as affected by the composition or concentration of the spiking solution. Surface area coverage, however, does not explain the differences in reactivity observed between the saturating cations on a given clay.

Surface acidity was investigated as an indicator of surface photoreaction properties. Silica gel and the calcium saturated clays have lower surface acidities ($H_o > +1.5$) than the aluminum saturated clays ($H_o = -3.0$ to -8.2). In general, surface acidity explains the reaction order of anthracene on the mineral surfaces, with silica gel being the most reactive and the calcium saturated clays being more reactive than the aluminum saturated clays. Again, however, surface acidity does not explain the lower reactivity of the montmorillonite and illite clays compared to the kaolinites.

Small Photoreactors--Soils. All chemicals showed some reactivity on Skumpah and McLaurin soils in the small photoreactor studies (Table 29). The relative order of photoreactivity, in general, was the same as in the large photoreactor study with cresol, anthracene, fluorene, and biphenyl being the most reactive. Contrary to the large photoreactor study, however, the McLaurin, not Skumpah soil, was the most reactive surface. Dibenzofuran, carbazole, quinoline, and PCP were not included in the small photoreactor study due to analytical difficulties using HPLC for quantitation of these compounds.

Differences in the rate of reactivity between the two photoreactor studies may be due to the higher exposure the soil has to the light in the small photoreactors study. The exposed surface areas of soil in the small photoreactors was 20 cm^2/g, whereas in the large photoreactors the light exposed surface was 4.4 cm^2/g. The relative reactivity between the studies reflect this surface exposure difference.

Table 28. Percent coverage of the total surface area of minerals by compounds under a variety of loading rate studies.[1]

	Anthracene only		Ten compound mixture		Seven compound mixture	
	1000 mg/kg	500 mg/kg	1000 mg/kg	500 mg/kg	1000 mg/kg	500 mg/kg
Silica gel	0.33	0.17	3.3	2.0	2.4	1.2
Ca-kaolinite	6.8	3.4	68	34	48	24
Al-kaolinite	7.4	3.7				
Ca-montmorillonite	0.29	0.15	2.9	1.5	2.0	1.0
Al-montmorillonite	0.33	0.16				
Ca-illite	1.4	0.7				
Al-illite	2.0	1.0				
Calcite (SA=13.7)	12.3	6.2				
Calcite (SA=2)	84	42				

[1]All compounds are assumed to occupy an average of 0.5 nm^2/molecule and have an average molecular weight of 178 g/mol

Amendments. Soil amendments were compared using one way ANOVA procedures to identify the particular soil/amendment combination resulting in a significant enhancement of the photodegradation rate. As shown in Table 15, there was apparent degradation enhancement for a small number of compound/soil/amendment combinations. Hydrogen peroxide was the amendment which produced the strongest indication of photodegradation enhancement. For example, when McLaurin soil was treated with hydrogen peroxide and irradiated under UV light, there was significant degradation enhancement over that seen in unamended soil for carbazole and biphenyl as indicated in Table 15. This enhancement was not evident for any of the compounds with the same soil and amendment under visible light. In fact, fluorene, phenanthrene and quinoline showed significant decreases in degradation under visible light with hydrogen peroxide amendment. Enhancement was also not observed in the samples amended with hydrogen peroxide on Durant soil and exposed to visible or UV light. This small number of positive enhancement results and the inability to observe them in other peroxide applications makes it unlikely that hydrogen peroxide significantly enhances photodegradation.

Table 29. Classification of test compounds in the seven and ten compound mixtures by photoreactivity (half-life, hr) on the soils using the small photoreactors.

Reactive (< 30 hr)	Moderately Reactive (< 70 hr)	Recalcitrant (> 70 hr)
Skumpah cresol (17.8)	Skumpah anthracene (49.5) fluorene (67)	Skumpah pyrene (151) biphenyl (210) phenanthrene (248)
McLaurin biphenyl (28.4)	McLaurin anthracene (34.4) fluorene (53) pyrene (66) cresol (30.5)	McLaurin phenanthrene (74.9)
	Durant cresol (53.3)	Durant anthracene (103) fluorene (152*) pyrene (no reaction) biphenyl (no reaction) phenanthrene (no reaction)

*Calculated half-life in excess of irradiation time.

Other soil amendments used in these experiments have produced positive effects in solution phase photodegradation processes (Sargent and Sanks 1976, Acher and Rosenthal 1977, Cooper and Zika 1983), but they did not appear to positively enhance soil-phase photochemistry in this study. An explanation for this could be the difficulty in relating solution conditions to experimental conditions in soil systems, specifically the concentrations of substrate and amendment. Sargent and Sanks (1976) suggest and optimum concentration of 1.5×10^{-5}M for dye and 5×10^{-4}M for substrate (cresol) for sensitized photooxidation of organic compounds. Given the mass of compounds and amendment added to the soil in these experiments, and taking the soil matrix as solvent, the concentrations of organic compounds ranged from 1.9×10^{-3}M to 4.6×10^{-3}M for each compound, while the methylene blue and riboflavin concentrations were 2.7×10^{-4}M and 1.9×10^{-4}M, respectively. For methylene blue and riboflavin, the ratio of substrate to sensitizer was in the correct proportion, the concentration of substrate was one order of magnitude larger than the sensitizer.

Diethylamine amendment. An ANOVA was performed on the data sets for Skumpah and Durant soils, with and without diethylamine amendment. ANOVA results indicated a significant decrease in degradation rates with diethylamine soil amendment at the 95% confidence level for fluorene, carbazole, and pyrene. It is significant that the diethylamine negatively affected degradation rates for two of the more reactive compounds in the mixture, carbazole and fluorene, and did not affect anthracene or m-cresol. This has implications with respect to the mechanism by which photodegradation of the test compound occurred.

Assuming that the test compounds comprise less than a monolayer, and that they have limited mobility on soil surfaces, it is possible to hypothesize an explanation for the results obtained with diethylamine. Absorption of light by anthracene is unaffected in samples with diethylamine as evidenced by the lack of an effect on anthracene's degradation rate and the fact that diethylamine has no absorption maxima which would compete with anthracene. The reactions of excited anthracene are relatively unhindered, and those pathways that do not involve energy transfer out of the immediate vicinity of anthracene proceed near their normal rates. Mechanisms which do involve transport of an excited species appear to be quenched. Davidson and Pratt (1984) suggest that amines may quench singlet oxygen. At the amendment concentration used in this study, the diethylamine may have been so abundant that it shielded other compounds from anthracene-produced excited species, providing sufficient collisions to deenergize the singlet oxygen and other energy transfer species before they could diffuse or migrate from the exciting molecule to a substrate molecule. The fact that cresol did not follow the trend observed with diethylamine amendment implies that it may be lost by a mechanism different than that of fluorene, suggesting that volatilization may be significant. Pyrene's inclusion in the group of affected compounds indicates that though its degradation is much slower than the reactive compounds, it probably degrades by the same mechanism. Verschueren (1983) reported the formation of pyrene diones similar to anthraquinone with the irradiation of pyrene on soils, supporting a photolysis mechanism similar to that of anthracene.

Silica gel. Because of the high reactivity of anthracene, cresol, and pyrene on silica gel, silica gel was added to Ca-kaolinite and Skumpah soil as an amendment. Enough silica gel was added to the mineral or soil to double the sample surface area. The addition of silica gel greatly enhanced anthracene loss from the calcium saturated kaolinite (Table 30), but had little effect on the other compounds present. Addition of silica gel had no effect on the photodegradation of any of the test compounds in Skumpah soil (Table 30).

Reaction Products

GC and HPLC Analysis. Analysis of irradiated soil and mineral extracts by GC or HPLC resulted in the identification of two unknown peaks that appeared regularly and increased in area over time. GC/MS analyses of these extracts identified these unknowns as anthraquinone and fluorenone, based on both a library match and retention time match with known standards. Two possible products of anthracene photodegradation, the 9, 10-dimer and 9,10-endoperoxide are thermally unstable. Analysis by GC or GC/MS causes decomposition of these photoproducts to anthracene and anthraquinine in a 50/50 ratio.

Analysis of the extracts by HPLC and NMR, however, did not show the production of either the dimer or endoperoxide on any surface studied. GC/MS analysis of the extracts yielded additional products but none with the quantitative yield and universal presence of anthraquinone and fluorenone. The additional products which were detected by GC/MS but were not confirmed by retention time match included: tetra- and tri-chlorophenol, a dimer of cresol, 9 (10H)-acridinone, 2-hydroxy-6-methyl-benzaldehyde, 3-methoxy-benzaldehyde, 4-hydroxy-3-methoxy-benzaldehyde, phthalic anhydride, 1,8-naphthalic anhydride, xanthene, xanthone, 9(10H)-anthracenone, 1H-phenalen-1-one, and benzoic acid.

Table 30. Effect of silica gel addition on rate of photodegradation of test compounds (half-life, hr).

	Anthracene	Fluorene	Cresol	Pyrene	Diphenyl	Phenan-thracene	Dibenzofuran
Ca kaolinite							
w/o silica gel	50.6	289[a]	31.0[a]	365*	364*	no loss	no loss
w silica gel	21.3	216[a]	21.1[a]	160*	no loss	no loss	no loss
Skumpah							
w/o silica gel	49.5[a†]	66.6[a]	17.3[a]	151[a]	210[a]	249[a]	
w silica gel	40.8[a]	67.3[a]	20.1[a]	136[a]	198	209[a]	

†Values within columns for given soil or mineral followed by the same letter are not significantly different by comparing slopes at $\alpha = 0.05$.

*Calculated half-life exceeds irradiation time.

The concentration of anthraquinone and fluorenone in the extracts were determined using GC or HPLC by calibration with external standards, and a direct relationship was established between the formation of the products and the disappearance of the parent compounds as shown in Figure 15 for fluorene and fluorenone on McLaurin soil. Results for fluorene and fluorenone and for anthracene and anthraquinone on all soils displayed similar trends. The ratio of $[product]_t/[parent]_o$ was plotted against the ratio of $[parent]_t/[parent]_o$ at each sampling time interval with the ratios calculated on a molar concentration basis. The slope of these regression lines is the average product yield. Figures 16 and 17 show a plot of fluorenone versus fluorene and anthraquinine versus anthracene product ratios, respectively, in all the samples analyzed from the Skumpah soil in the large photoreactor study. The linear relationship between fluorene and fluorenone can be observed by noting that the x and y intercepts of the linear regression are approximately equal. This confirms the accuracy of the analytical procedures and indicates

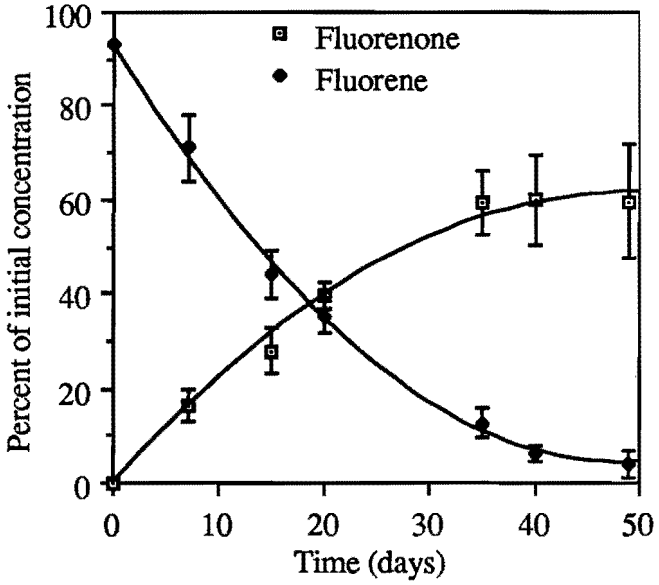

Figure 15. Reactant loss and product formation for fluorene and fluorenone on the McLaurin soil.

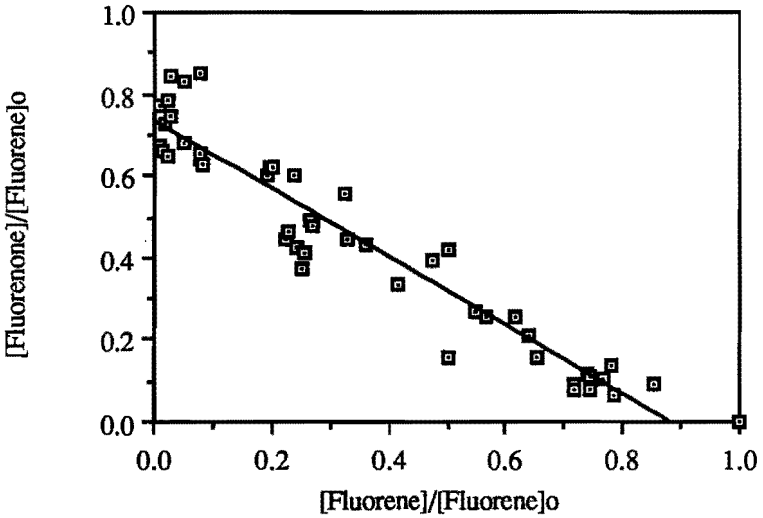

Figure 16. Study product versus reactant summary plot, fluorene and fluorenone on Skumpah soil.

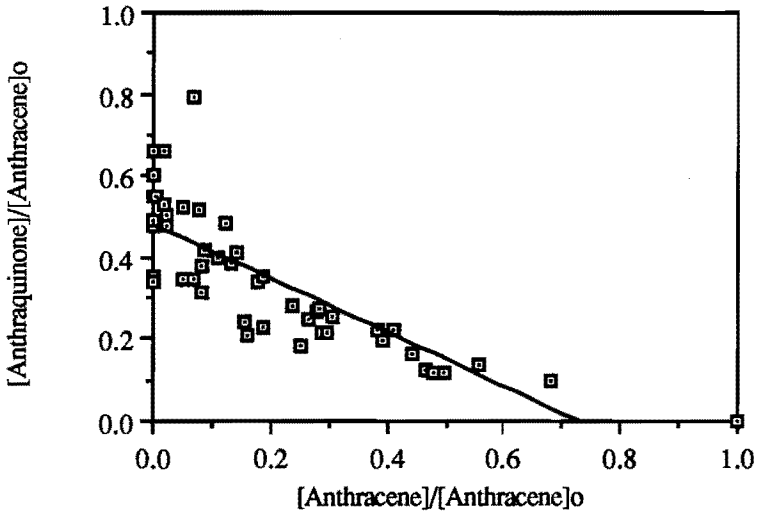

Figure 17. Study product versus reactant summary plot, anthracene and anthraquinone in Skumpah soil.

that the mechanisms of reactant loss and product formation remained constant over the duration of the experiments. For the anthraquinone and anthracene relationship, the x and y intercepts were not the same and the coefficient of determination for the regression was only 0.66. Information on the initial relationship between reactant and product formation was lost due to the fact that 40 percent of the anthracene had reacted by the first sampling time.

Photoproduct yields were calculated, as described above, for all surfaces studied. Results for soils are reported in Table 31 and for minerals in Table 32. Yield of the two photoproducts, anthraquinone and fluorenone were highest from the Skumpah soil in the large photoreactor study and from the Durant soil in the small photoreactor study (Table 31). The differences in yield of the photoproducts between these studies may be caused by two factors, i.e., method of analysis and method of extraction. In the large photoreactor study, GC rather than HPLC methods were used to quantify the products formed. Using GC methods, any 9,10-endoperoxide formed will decompose to anthracene and anthraquinone in a 50/50 ratio due to the high temperature required for sample injection. Any 9,10-dimer would also decompose to anthracene. Anthraquinone was reported as the major product in all GC studies. However, this does not fully explain the higher yields of anthraquinone that were observed using GC compared to HPLC analyses since the decomposition of endoperoxide could only yield 50 percent of the anthracene photoproduct.

Table 31. Percent of initial concentration of anthracene and fluorene accounted for in the production of anthraquinone and fluorenone.

Soil	Mixture/Conc. (mg/L)	% Anthraquinone/ anthracene	% Fluorenone/ fluorene
Skumpah Soil	7 cpd/500	29*	50*
McLaurin Soil	7 cpd/500	33*	26*
Durant Soil	7 cpd/500	62*	68*
Skumpah Soil	10 cpd/500	66**	85**
McLaurin Soil††	10 cpd/500	43**	65**
Durant Soil††	10 cpd/500	49**	62**

*Analyzed by HPLC
**Analyzed by GC
††Light intensity = Io x 4.4 (cm^2/g substrate)

The extraction methods used may also influence photoproduct yields. For the small photoreactor study, extractions were performed by manually shaking the soil with methylene chloride rather than using the more rigorous acid/base-neutral Tissumizer® method used in the large photoreactor study. As stated previously, the manual shaking method was effective in extracting anthraquinone and fluorenone from the McLaurin and Durant Soil (Table 11). The extraction of photoproducts from Durant soil may be facilitated by manual shaking since the emulsion formed using the Tissumizer and the resulting erratic recovery efficiencies was not observed. The extraction efficiency for the Skumpah soil, however, using manual shaking, decreased with time. The milder shaking method and the use of methylene chloride alone was not effective in removing the more hydrophilic photoproducts from this soil.

Although silica gel exhibited the highest rate of loss of anthracene and fluorene of all the test minerals evaluated, little anthraquinone or fluorenone was detected in the extract from these silica gel studies regardless of the compound loading rate or mixture utilized (Table 32). The calcite surfaces had the highest recovery of anthraquinone of the soil minerals studied. The kaolinite clays produced higher yields of anthraquinone and fluorenone than the other clay surfaces tested. As stated previously, manual shaking with methylene chloride may not be effective in removing the photoproducts sorbed to the mineral surfaces over long-reaction periods. The relative recovery of the photoproducts among the minerals reflects the potential strength of the surface interaction with hydrophilic

Table 32. Percent of initial concentration of anthracene and fluorene accounted for in the production of anthraquinone and fluorenone.

Minerals	Mixture/Conc. (mg/L)	% Anthraquinone/ anthracene	% Fluorenone/ fluorene
Ca kaolinite	Anthracene only		
	1000	34*, 63**	
	500	20*	
	10 cpd		
	1000	18*	****
	500	20*	****
	7 cpd		
	1000	42*	36*
	500	43*	40*
Ca montmorillonite	An only		
	1000	7.5*, 16**	
	500	4.9*	
	10 cpd		
	1000	8.3*	****
	500	7.3*	****
	7 cpd		
	1000	25*	5.9*
	500	22*	5.9*
Ca illite	An only		
	1000	22**	
Al kaolinite	An only		
	1000	46**	
Al montmorillonite	An only		
	1000	19*	
Al illite	An only		
	1000	26**	
Silica gel	An only		
	1000	5.3*, 9.6**, 40***	
	500	7.6*	
	10 cpd		
	1000	3.0*	****
	500	4.9*	****
	7 cpd		
	1000	7.1*	8.0*
	500	5.8*	14.5*

Table 32 (Cont'd)

Minerals	Mixture/Conc. (mg/L)	% Anthraquinone/ anthracene	% Fluorenone/ fluorene
Calcite (SA=13.5)	An only 1000	42*	
Calcite (SA=2)	An only 1000	72*	

*Analyzed by HPLC
**Analyzed by GC
***Analyzed by NMR
****Fluorenone could not be determined in the ten compound mixture because the LC retention time was the same as carbazole
†Light intensity=Io x 20 (cm^2/g substrate)
††Light intensity = Io x 4.4 (cm^2/g substrate)

photoproducts, with calcite having the lowest sorption capacity and silica gel and the 2:1 clays having the highest. For the anthracene only studies, anthraquinone formation on some of the mineral surfaces was quantified by both HPLC and GC. Higher yields of anthraquinone were again observed using GC compared to HPLC analyses.

Anthracene Reactivity

Anthracene has the most distinctive ultraviolet-visible absorption spectrum of any of the ten test compounds used in the model waste system. It is the only compound which strongly absorbs light in the range of the solar spectrum. Anthracene was of particular interest in the simulated waste mixture as it demonstrated one of the highest photodegradation rates of all the test compounds. Additionally, it formed a quantitative product and was suspected of playing a role as a sensitizer in the overall photooxidation process. The solution photochemistry of anthracene has been extensively studied, so it also provided a means of exploring the mechanisms of surface adsorbed photochemistry through a comparison with solution reaction pathways.

Anthracene Solution Photochemistry. In solution chemistry in the absence of oxygen, anthracene forms a photo-dimer, where the bonding occurs at the 9, 10 center positions. In the presence of sufficient oxygen and light, anthracene forms the 9,10-endoperoxide. This reaction takes place in any solvent which is transparent to light above a wavelength of 300 nm. Anthraquinone has not been reported as a photoproduct of anthracene in solution. The mechanism of anthracene photochemistry in solution is given in Equations 16 through 24 (Saltiel and Atwater 1988, Stevens and Perez 1974). The notation used is as follows:

A is ground state anthracene; ^1A is the excited singlet; ^3A is the associated triplet; $^1O_2$ is the first excited singlet delta state of oxygen; I_a and I_o are the absorbed and incident light intensities, respectively; ε is the molar extinction coefficient; and L is the path length through the medium where absorption of light takes place.

$A + h\gamma \rightarrow {}^1A$	Rate = $I_a/L = I_o(1 - e^{(-2.3\varepsilon L[A])})/L$	(16)
$^1A + A \rightarrow$ 9,10-dimer	$k_a = 1 \times 10^{10}$ $(M\text{-}s)^{-1}$	(17)
$^1A + O_2 \rightarrow A + O_2 +$ heat	$k_{q1} = 3 \times 10^{10}$ $(M\text{-}s)^{-1}$	(18)
$^1A \rightarrow A + h\gamma'$	$k_f = 6.4 \times 10^7$ $(s)^{-1}$	(19)
$^1A \rightarrow {}^3A$	$k_{isc} = 1.7 \times 10^8$ $(s)^{-1}$	(20)
$^3A + O_2 \rightarrow A + {}^1O_2$	$k_{q3} = 3 \times 10^9$ $(M\text{-}s)^{-1}$	(21)
$A + {}^1O_2 \rightarrow$ 9,10-endoperoxide	$k_e = 1.5 \times 10^5$ $(M\text{-}s)^{-1}$	(22)
$^1O_2 +$ solvent $\rightarrow O_2 +$ solvent + heat	$k_1 = 1 \times 10^4$ $(s)^{-1}$	(23)
$^3A +$ solvent $\rightarrow A +$ solvent + heat	$k_{t3} \approx 100$ $(s)^{-1}$	(24)

The rate of dimer formation from the excited singlet state is given as:

$$\frac{d[A_2]}{dt} = \frac{I_a \bullet k_a \bullet [A]}{k_a[A] + k_{q1}[O_2] + k_f + k_{isc}} \qquad (25)$$

The quantum yield is given by dividing this rate by I_a, assuming that I_a is $\approx I_o$. The limiting quantum yield for dimer formation as determined by Bowen and Tanner (1954), is 0.1 to 0.2 (depending on the solvent), while the limiting yield of fluorescence is 0.3. The dominant term in this anthracene reaction mechanism is Equation 20, the intersystem crossing to the triplet state.

The rate of reactions involving the triplet state are more complex since every excited molecule must first pass through the singlet state. It is now known that photochemical oxygen additions proceed via energy transfer between the excited triplet state of the organic

molecule and the ground state triplet oxygen (Saltiel and Atwater 1988). Although oxygen quenches the excited singlet state of anthracene (Equation 18), generation of singlet oxygen is spin forbidden (unless there is a simultaneous triplet conversion of anthracene), consequently this process must occur from the triplet state of anthracene (Equation 21). The lifetime of singlet oxygen is dependent on the solvent (Equation 23), with values reported in the literature presented in Table 33.

Table 33. The lifetime of $^1O_2$ in various solvents.

Solvent	Lifetime/(10^{-6} s)	Reference
Carbon Disulfide	200-250	Merkel and Kearns (1972)
Carbon Tetrachloride	700	Merkel and Kearns (1972)
Bromobenzene	34	Stevens and Perez (1974)
Methylene Chloride	105	Carlson et al. (1974)
Benzene	11	Carlson et al. (1974)
Chlorobenzene	91	Carlson et al. (1974)
Chloroform	60	Merkel and Kearns (1972)

The rate of endoperoxide formation is given as:

$$\frac{d[endo]}{dt} = \frac{I_a \bullet k_{isc} \bullet [A] \bullet [O_2] \bullet k_{q3} \bullet k_e}{(k_a [A] + k_{q1}[O_2] + k_f + k_{isc}) \bullet (k_{q3}[O_2] + k_{t3}) \bullet (k_e [A] + k_1)} \quad (26)$$

Again the results obtained by Bowen and Tanner (1954) show that for carbon disulfide and chloroform the sequence of Equation 21 followed by Equation 22 must dominate over the deactivating steps Equations 23 and 24. Under these conditions, Equation 26 reduces to:

$$\Phi_{endo} = \frac{d[endo]}{dt} / I_a = \frac{\Phi_{isc}\, k_e\, [A]}{k_e[A] + k_1} \quad (27)$$

where $\Phi_{isc} = k_{isc}/(k_a \bullet [A] + k_{q1}[O_2] + k_f + k_{isc})$. The limiting quantum yield, Φ_{endo}, for endoperoxide formation was 0.9. While these authors showed only a slight dependence on oxygen concentration, the reciprocal of the quantum yield had a linear dependence on the reciprocal of the anthracene concentration.

The main points of this kinetic analysis were verified in this study using the analytical technique of proton NMR analysis. Solution experiments, using methylene chloride, benzene, chloroform, hexane, acetone, and carbon disulfide were conducted as part of this study, using proton NMR, for a quantitative analysis of potential anthracene reaction mechanisms in the soil/mineral studies. The NMR peaks of anthracene and its reaction products are chemically shifted in such a way that each of the reaction/product components can be identified and determined quantitatively in the presence of all of the others. This is rather unique in NMR studies.

The proton NMR of anthracene and several of its derivatives have been determined. The chemical shifts and spin-spin couplings for these materials are reported in Table 34. Endoperoxide, dienthrenyl, the photo-dimer, and several unidentified photoproducts were formed in various proportions in the different solvents analyzed in this study. There was always some anthraquinone produced regardless of the solvent used upon long irradiation times, however, which was thought to be due to a surface reactions at the glass-solvent interface.

Anthracene Photochemistry on Silica Gel. The contrast between solution photochemistry and surface adsorbed photochemistry of anthracene is dramatic. It is not possible to accurately determine the light intensity absorbed by granular surfaces, so anthracene adsorbed on silica gel was used as the actinometric standard in this study. Silica gel particles produce multiple light reflections, and since the anthracene concentration on the surface was monomolecular, light absorption is very small upon each reflection. This system is labelled optically thin, or $I_a = 2.3\ I_o \cdot E \cdot L \cdot [A]$, where L is difficult to determine. As the particles must be shaken periodically to expose every surface to light, if the period of shaking is long, the physical process rather than photochemistry becomes reaction rate limiting.

The silica gel system has been analyzed separately by: (1) gas chromatography, (2) high pressure liquid chromatography, and (3) proton NMR. The advantage of NMR is that all compounds have the same sensitivity to the technique. However, it will not work with mixtures where spectral features overlap. Two different types of anthracene irradiation experiments were performed using silica gel. In one experiment, the methylene chloride solvent was not allowed to completely evaporate before irradiation of the sample (wet experiment). In the other experiment, the sample was heated using a sand bath before irradiation (dry experiment). The rate of anthracene loss was the same in both experiments, however, product formation was significantly different. In the wet experiments, the first products formed were the dimer and the endoperoxide. After a delay period, production of 9,10-anthraquinone began. In the dry experiments, for the NMR experiments only anthraquinone was observed as a product. The concentration dependent time data for these experiments is shown in Figure 18.

The product ratio relating anthraquinone to anthracene for the dry experiment is shown in Figure 19. The yield of anthraquinone was 42 percent in the dry experiment. In the wet experiment, where solvent was still present, the product ratio curve was concave, indicating that anthraquinone was produced in secondary photoreactions. The photo-production of anthraquinone from anthracene on solids was first observed by Kortum and

Table 34. Chemical shifts for the proton NMR spectra of anthracene and its photoproducts.

Compound	Chemical shift	Splitting	No. of protons
Anthracene	8.46	singlet	2
	8.01	multiplet	4
	7.50	multiplet	4
Anthraquinone	8.33	multiplet	4
(9,10)	7.82	multiplet	4
Endoperoxide	7.40	multiplet	4
(9,10)	7.30	multiplet	4
	6.03	singlet	2
9,10-Dimer	6.82	multiplet	8
	6.92	multiplet	8
	4.57	singlet	4
Anthrone	8.36	doublet	2
(9-keto-10-	7.61	multiplet	6
hydro-anthracene)	7.47	multiplet	-
	4.35	singlet	2
Dianthrone	7.93	multiplet	4
	7.42	multiplet	8
	6.87	multiplet	4
	4.77	singlet	2

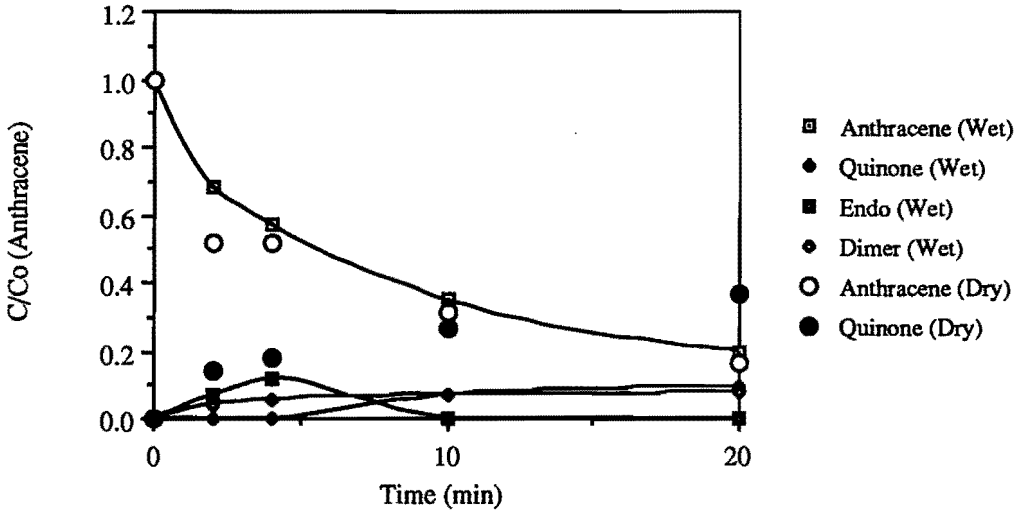

Figure 18. Anthracene on silica gel. Proton NMR wet and dry experiment results.

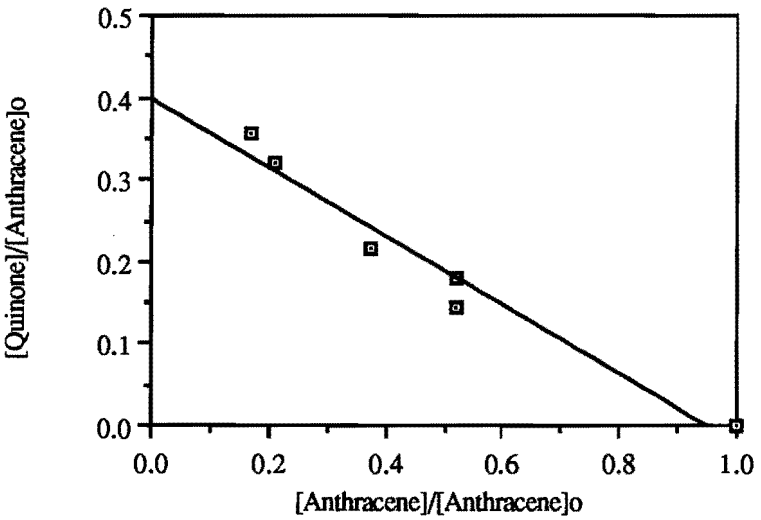

Figure 19. Anthracene on silica gel. Product ratio from dry experiment results.

Braun (1960). They observed that anthraquinone was not the sole product from the photolysis of anthracene on silica gel, but were not able to identify other products by reflectance spectroscopy. They did find however, that 9,10-diphenyl anthracene on silica gel converted quantitatively to the 9,10-endoperoxide when irradiated. The "dryness" of their system is unknown.

The mechanism presented in Equations 17 through 26 has to be modified to provide for the production of anthraquinone on a surface. If endoperoxide is an intermediate in anthraquinone formation, it is so reactive on surfaces that its concentration never reaches measurable levels. However, endoperoxide applied to silica gel in this study was not found to be converted to anthraquinone immediately. The combination of adsorbed anthracene, light, and oxygen is necessary for the reaction to take place. The reaction step can be postulated as:

$$^3A_{ads} + 2O_2 \rightarrow \text{anthraquinone}_{ads} + H_2O_2\,Ks \qquad (28)$$

In this reaction scheme triplet anthracene is oxidized and hydrogen peroxide is formed. The nature of the surface is critical for the efficiency of this reaction. The rate law with an optically thin absorption layer becomes:

$$-\frac{d[A]}{dt} = \frac{I_o \bullet \Phi_{isc} \bullet k_s \bullet \varepsilon \bullet [A]_{ads} \bullet [O_2]}{k_{t3} + k_2\,[O_2] + kq_3\,[O_2]} \qquad (29)$$

where k_{t3} now refers to deactivation of the anthracene triplet on the surface by processes other than conversion to anthraquinone. The integration of Equation 29 yields a first order relationship for anthracene dependence, the validity of this first order dependence being based on there being no competition for light absorption by the photoproducts. This condition could be expected to hold for no more than two half-lives, as was observed in this study. When there is a solvent film on the silica gel, solution type photochemistry exists on its surface, and the solution products of the 9,10-dimer and the 9,10-endoperoxide appear in addition to 9,10-anthraquinone.

With long irradiation times (greater than 2 hr), anthraquinone is photochemically converted into a number of new products. Those separated by HPLC include: hydroxy-anthraquinone, dianthanyl, and anthrone. This provides evidence that once the initial anthracene photochemical reactions are complete, secondary photoreactions can take place.

DeMayo and coworkers (De Mayo et al. 1984) have shown that polycyclic aromatic molecules have high mobilities on silica gel surfaces. This mobility is sufficient to facilitate energy transfer from excited state molecules to other molecules on the surface. When the concentration of anthracene on silica gel is increased from 1000 mg/kg to 5000 mg/kg, the photodimer is produced. When other compounds are added to the silica gel (binary mixtures and seven and ten compound mixtures), the rate of anthracene loss decreases.

Anthracene Photochemistry on Minerals. Anthracene was the most reactive on Ca kaolinite when it was added alone. The first order rate constant (Table 16) for anthracene loss under this condition averaged 0.16±0.05 hr^{-1}. This reaction is 30 times less efficient than anthracene loss from silica gel. There was no significant differences in reaction rates for anthracene from Ca montmorillonite, Ca illite, and the two calcite surfaces, when anthracene was added alone. The first order rate constant for these surfaces averaged 0.056±0.012 hr^{-1}.

The reactivity of anthracene decreased on Ca kaolinite in the seven and ten compound mixtures compared to the anthracene only study. Also the reactivity of anthracene decreased as the concentration within each mixture was increased from 500 to 1000 mg/kg soil. For Ca montmorillonite, unlike Ca kaolinite, anthracene reactivity was not affected by either solution composition or concentration. The reactivity of anthracene in the seven compound mixture for the Ca montmorillonite and Ca kaolinite was the same. Averaging first order rate constants for all surfaces that did not display significantly different reaction rates (Ca montmorillonite studies, Ca illite, the calcites, and Ca kaolinite with the seven compound mixture and ten compound mixture at 500 mg/L) results in a rate constant that is independent of surface type, solution composition, and concentration. This surface independent rate constant equals 0.061±0.035hr^{-1} ($t_{1/2}$=11.4 hr). Compared to this "standard" surface, Ca kaolinite displayed a faster loss rate when anthracene was added alone by a factor of 2.7 whereas the loss was slower on this mineral in the 10 compound mixture at the 1000 mg/L loading rate by a factor of 4.4.

Anthracene reaction on the mineral surfaces produced the same photoproduct as on the silica gel, implying a similar reaction mechanism. The principal site of organic sorption on silica gel is the surface silanol groups and the principal force responsible for sorption is assumed to be electrostatic interactions, hydrogen bonding, and dispersion forces (Bauer et al. 1982). Binding of molecules with π system or with lone pair electrons should largely be by hydrogen bonding to the silanol or to the physical adsorbed water molecules. Hydrogen bonding of anthracene and pyrene to silica gel was the principal mechanism of sorption reported by Bauer et al. (1982).

When silica gel is heated to 550°C in air and cooled, as was done in this study, it will adsorb moisture from the atmosphere. This leads to partial hydrolysis of siloxane bonds formed during heating. The extent of hydrolysis of the silica gel surface effects the reactivity of the surface by affecting the number and distribution of silanol and hydrated silanol groups (Bauer et al. 1984, De Mayo et al. 1984). The extent of hydrolysis of the silica gel used in this study is unknown.

The interaction of the silanol surface of silica gel and anthracene enhances photoreactivity compared to other surfaces tested. The broken edges of kaolinite consist of silanol and aluminol groups. These broken edges account for 10 to 20 percent of the total surface area and for the majority of the surface reactivity of this clay. Calcium kaolinite has far fewer silanol sites than silica gel which accounts for its lower photoreactivity. These edge silanol sites may, however, account for its higher reactivity compared to the other surfaces tested. Montmorillonite and illite have less than 10 percent of their total surface area as broken edges and with their more reactive basal and inter layer surfaces, anthracene

interaction with the silanol groups may be limited. These 2:1 Ca saturated clays do not behave any differently than calcite. Anthracene photodegradation is enhanced when silanol groups are present but the reaction will proceed at a slower rate with the same photoproducts on any of the surface tested, even ones with no silanol (i.e., calcite). For Ca kaolinite, with the addition of the seven and ten compound mixtures, anthracene sorption at the silanol sites, and hence photoreactivity, is decreased due to competition for sorption with the other chemicals present.

The reactivity of Al saturated kaolinite and illite in the anthracene only study was less than the "standard" surface by a factor of 2. The aluminum kaolinite and illite were less reactive but reaction rates were of the same order of magnitude as their calcium counter parts, whereas anthracene was virtually non-reactive on Al montmorillonite. The aluminum saturated clays had much more acidic surface than the Ca saturated clays, calcite, or silica gel (Table 7), and anthracene reactivity seems to be somewhat related to surface pH characteristics.

Anthracene Photochemistry in Soils. A series of simplified experiments was performed to evaluate the effect of anthracene on the photodegradation rates of other compounds in a binary mixture on Skumpah soil using the large photoreactors. Six pairs of samples were prepared in duplicate, each pair consisting of one sample spiked with a single compound only (substrate) and the second sample spiked with the substrate compound plus anthracene. Samples were irradiated for 15 days with normal maintenance, and were extracted and analyzed according to standard methods for soils described above. Dark controls for each irradiated sample were also incubated for 15 days as per standard protocol. The concentration of anthracene and substrate in each extract was normalized by comparison with initial concentrations, i.e., C_t/C_o. The normalized raw data (Figure 20) showed an obvious trend. For each pair of sample, the substrate alone simple showed less degradation than the same substrate sample when combined with anthracene.

These data were evaluated statistically by comparing the difference between the dark controls and irradiated samples using ANOVA procedures. ANOVA results showed a significant difference (at $\alpha = 0.05$) in the degradation of the substrate compound with and without anthracene. This demonstrates that, under the conditions of these experiments, the degradation of the substrate in binary mixtures was enhanced by the presence of anthracene as a photosensitizer. These sensitization experiments also included samples with fluorene as the substrate and anthraquinone added in place of the anthracene as the potential sensitizer. Anthraquinone has been shown to be a photosensitizer in aqueous systems (Spikes and Straight 1963), but gave no indication of enhancing photolysis in these soil-phase experiments. ANOVA results showed no difference between fluorene alone and fluorene with anthraquinone results. In addition, there was no detectable anthracene in the anthraquinone spiked sample after irradiation, indicating the absence of a back reaction. Finally, ANOVA results indicated no significant differences in the amount of anthracene degradation with or without substrate present. This indicates that the mechanism by which anthracene is sensitizing the photolysis of other compounds does not significantly reduce the rate of degradation of anthracene itself.

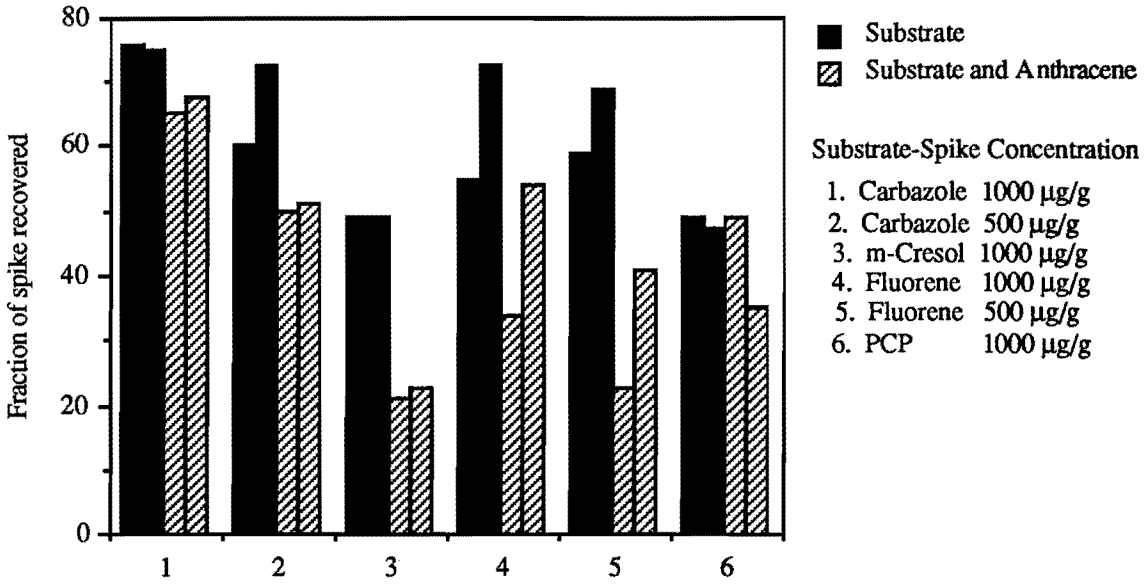

Figure 20. Results of anthracene sensitization experiments. Two replicates were used for each set of experimental conditions. Anthracene was added to the indicated samples at the same concentration as the substrate compound.

The most active of the test soils was the light colored Skumpah with a mean first order rate constant for anthracene loss of 0.09 d^{-1} (a half-life of 7.7 days). The only identifiable product, (using gas chromatography) was 9,10-anthraquinone for this reaction system. The yield from the photodegradation of anthracene on the Skumpah soil was high, ranging from 60 to 70 percent over the entire course of the reaction.

The use of amines as an amendment for the non-acidic soils, Skumpah and Durant, gave some intriguing results as summarized in Table 15. Anthracene photochemistry was unaffected by the addition of diethylamine, whereas the photodegradation of many of the other compounds was quenched. The most dramatic changes were for carbazole and fluorene. The first order rate constants were reduced by 56 percent for these compounds on both the Skumpah and Durant soils following amine amendment.

Although amines are possible hydrogen or electron donors, they are also capable of quenching singlet oxygen. The process for this mechanism has been reviewed by Bellus (1979). Specifically, the quenching of singlet oxygen by diethylamine has been measured to be 2 x 10^6 $(M\text{-}s)^{-1}$ in nonpolar organic solvents (Young et al. 1973). Since the concentration of diethylamine at 10 mg/kg soil was greater than the total concentration of all of the aromatic hydrocarbons added (5 mg/kg soil), it is possible that any singlet oxygen generated photochemically would be quenched by the amine.

Since the photodegradation of anthracene was unaffected by the amine addition, this evidence again supports the suggestion that the anthracene photochemistry may proceed by another pathway independent of singlet oxygen.

ENGINEERING APPLICATIONS

The intent of this research was to evaluate the photodegradation of a simulated creosote waste and to assess the potential for the enhancement of photodegradation using several easily applied engineering management techniques. Though no significant enhancement of photodegradation by any of the evaluated soil amendments was observed, photolysis was clearly shown to be a significant factor in the fate of the test compounds in the soil and mineral systems. First order modeling allowed the derivation of rate expressions and pseudo-first order degradation rate constants for the test compounds, from which the half lives of the compounds under given experimental conditions were calculated.

It has become apparent from results of this study that these laboratory results are only applicable to environmental situations when mixing half lives of the soil matrix are considered. For systems in which there is a thick soil layer containing contamination, mixing could be important even for the less reactive compounds. It appears, then that mixing is an important engineering management option that should be evaluated for determining optimum treatment strategies.

The complicating factor for analysis of the kinetics of the photoreaction systems is the frequency used for stirring of the soil/minerals. This frequency may limit the overall observed rate constant. It is apparent that a particle must be exposed to light before the organic contaminants adsorbed on it may undergo photolysis. In these experiments, the test compounds were present throughout the depth of the matrix; therefore, only a fraction of the particles with adsorbed test compounds were exposed to light at a given time. The physical process of bringing particles to the soil surface, where they can be exposed to light, must be included in an overall model of the photolysis process. Mixing is, by its nature, a first order process which converts unexposed particles, A, into exposed particles, B, in proportion to the concentration of unexposed particles in the soil.

Photolysis Process Scheme

An overall scheme to illustrate the photodegradation process observed in these experiments must incorporate the loss processes observed in the dark controls, loss due to photodegradation, and the influence of mixing rate on the overall reaction. A proposed scheme is shown in Figure 21.

The dark control loss processes act on all of the test compounds at all depths in the irradiation dishes. The mixing process is required to bring the unexposed reactants to the surface, where the photodegradation mechanisms described above take place. This step

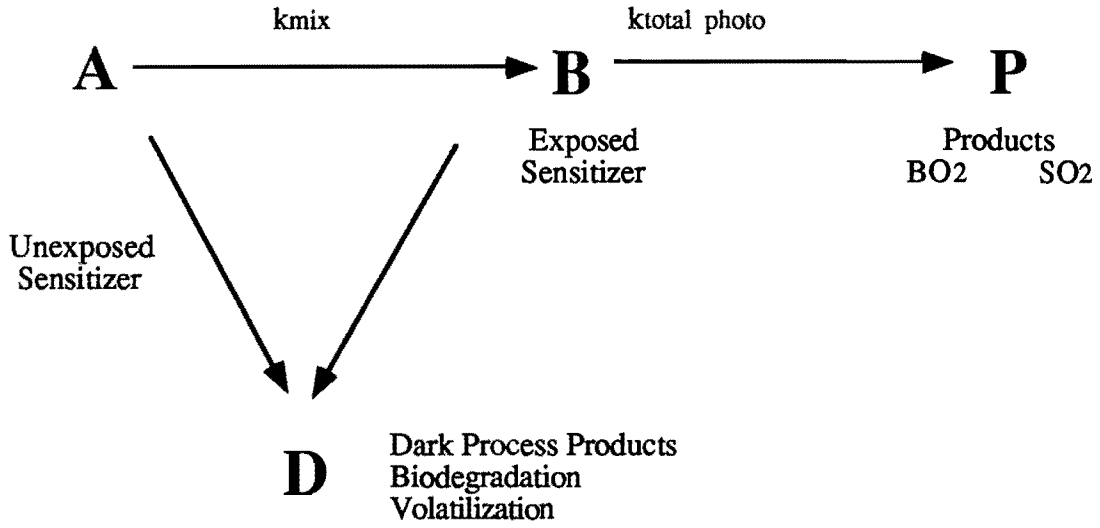

Figure 21. Overall soil phase photolysis reaction scheme.

requires the presence of light and oxygen. Implicit in the derivation of first order photolysis rate constants is the assumption that the dark processes and photodegradation mechanisms are slow processes compared to the mixing process.

The mixing effectiveness, given by k_{mix}, is determined by how thorough the mixing process is and by the thickness or number of effective layers of the soil being mixed. An effective soil layer can be defined as the depth of soil to which some finite portion of the incident light penetrates. The thickness of the effective layer is dependent on the roughness of the soil surface, which is related to the particle size of the soil, and the internal reflectance of the soil particles, all influencing the transmittance of light throughout the soil matrix.

Using a Monte Carlo simulation applied to simple spherical particles, with ten effective layers one particle deep, and assuming that one half of the surface of the particle was irradiated per light exposure event, half lives for exposure of the particles to light were estimated to be on the order of 5 to 6 days (i.e., five to six days of mixing is required to expose half of the particles to light). This model is a reasonable approximation of the conditions which existed in this study with McLaurin soil based on its particle size distribution and the total thickness of the soil in the 150 mm diameter irradiation dishes. When the half life of the compound approaches the half life for mixing, mixing can become the controlling factor in determining the degradation rate of the compound. This estimated mixing half life is on the order of the observed half lives of the more reactive compounds in the test mixture as shown in Table 35.

Table 35. Experimental half lives of test compounds.

Compounds	Soil Type		
	Skumpah	McLaurin	Durant
m-Cresol	7 ± 1	14 ± 3	10 ± 1
Anthracene	9 ± 1	12 ± 1	20 ± 2
Fluorene	9 ± 1	10 ± 1	27 ± 4
PCP	10 ± 1	46 ± 17	36 ± 10
Carbazole	24 ± 4	31 ± 4	33 ± 5
Biphenyl	24 ± 4	17 ± 1	83 ± 14
Recalcitrant Compounds	50 to 180	53 to 180	72 to 180

This implies that increased mixing rates may have resulted in even higher rates of degradation for the most reactive compounds. However, this does not appear to be the case in this study as replicate experiments with 1 g soil samples in the 50 mm irradiation dishes as compared to 40 g of soil in 150 mm dishes have yielded comparable results when the rate constants are normalized to the incident light intensity per gram of soil.

If the photodegradation of hazardous compounds on soil is to be carried out as an effective engineering treatment option in the natural environment, the influence of mixing on the rate of photodegradation is likely to become paramount. When considering a soil with a number of compounds that have different photolytic half-lives, a dilemma is presented to the site manager. The rate of soil mixing should be maintained high enough so as not to limit photodegradation. However, mixing rates which are high enough to maximize degradation of the more reactive compounds will cause unreacted amounts of the less reactive compounds to be tilled back into the subsurface. Waste constituent analysis, available financial and physical resources for remediation, the objectives of the remediation efforts, and the relative photodegradation rates of the waste constituents must be considered in developing an optimal plan for site hazard mitigation. This photolysis reaction could be a significant contributor to the detoxification of sites with relatively thin layers of contaminated soil that covers large areas. This situation would most likely be found at uncontrolled hazardous waste sites after the completion of initial, large scale clean-up efforts. Knowledge of photolysis rates could also contribute to the post closure, 30 year treatment and monitoring efforts at hazardous waste sites.

One of the important results of these experiments was the confirmation of effectiveness of anthracene as a sensitizer for photodegradation on soil. This emphasizes the importance of the presence of a sensitizer for effective photodegradation, whether this sensitizer is contained in the contaminated mixture or is artificially introduced prior to treatment. The

role of singlet oxygen in soil systems was implicated from these results. Further work should be done with singlet oxygen sensitizers to determine optimum concentrations and to evaluate other methods of their amendment to contaminated soil systems.

Diethylamine should not be pursued further as a means of enhancing degradation because of its quenching effects on photolysis rates.

A positive result was obtained for a non-destructive means of hazardous waste management in soil systems, specifically immobilization. From the extraction efficiency estimations made, there is support for the enhancement of polycyclic aromatic hydrocarbon immobilization by increasing the organic content of the soil. This could provide a means for retaining hazardous compounds in the treatment zone of a land treatment or soil remediation site, allowing further long-term treatment by photochemical, biological, or other destructive means.

CONCLUSIONS

Based on results of this study from soil and pure mineral experiments using individual compounds and complex mixtures of creosote waste constituents, the following conclusions can be reached.

1. Under the conditions of this experiment, significant degradation was observed for all ten test compounds in the test soils and in all but one mineral sample. Degradation was shown to be attributable to photochemical activity.

2. First order modeling adequately described the degradation of the test compounds based upon significant r^2 values and observed first order degradation rates were significantly different from zero at α=0.05. Anthracene and cresol were the most reactive compounds on all surfaces studied.

3. Under the experimental conditions of this study, none of the amendments significantly enhanced the photodegradation of the test compounds. Soils amended with diethylamine displayed significantly inhibited photodegradation of several compounds. Sensitization of singlet oxygen production by organic dye amendments in the visible irradiation chamber may have been masked by the high output of light at 365 nm, providing the needed energy for anthracene sensitization.

4. Soil and mineral type proved to be a significant factor in the rate of degradation observed for all test compounds. Reaction rates of anthracene on silica gel and Ca kaolinite in the anthracene only studies were significantly different than for the other surfaces tested. The presence of silanol groups on the silica gel on Ca kaolinite leads to enhanced reactivity of anthracene compared with other surfaces, i.e., the "standard" surfaces, Ca Montmorillonite, Ca illite, and calcite, which were not significantly different in reaction rates. Aluminum saturated clays inhibited anthracene reactivity compared with the "standard surfaces." The complex nature of the three soils also inhibited reactivity of all the test compounds as compared to the pure minerals.

5. Photosensitization by anthracene was shown to be significant in enhancing the rate of degradation of other test compounds.

6. The rate of mixing of the test soil/minerals was postulated to be a significant determinant of observable photochemical degradation rates and may be the primary management technique for enhancing photodegradation at the field scale.

REFERENCES

Acher, A.J., and J. Rosenthal. (1977). "Dye-sensitized photooxidation-a new approach to the treatment of organic matter in sewage effluents." Water Resources 92:59-112.

Altschuller, A.P., and J.J. Bufalini. (1971). Photochemical aspects of air pollution: A review. Environmental Science and Technology 5:39-64.

Bauer, R. K., R. Borenstein, P. De Mayo, K. Okada, M. Rafalska, W.R. Ware and K. C. Wu. (1982). "Surface photochemistry. Translational motion of organic molecules adsorbed on silica gel and its consequences," Journal of the American Chemical Society 104(17):4635.

Bauer, R.K., P. De Mayo, L.V. Natarajan and W. R. Ware. (1984). "Surface photochemistry. The effect of surface modification on the photophysics of naphthalene and pyrene adsorbed on silica gel," Canadian Journal of Chemistry 62(7):1279.

Behymer, T.D., and R.A. Hites. (1985). "Photolysis of polycyclic aromatic hydrocarbons adsorbed on simulated atmospheric particulates." Environmental Science and Technology 19(10):1004-1006.

Bellus, D. (1979). Physical quenchers of singlet oxygen, Advances in Photochemistry 11:105-205.

Benesi, H.A. (1956). "Acidity of catalyst surfaces, I. acid strength from colors of adsorbed indicators." Journal of the American Chemical Society 78:5490-5494.

Bonneau, R., R. Pottier, O. Bagno, and J. Joussot-Dubien. (1975). "pH dependence of singlet oxygen production in aqueous solutions using thiazine dyes as photosensitizers." Photochemistry and Photobiology 21:159-163.

Bowen, E.J., and D.W. Tanner. (1954). "The Photochemistry of Anthracenes." Trans. Faraday Soc. 50:475-481.

Bulman, T.L., S. Lesage, P.J.A. Fowlie, and M.D. Webber. (1985). "The persistence of polynuclear aromatic hydrocarbons in soil." Petroleum Association for Conservation of the Canadian Environment, Report No. 85-2, Ottawa, Ontario.

Burkhard, N., and J.A.Guth. (1979). "Photolysis of organophosphorus insecticides on soil surfaces." Pesticide Science 10(4):313-319.

Calvert, J.G. and N.J. Pitts. (1966). Photochemistry. John Wiley and Sons, Inc., New York, p. 688.

Carroll, D. (1970). "Clay minerals: A guide to their x-ray identification." The Geological Society of America. Special paper 26, Boulder, CO.

Carlson, D.J. et al. (1974). Canadian Journal of Chemistry 52:3728.

Carter, D.L., M.M. Mortland, and W.D. Kemper. (1986). "Specific surface," In A. Klute, (Ed.), Methods of Soil Analysis, Part 1- Physical and Mineralogical Methods, 2nd Ed., American Society of Agronomy, Madison, Wisconsin, 654p.

Choudhry, G.G. and G.R.B. Webster. (1985). "Protocol guidelines for the investigations of photochemical fate of pesticides in water, air, and soils." Residue Reviews 96:80-137.

Choudhry. G.G. (1984). "Photophysical and photochemical properties of soil and aquatic humic materials."

Choudhry, G.G. and O. Hutzinger. (1982). "Photochemical formation and degradation of polychlorinated dibenzofurans and dibenzo-p-dioxins." Residue Reviews 84:111-161.

Christensen, D.C., and W.C. Weimer. (1979). "Enhanced photodegradation of persistent halogenated organic materials." Proceedings of 34th Industrial Waste Conference, Purdue University. 160-166.

Cooper, W. J. and R. G. Zika. (1983). "Photochemical formation of hydrogen peroxide in surface and ground waters exposed to sunlight." Science 220(4598):711.

Coover, M.P. (1987). Studies of the persistence of polycyclic aromatic hydrocarbons in two unacclimated agricultural soils. M.S. thesis, Utah State University, Logan, UT.

Crosby, D.G. (1971). "Environmental photoxidation of pesticides in degradation of synthetic organic molecules in the biosphere." National Academy of Sciences, Washington, D.C. 260-290.

Davidson, R.S., and J.E. Pratt. (1984). "Excimers and exciplexes as sensitizers for photooxidation reactions." Tetrahedron Letters 40(6):999.

De Mayo, P., L.V. Natarajan, and W.R. Ware. (1984). "Surface photochemistry: The effect of surface modification on the singlet quenching of pyrene adsorbed on silica gel by 2-bromonaphthalene." Chemical Physics Letters 107(2):187-192.

Dunstan, T.D.J., R.E. Mauldin, J. Zhong, A.D. Hipps, E.L. Wehry, and G. Mamantov. (1989). "Adsorption and photodegradation of pyrene on magnetic carbonaceous and minerals subfractions of coal stack ash." Environmental Science and Technology 23:303-309.

Farmer, V.C. (1971). "The characterization of adsorption bonds in clays by infrared spectroscopy." Soil Science 112:62-68.

Federal Register 40 CFR 264.113.

Feldman, D.S. J. Gagnun, R. Hofman, J. Simpson, and M. Cuneo. (1986). Statview 512+ (Software and documentation). Brainpower, Inc., Calabasas, California.

Fife, D.J., and W.M. Moore. (1979). "The reduction and quenching of photoexcited flavins by EDTA." Photochemistry and Photobiology. 29(1):43-47.

Foote, C. S. (1968). "Mechanisms of photosensitized oxidation." Science, 162(3857):963-970.

Freeman, D.H. and L.S. Cheung. (1981). "A gel partition model for organic desorption from pond sediments." Science 214:790-792.

Gohre, K., and G.C. Miller. (1983). "Singlet oxygen generation on soil surfaces." Journal of Agricultural and Food Chemistry 31(5):1104-1108.

Groenewegen, D., and H. Stolp. (1981). "Microbial breakdown of polycyclic aromatic hydrocarbons," In M. R. Overcash, Ed., Decomposition of Toxic and Nontoxic Organic Compounds in Soils, Ann Arbor Science Publishers, Inc., Ann Arbor, MI.

Guthrie, M.A., E.J. Kirsch, R.F. Wukash, and C.P.L. Grady. (1984). "Pentachlorophenol degradation: anaerobic," Water Research 18(4):451.

Haddock, J.D., P.F. Landrum, and J.P. Glesy. (1983). "Extraction efficiency of anthracene from sediments." Analytical Chemistry 55(7):1197.

Hansch, C. and A. Leo. (1979). Substituent Constants for Correlation Analysis in Chemistry and Biology. John Wiley and Sons, New York.

Hautala, R. (1978). Surfactant effects on pesticide photochemistry in water and soil. U.S. Environmental Protection Agency, Athens, Georgia, EPA-600/3-78-060.

Helling, C. S., P. C. Kearney, and M. Alexander. (1971). Behavior of pesticides in soils. p. 147-240. In C. N. Brady (ed.) Advances in Agronomy. Vol. 23. Academic Press, New York.

Jackson, M.L. (1956). Soil chemical analysis--advanced course. Published by author. University of Wisconsin, Madison, WI.

Johnston, L.J., P. De Mayo, and S.K. Wong. (1982). "Surface photochemistry: Evidence for rotational and translational movement of cyanopropyl radicals on a silica gel surface." Journal of the Chemical Society, Chemical Communications 1982(19):1106-1108.

Karickhoff, S.W., D.S. Brown, and T.A. Scott. (1979). "Sorption of hydrophobic pollutants on natural sediments." Water Research 13(3):241-248.

Karickhoff, S.W. (1981). "Semi-empirical estimation of sorption of hydrophobic pollutants on natural sediments and soils." Chemosphere 10(8):833-846.

Kearns, D. R. (1971). "Physical and chemical properties of singlet molecular oxygen." Chemical Reviews 71(4):395-427.

Kenaga, E.E. and C.A.I. Goring. (1980). "Relationship between water solubility, soil sorption, octanol water partitioning, and concentration of chemicals in biota." pp. 78-115 in Eaton, J.C., Parrish, P.R., and Hendriks, A. C., eds. Aquatic Toxicology. Special Publication Number 707, American Society of Testing and Materials. Washington, D.C.

Kleinbaum, D.G. and L.L. Kupper. (1978). Applied regression analysis and other multivariable methods. Duxbury Press, North Scituate, Massachusetts.

Klute, A. (Ed.). (1986). Methods of soil analysis. Part I. Physical and Mineralogical Properties. 2nd Ed. American Society of Agronomy, Madison, WI.

Korfmacher, W.A., E.L. Wehry, G. Mamatov, and D.F.S. Natusch. (1980). "Resistance to photochemical decomposition of polycyclic aromatic hydrocarbons vapor adsorbed on coal fly ash." Environmental Science and Technology 14(9):1094-1099.

Kortum, G. and W. Braun. (1960). Liebigs Annalytical Chemistry 632:104-115.

Lambert, S.M. (1967). "Functional relationship between sorption in soil and chemical structure." Soil Science 106:248-261.

Lambert, S.M., P.E. Porter, and H. Schieferstein. (1965). "Movement and sorption of chemicals applied to the soil." Weeds 13(3):185.

Leighton, P.A. (1961). Photochemistry of Air Pollution. Academic Press, New York, New York. 300 p.

Lemaire, J., I. Campbell, H. Hulpke, J.A. Guth, W. Merz, L. Philip, and C. Von Waldow. (1982). An assessment of test methods for photodegradation of chemicals in the environment. Chemosphere 11(2):119-164.

Liberti, A. D. Brocco, I. Allegrini, and G. Bertoni. (1978). "Field photodegradation of TCDD by ultra-violet radiations." p. 195-200. In F. Cattabeni, A. Cavallero, and G. Galli (Eds.). Dioxin: Toxicological and chemical aspects. Spectrum Publications, Inc., New York. 195-200.

Lorenz, L.F. and L.R. Gjovik. (1972). "Analyzing creosote by gas chromatography: Relationship to creosote specifications." Proceedings, American Wood Preservation Association, 68:32-42.

Lyman, W.J., W.F. Reehl, and D.H. Rosenblatt. (1982). Handbook of Chemical Property Estimation Methods. McGraw-Hill Book Company, New York.

Mabey, W.R., T. Mill, and D. G. Hendry. (1982). Photolysis in water. pp. 49-102. In: Laboratory protocols for evaluating the fate of organic chemicals in air and water. EPA-600/3-82-022. Athens, Georgia.

Mackay, D., Bobra, A., Chan, D.W., and Shui, W.Y. (1982). "Vapor pressure correlations for low volatility environmental chemicals." Environmental Science and Technology 16:645.

Masnovi, J.M., E.A. Seddon,and J.K. Koch. (1984). "Electron transfer from anthracenes: Comparison of photoionization, charge-transfer excitation and electrochemical oxidation." Canadian Journal of Chemistry 62(12):2552-2559.

McKenna, E.J. and R.D. Heath. (1976). "Biodegradation of polynuclear aromatic hydrocarbon pollutants by soil and water microorganisms." Water Resources Center, University of Illinois, Research Report No. 113, UILU-WRC-76-0113.

Merck. (1983). Merck Index. 10th ed. Merck and Company, Inc., Rahway, New Jersey.

Merkel, P.B., and D.R. Kearns. (1972). Journal of the American Chemical Society 94:7244.

Miles, C.J., and P.L. Brezonik. (1981). Oxygen consumption in humic-color waters by a photochemical ferrous-ferric catalytic cycle. Environmental Science and Technology 15:1089.

Miller, G.C., and R.G. Zepp. (1983). "Extrapolating photolysis rates from the laboratory to the environment." Residue Reviews 85:89-110.

Mingelgrin, U.S. Yarin and S. Saltzman. (1978). Differential infrared spectroscopy in the study of parathion-bentonite complexes. Soil Science Society of American Journal 42:664-665.

Moersen, A. and H.J. Rehm. (1987). "Degradation of phenol by a mixed culture of pseudomonas putida and cryptococcus elinovii on activated carbon." Applied Microbiology and Biotechnology, 26(3):283-288.

Moos, L.P., E.J. Kirsch, R.F. Wukash, and C.P.L. Grady. (1983). "Pentachlorophenol degradation: Aerobic." Water Research 17(11):1575-1584.

Mortland, M.M. (1970). Clay-organic complexes and interactions. Advances in Agronomy 22:75.

Murphy, N.B.K., D.D. Kaufman, and G.F. Fries. (1979). "Degradation of pentachlorophenol in aerobic and anaerobic soils." Journal of Environmental Science and Health B14(1):1-14.

Naeger, B.A. (1985). Engineering treatment of hazardous wastewater utilizing dye-sensitized photooxidation. M.S. Thesis, Utah State University, Logan, Utah.

Nester, J. and W. Wasserman. (1974). Applied linear statistical models. Irwin, Inc. Homewood, Il.

Nilles, G.P., and M.J. Zabik. (1975). "Photochemistry of bioactive compounds. Multiple photodegradation and mass spectral analysis of basagran." Journal of Agricultural and Food Chemistry. 23(3):410-415.

Office of Technology Assessment, (1983). Technologies and Management Strategies for Hazardous Waste Control. Superintendent of Documents, U.S. Government Printing Office, Washington, D.C., 407p.

Page, A.L. (Ed.). (1982). Methods of soil analysis. Part 2. Chemical and microbiological properties. 2nd Ed. American Society of Agronomy, Madison, WI.

Plimmer, J.R. and U.I. Kligebiel. (1973). "Photochemistry of dibenzo-p-dioxins." p. 44-54. In E.H. Blair (Ed.)., Chlorodioxins-origins and fate. American Chemical Society, Washington, D.C.

Roy, W.R. and R.A. Griffin. (1985). "Mobility of organic solvents in water saturated soil materials." Environmental and Geological Water Science 7(4):241-247.

Saltiel, J., and B.W. Atwater. (1988). "Spin-statistical factors in diffusion controlled reactions." Advanced Photochemistry 14:1-90.

Sargent, J.W., and R.L. Sanks. (1974). Light energized oxidation of organic wastes. Journal of the Water Pollution Control Federation 46:2547-2554.

Sargent, J.W. and R.L. Sanks. (1976). "Dye catalyzed oxidation of industrial wastes." Journal of Environmental Engineering, ASCE 102(EE5):879-895.

Sims, R.C. (1982). Land treatment of polynuclear aromatic compound. Ph.D. Dissertation, North Carolina State University, Raleigh, N.C.

Sims, R.C. and M.R. Overcash. (1983). "Fate of polynuclear aromatic compounds (PNAs) in soil-plant systems." Residue Reviews 88:1-68.

Sims, R.C. (1986). Land Treatment: A Waste Management Alternative. Loehr, R.C. and Malina, J. F., Eds. University of Texas Center for Research in Water Resources. Austin, Texas. 151.

Sims, R.C., J.L. Sims, D.L. Sorensen, and L.L. Hastings. (1986). Waste/soil treatability studies for four complex industrial wastes: Methodologies and results. Volume 1. U.S. Environmental Protection Agency, Ada, Oklahoma, October 1986, EPA/600/6-86/003a.

Smith, J.H., W.R. Mabey, N. Bohonos, B.R. Holt, S.S. Lee, T.W. Chou, D.C. Bomberger, and T. Mill. (1978). Environmental pathways of selected chemicals in freshwater systems. II. Laboratory studies. Report No. EPA-560/5-78-002, U.S. Environmental Protection Agency, Washington, D.C.

Spikes, J. D., and R. Straight. (1967). Sensitized photochemical processes in biological systems. Annual Review of Physical Chemistry 18:409-440.

Stakey, H.C., P.B. Blackman, and P.L. Hauff. (1984). "The routine mineralogical analysis of clay-bearing samples." U.S. Geological Survey Bulletin 1563.

Stevens, B. and S.R. Perez. (1974). Molecular Photochemistry 6:1.

Swann, R.L., D.A. Laskowki, P.J. McCall, and K. Van der Kuy. (1983). "A rapid method for the estimation of environmental parameters Kow, Koc, and water solubility." Residue Reviews 8:15.

U.S. Environmental Protection Agency. (1986). Test methods for evaluating solid wastes. Volume 1B: laboratory manual physical/chemical methods, 3rd Ed, SW-846, Office of Solid Waste and Emergency Response, Washington, D.C.

Verschueren, K., (Ed.). (1983). Handbook of Environmental Data on Organic Chemicals, 2nd Ed., Van Nostrand Reinhold Company, New York, 650p.

Wasik, S.P. M.M. Miller, Y.B. Tewari, W.E. May, W.J. Sonnefeld, H. DeVoe, and W.H. Zoller. (1983). "Determination of the vapor pressure, aqueous solubility, and octanol/water partition coefficient of hydrophobic substances by coupled generator column/liquid chromatographic methods." Residue Reviews 85:27-42.

Watts, R.J. (1983). The development of design criteria for the construction of sensitized photooxidation lagoons for the treatment of toxic and biologically recalcitrant industrial wastes. Ph.D. Dissertation, Utah State University, Logan, Utah.

Winslow, H.H. (1973). "Chemical and physical properties of wood preservatives and wood-preserving systems." In Nicholas, D.D. Ed., Wood Deterioration and its Prevention by Preservative Treatments. Syracuse University Press, Syracuse, NY.

Wipf, H.K., E. Humberger, N. Neuner, and F. Schenker. (1978). "Field trials on photodegradation of TCDD on vegetation after spraying with vegetable oil." p. 201-217. In F. Cattabeni, A. Cavallero, and G. Galli (Eds.). Dioxins: Toxicological and chemical aspects. Spectrum Publications, Inc., New York.

Yokley, R.A., A.A. Garrison, E.L. Wehry, and G. Mamantov. (1986). "Photochemical transformation of pyrene and benzo[a]pyrene vapor deposited on eight coal stack ashes." Environmental Science and Technology 20:86-91.

Young, R.H., R.L. Martin, D. Feriozi, D. Brewer, and R. Kayser. (1973). "On the mechanism of quenching of singlet oxygen by amines." Photochemistry and Photobiology 17:233-244.

Zepp, R. G., and D. M. Cline. (1977). Rates of direct photolysis in aquatic environment. Environmental Science and Technology 11:359-366.

Zepp, R. G., G. N. L. Wolfe, G. L. Baughman, and R. C. Hollis. (1977). Singlet oxygen in natural waters. Nature 267:421.

APPENDIXES

Table 1A. Physical and chemical properties of the Skumpah soil used in the study.

Soil Classification	Fine silty, mixed typic natragid		
Sample Location	Tooele, Co., UT		
PROPERTIES	Skumpah 2 mm	Skumpah < 60 mesh	Skumpah < 60 mesh w/ MeCl
PHYSICAL PROPERTIES			
Texture	Silty clay loam	Silty clay	Clay loam
Bulk density (g/cc)	1.65		
Effective Size, mm*	0.048		
Uniformity Coefficient*	8.33		
% Moisture at			
Saturation	36	35.7	
1/3 bar	23		
15 bar	9		
Particle Size Distribution			
Clay (<2um)	34	32	30
Silt (0.050-0.002mm)	51	52	48
Sand (2-0.05mm)	15	16	22
Surface area m2/g			
Total		57.25** (118.5)	
External		13.45** (51.22)	
Surface Charge Density (C/m2)		0.218	
Munsell Color Designation		10YR 7/2	
CHEMICAL PROPERTIES			
pH	8	8.3	
CEC (meg/100g)	12.4	12.5	12.2
% Organic Carbon	0.9	0.7	0.7
Total Phosphorus (%)		0.071	
Total Nitrogen (%)		0.06	
Nitrate Nitrogen (mg/Kg)		28.3	
Sulfate in Sat'd Extract (meg/L)		25	
EC in Sat'd Extract (mmhos/cm)	54	40	
Fe (mg/Kg) DTPA Extract		5.3	
Zn (mg/Kg) DTPA Extract		3.9	
Total Fe(%)	1.07	1.03	
Total Al (%)	1.08	1.79	
Total Mn (mg/Kg)	326	298	
P Bicarbonate Extract (mg/Kg)		18	
K (mg/Kg) Bicarbonate Extract		>400	
NH4OAcExtraction (meg/100g)			
Na	22.4	19.2	18
K	2.28	3.27	3.33
Ca	40.9	44.4	44.4
Mg	3.62	3.29	3.56
Al		0.03	0.028
H			
Water Soluble (meg/100g)			
Na	17.3	6.8	
K	0.81	0.93	
Ca	0.52	0.38	
Mg	0.39	0.31	
Calcium Carbonate %	30.8		

* Determination made from dry sieve analysis conducted at the UWRL.

** Surface area determined without standard chemical pretreatment to remove organic matter and carbonates (with pretreatment).

Table 2A. Physical and chemical properties of the McLaurin soil used in the study.

Soil Classification	Course loamy, siliceous thermic typic palendulfs		
Sample Location	Stone Co. MS		
PROPERTIES	McLaurin 2 mm	McLaurin < 60 mesh	McLaurin < 60 mesh w/ MeCl
PHYSICAL PROPERTIES			
Texture	Sandy loam	Loam	Sandy loam
Bulk density (g/cc)	1.41		
Effective Size, mm*			
Uniformity Coefficient*			
% Moisture at			
Saturation	25.7		
1/3 bar	12.4		
15 bar	8.2		
Particle Size Distribution			
Clay (<2um)	3.3	8	10
Silt (0.050-0.002mm)	24.2	41	23
Sand (2-0.05mm)	72.6	51	67
Surface area m2/g			
Total		4.79	
External		2.7	
Surface Charge Density (C/m2)		0.766	
Munsell Color Designation		10YR6/3 (pale brown)	
CHEMICAL PROPERTIES			
pH	4.8	5.3	
CEC (meg/100g)	6.4	3.8	3.6
% Organic Carbon	0.94	0.7	0.6
Total Phosphorus (%)	0.003		
Total Nitrogen (%)	0.02		
Nitrate Nitrogen (mg/Kg)	0.8		
Sulfate in Sat'd Extract (meg/L)	13.7		
EC in Sat'd Extract (mmhos/cm)	0.1	0.25	0.26
Fe (mg/Kg) DTPA Extract	18		
Zn (mg/Kg) DTPA Extract	0.64		
Total Fe(%)	0.2	0.452	0.433
Total Al (%)	0.42	0.89	0.92
Total Mn (mg/Kg)	19	44	45
P Bicarbonate Extract (mg/Kg)	2.2		
K (mg/Kg) Bicarbonate Extract	19		
NH4OAcExtraction (meg/100g)			
Na	0.02	<	>
K	0.07	0.1	0.09
Ca	0.3	1.08	0.85
Mg	0.06	0.2	0.16
Al	1.4	0.11	0.12
H	5.9		
Water Soluble (meg/100g)			
Na	0.1		
K	0.003		
Ca	0.27		
Mg	0.088		

* Determination made from dry sieve analysis conducted at the UWRL.

Table 3A. Physical and chemical properties of the Durant soil used in the study.

Soil Classification	Fine montmorillonite thermic vertic agrigstolls		
Sample Location	Pentotoc Co., OK		
PROPERTIES	Durant 2 mm	Durant < 60 mesh	Durant < 60 mesh w/ MeCl
PHYSICAL PROPERTIES			
Texture	Silt loam	Clay loam	Clay loam
Bulk density (g/cc)	1.59		
Effective Size, mm*	0.29		
Uniformity Coefficient*	12.8		
% Moisture at			
Saturation	55		
1/3 bar	41.6		
15 bar	12		
Particle Size Distribution			
Clay (<2um)	15.2	30	29
Silt (0.050-0.002mm)	53.6	46	46
Sand (2-0.05mm)	31.2	24	25
Surface area m2/g			
Total		128	
External		33.9	
Surface Charge Density (C/m2)		0.188	
Munsell Color Designation		10YR4/2 (dark greyish brown)	
CHEMICAL PROPERTIES			
pH	6.6		
CEC (meg/100g)	20.5	24.9	24.8
% Organic Carbon	2.88	2.2	2.2
Total Phosphorus (%)	0.03		
Total Nitrogen (%)	0.21		
Nitrate Nitrogen (mg/Kg)	18		
Sulfate in Sat'd Extract (meg/L)	0.3		
EC in Sat'd Extract (mmhos/cm)	0.5	0.78	0.68
Fe (mg/Kg) DTPA Extract	28		
Zn (mg/Kg) DTPA Extract	3.8		
Total Fe(%)		1.72	1.72
Total Al.(%)		3.2	3.22
Total Mn (mg/Kg)		464	490
P Bicarbonate Extract (mg/Kg)	3		
K (mg/Kg) Bicarbonate Extract	177		
NH4OAcExtraction (meg/100g)			
Na	0.2	0.1	0.04
K	0.7	0.83	0.79
Ca	19.4	19.6	19.7
Mg	14.7	5.01	5.08
Al		0.019	0.021
H			
Water Soluble (meg/100g)			
Na	0.002		
K	0.0006		
Ca	0.12		
Mg	0.004		

* Determination made from dry sieve analysis conducted at the UWRL.

Table 4A. Summary of first order kinetics of anthracene on minerals and soils using UV radiation.*

	Half Life (hr)					
	Chemical Mixture/Concentration mg/L					
	Anthracene only		10 cpd mixture		7 cpd mixture	
Mineral/Soil	1000	500	1000	500	1000	500
Silical gel	0.18 a†	0.10 a	0.57 b,d,(1)††	0.37 b,e	0.25 c,d	0.17 c,e
Ca kaolinite	4.5 a	3.5 a,b	50.6	10.9 b,c	25.7 (1)	16.5 c,(1)
Ca montmorillonite	11.2 a,d,(1)	19.8 a,e	7.21b,d,(1)	4.33 b,f	16.9 c,d,(1)	10.8 c,e,f,(1)
Ca illite	10.3 (1)					
Al kaolinite	7.7					
Al montmorillonite	61†††					
Al illite	22.6†††					
Calcite (surface area = 13.6)	17.3 (1)					
Calcite (surface area =2)	13.0 (1)					
Skumpah				219**		49.5 (2)
Durant				480**		103
McLaurin				288**		34.3 (2)

*Light intensity = Iox20 (cm^2/g substrate) small photoreactors.
**Light intensity = Iox4.4 (cm^2/g substrate) large photoreactors.
†Values within rows followed by the same letter are not significantly different (α=0.05).
††Values within column followed by the same number are not significantly different (α=0.05).
†††Calculated half life exceeds experimental irradiation time.

Table 5A. Summary of first order kinetics of fluorene on minerals and soils using UV radiation.*

	Half Life (hr)			
	Chemical Mixture/ Concentration mg/L			
	10 cpd mixture		7 cpd mixture	
Mineral/Soil	1000	500	1000	500
Silical gel	87††	50††	51††	51††
Ca kaolinite	289††	52 a†	74 b	55 a,b
Ca montmorillonite	no reaction	173††	231††	231††
Skumpah		216**		67
Durant		648**		152††
McLaurin		240**		53

*Light intensity = Iox20 (cm^2/g substrate) small photoreactors.
**Light intensity = Iox4.4 (cm^2/g substrate) large photoreactors.
†Values within rows followed by the same letter are not significantly different (α=0.05).
††Calculated half life exceeds experimental irradiation time.

Table 6A. Summary of first order kinetics of cresol on minerals and soils using UV radiation.*

	Half Life (hr)			
	Chemical Mixture/ Concentration mg/L			
	10 cpd mixture		7 cpd mixture	
Mineral/Soil	1000	500	1000	500
Silical gel	5.7 a,c†	3.6 a,d(1)††	6.3 b,c(1)	2.3 b,d(1),(2)
Ca kaolinite	31	6.3 a,(1)	2.2 b,(1)	3.9 a,b,(1)
Ca montmorillonite	231†††	173†††	73 a	55 a,(2)
Skumpah		168**		17.8
Durant		240**		53.3 (3)
McLaurin		336**		30.5 (3)

*Light intensity = Iox20 (cm^2/g substrate) small photoreactors.
**Light intensity = Iox4.4 (cm^2/g substrate) large photoreactors.
†Values within rows followed by the same letter are not significantly different (α=0.05).
††Values within columns followed by the same letter are not significantly different (α=0.05).
†††Calculated half life exceeds experimental irradiation time.

Table 7A. Summary of first order kinetics of pyrene on minerals and soils using UV radiation.*

	Half Life (hr)			
	Chemical Mixture/ Concentration mg/L			
	10 cpd mixture		7 cpd mixture	
Mineral/Soil	1000	500	1000	500
Silical gel	26 a†	10 a	25 b	12 1,b
Ca kaolinite	365††	196††	173	115††
Ca montmorillonite	173††	139††	139††	116††
Skumpah		no reaction**		151
Durant reaction		no reaction**		no
McLaurin		no reaction**		66

*Light intensity = Iox20 (cm^2/g substrate) small photoreactors.
**Light intensity = Iox4.4 (cm^2/g substrate) large photoreactors.
†Values within rows followed by the same letter are not significantly different (α=0.05).
††Calculated half life exceeds experimental irradiation time.

Table 8A. Summary of first order kinetics of biphenyl on minerals and soils using UV radiation.*

	Half Life (hr)			
	Chemical Mixture/ Concentration mg/L			
	10 cpd mixture		7 cpd mixture	
Mineral/Soil	1000	500	1000	500
Silical gel	no reaction	no reaction	no reaction	no reaction
Ca kaolinite	364†	116†	173	125†
Ca montmorillonite	no reaction	no reaction	346†	346†
Skumpah		648**		210
Durant		1992**		no reaction
McLaurin		408**		28.4

*Light intensity = Iox20 (cm^2/g substrate) small photoreactors.
**Light intensity = Iox4.4 (cm^2/g substrate) large photoreactors.
†Calculated half life exceeds experimental irradiation time.

Table 9A. Summary of first order kinetics of phenanthracene on minerals and soils using UV radiation.*

	Half Life (hr)			
	Chemical Mixture/ Concentration mg/L			
	10 cpd mixture		7 cpd mixture	
Mineral/Soil	1000	500	1000	500
Silical gel	69†	52†	no reaction	87†
Ca kaolinite	no reaction	no reaction	204	185†
Ca montmorillonite	231†	173†	231†	173†
Skumpah		no reaction**		248
Durant		no reaction**		no reaction
McLaurin		no reaction**		74.9

*Light intensity = Iox20 (cm^2/g substrate) small photoreactors.
**Light intensity = Iox4.4 (cm^2/g substrate) large photoreactors.
†Calculated half life exceeds experimental irradiation time.

Table 10A. Summary of first order kinetics of dibenzofuran on minerals and soils using UV radiation.*

	Half Life (hr)	
	Chemical Mixture/Concentration mg/L	
	10 cpd mixture	
Mineral/Soil	1000	500
Silical gel	no reaction	52†
Ca kaolinite	no reaction	266†
Ca montmorillonite	no reaction	no reaction
Skumpah		no reaction**
Durant		no reaction**
McLaurin		no reaction**

*Light intensity = Iox20 (cm^2/g substrate) small photoreactors.
**Light intensity = Iox4.4 (cm^2/g substrate) large photoreactors.
†Calculated half life exceeds experimental irradiation time.

Table 11A. Summary of first order kinetics of quinoline on minerals and soils using UV radiation.*

	Half Life (hr)	
	Chemical Mixture/Concentration mg/L	
	10 cpd mixture	
Mineral/Soil	1000	500
Silical gel†		
Ca kaolinite†		
Ca montmorillonite†		
Skumpah		no reaction**
Durant		no reaction**
McLaurin		no reaction**

*Light intensity = Iox20 (cm^2/g substrate) small photoreactors.
**Light intensity = Iox4.4 (cm^2/g substrate) large photoreactors.
†Quinoline in the 10 compound mixture not extracted with MeCl used in the mineral studies.

Table 12A. Summary of first order kinetics of carbazole on minerals and soils using UV radiation.*

	Half Life (hr)	
	Chemical Mixture/Concentration mg/L	
	10 cpd mixture	
Mineral/Soil	1000	500
Silical gel†		
Ca kaolinite†		
Ca montmorillonite†		
Skumpah		576**
Durant		792**
McLaurin		744**

*Light intensity = Iox20 (cm^2/g substrate) small photoreactors.
**Light intensity = Iox4.4 (cm^2/g substrate) large photoreactors.
†Carbazole not quintified for mineral study, similar retention time to fluorene by LC analysis.